# THESIS APPROVAL

## GRADUATE SCHOOL, KASETSART UNIVERSITY

Doctor of Engineering (Environmental Engineering)

**DEGREE**

Environmental Engineering — **FIELD**

Environmental Engineering — **DEPARTMENT**

**TITLE:** Development of Sediment Transport Model with Application to Songkhla Lake

**NAME:** Miss Sucheewan Yoyrurob

**THIS THESIS HAS BEEN ACCEPTED BY**

**THESIS ADVISOR**

( Associate Professor Winai Liengcharernsit, D.Eng. )

**THESIS CO-ADVISOR**

( Mr. Suchart Leungprasert, Ph.D. )

**DEPARTMENT HEAD**

( Assistant Professor Mongkol Damrongsri, Dr.Ing. )

**APPROVED BY THE GRADUATE SCHOOL ON** _____

**DEAN**

( Associate Professor Gunjana Theeragool, D.Agr. )

THESIS

# DEVELOPMENT OF SEDIMENT TRANSPORT MODEL WITH APPLICATION TO SONGKHLA LAKE

SUCHEEWAN YOYRUROB

A Thesis Submitted in Partial Fulfillment of
the Requirements for the Degree of
Doctor of Engineering (Environmental Engineering)
Graduate School, Kasetsart University
2011

Sucheewan Yoyrurob 2011: Development of Sediment Transport Model with Application to Songkhla Lake. Doctor of Engineering (Environmental Engineering), Major Field: Environmental Engineering, Department of Environmental Engineering. Thesis Advisor:
Associate Professor Winai Liengcharernsit, D.Eng. 165 pages.

In the past few decades, rapid population growth in Thailand has resulted in excess utilization of natural resources and degradation of environmental quality. Deforestation in sloping areas for agricultural and residential purposes has resulted in soil erosion from deforested areas with subsequent sediment transport and deposition in receiving water bodies. In order to evaluate the severity of this problem, a mathematical model is developed to simulate sediment transport phenomena in a receiving water body. In model development, total sediment transport is classified as bedload transport and suspended load transport, which result in two interrelated transport models. Three-dimensional mass balance equation is used as a basic governing equation for the suspended load transport model, whereas two-dimensional mass balance equation is used as a basic governing equation for the bedload transport model. The finite element method is used to solve these governing equations. Since sediment grain size and specific gravity are important factors affecting sediment transport either in the form of bedload or suspended load, the simulation models are developed for each group of sediment grain size and specific gravity, then the simulated sediment concentrations of various groups are combined to obtain spatial distribution of total sediment load at each time step. Inflow sediment load along the water body boundary is classified into corresponding groups based on their grain size and specific gravity. The developed model is applied to simulate sediment transport pattern in Songkhla Lake which is one of the most important water resources in southern Thailand.

_____ _____ __ / __ / __

Student's signature Thesis Advisor's signature

# ACKNOWLEDGMENTS

I would like to express my sincere gratitude and deepest appreciation to my thesis advisor Assoc. Prof. Dr. Winai Liengcharernsit and committees Asst. Prof. Dr. Narumol Vongthanasunthorn and Dr. Suchart Leungprasert for their excellent guidline, problem solving, invaluable suggestion, proofreading of this thesis and encouragement throughout the study which made this thesis complete in appropriate time.

Especially, I would like to give special thankfulness and deepest appreciation to all research participants for their excellent cooperation.

Thankfulness also goes to the staff of the Faculty of Environmental Management, Prince of Songkhla University for laboratory supports. I am equally grateful and deepest appreciation to Asst. Prof. Dr. Penjai Sompongchaikul for her worthy advice and valuable suggestion in laboratory technically.

In addition, I wish to thank all my friends for their suggestion, helpful and kind support.

Finally, I am particularly indepted to the Songkhla Rajabhat University for giving me a chance and funds to study at the Graduate School, Kasetsart University and I wish to express my gratefulness to my family and Mr. Palakorn Boonsai for their love, understanding, warmest encouragement, assistance throughout the study.

Sucheewan Yoyrurob

April 2011

# TABLE OF CONTENTS

# LIST OF TABLES

# LIST OF FIGURES

# LIST OF FIGURES (continued)

# LIST OF ABBREVIATIONS

| | | |
|---|---|---|
| A | = | Area of each element |
| Ci | = | Nodal values of substance concentration |
| C | = | Substance concentration |
| Kx | = | The dispersion coefficient in x-direction |
| Ky | = | The dispersion coefficient in y-direction |
| Kz | = | The dispersion coefficient in z-direction |
| Ni | = | Interpolation functions of node i |
| Psu | = | Practical salnity unit |
| t | = | time |
| $\Delta t$ | = | Time increment |
| Ui | = | Nodal values of flow velocity in x-direction |
| u | = | Flow velocities in x-direction |
| Vi | = | Nodal values of flow velocity in y-direction |
| v | = | Flow velocities in x-direction |
| Wi | = | Nodal values of flow velocity in z-direction |
| w | = | Flow velocities in x-direction |
| $\xi$ | = | Natural coordinate of node i in x-direction |
| $\eta$ | = | Natural coordinate of node i in y-direction |
| $\mu$ | = | Natural coordinate of node i in z-direction |

# DEVELOPMENT OF SEDIMENT TRANSPORT MODEL WITH APPLICATION TO SONGKHLA LAKE

## INTRODUCTION

Erosion and sedimentation represent the processes of erosion, transportation, and deposition of solid particles, often called sediments. These natural processes have been active throughout geological time and have shaped the present landscape of our world. Nowadays, erosion, transportation, and sedimentation can cause severe engineering and environmental problems. Human activities exert a profound influence on erosion. Under some circumstances, the erosion rate is 100 times greater than the normal, or geological, erosion rate.

Sediment transport affects water quality and its suitability for human consumption or use in various enterprises. Numerous industries cannot tolerate even the smallest amount of sediment in the water that is necessary for manufacturing processes, and the public pays a large price for the removal of sediments from water it consumes every day. Sediment is not only the major water pollutant, but also serves as a catalyst, carrier, and storage agent of other forms of pollution. Sediment alone degrades water quality for municipal supply, recreation, industrial consumption and cooling, hydroelectric facilities, and aquatic life. In addition, chemicals and waste are assimilated onto and into sediment particles. Ion exchange occurs between solutes and sediments. Thus, sediment particles have become a source of increased concern as carriers and storage agents of pesticides, residues, adsorbed phosphorus, nitrogen, and other organic compounds, and pathogenic bacteria and viruses.

The problems caused by sediment deposition are diverse. Sediments deposited in stream channels reduce flood-carrying capacity, resulting in more frequent overflows and greater flood damage to adjacent properties. Deposition of sediments in irrigation and drainage canals, in navigation channels and floodways, in reservoirs and harbors, on streets and highways, and in buildings. It not only creates a

nuisance but inflicts a high public cost in maintenance, removal or in reduced services.

Songkhla lake is one of the most important water resources in the southern part of Thailand. It has very unique feature characterized by the 3-water ecosystem. Seasonal variations in freshwater runoff from its watershed and saline water intruded from the Gulf of Thailand cause spatial and temporal distributions of salinity of Songkhla lake water. In general, three distinct parts in Songkhla lake are recognized, i.e., fresh water in the upper part, brackish water in the middle part, and saline water in the lower part of the lake. Usually, in the rainy season larger extent of the freshwater part occurs while in the dry season more saline water intrudes further north into the lake. Besides saline water intrusion large portion of the lake has faced sediment deposition problem, caused by increasing rate of soil erosion from the watershed area. It was reported that a total area of approximately 1.8 million rais, equivalent to 27.3% of the Songkhla lake basin area (SLB), has soil erosion rate exceeding 2 tons/rai/year. Out of this, the area of about 0.7 million rais has soil erosion rate exceeding 15 tons/rai/year which is considered very severe (Master Plan for Songkhla Lake Basin Development, 2006). Sediment entering the Songkhla lake occurs from 3 sources, i.e., 1) sediment from its coastline, 2) sediment from river runoff, and 3) sediment from decomposition of humus.

# OBJECTIVES

The objectives of this study are:

1) To develop a sediment transport model consisting of suspended sediment transport model and bedload transport model which are linked to each other, taken into consideration the effects of sediment grain size and specific gravity.

2) To apply the developed model to determine sediment transport patterns in the Songkhla lake.

# LITERATURE REVIEW

## 1. Songkhla Lake Basin.

### 1.1 Topography

Songkhla Lake Basin (SLB) lies in 3 provinces, i.e., all 11 districts of Phattalung Province, 12 (out of 16) districts of Songkhla Province and 2 (out of 23) districts of Nakhon Si Thammarat Province (Figure 1). The Basin covers approximately 8,729 sq.km, consisting of 7,687 sq.km of land area and 1,042 sq.km of lake area. The Basin spans approximately 150 km from the north to the south, and approximately 65 km from the east to the west. The SLB is the only basin in Thailand where freshwater from precipitation, stream runoff and overland flow, draining into the lake, has been mixing with saline water from the sea. This makes the Songkhla lake a large lagoon with 3-water ecosystem, consisting of freshwater, brackish water, and saline water ecosystems (Master Plan for Songkhla Lake Basin Development, 2006).

The basin is bounded by two mountain ranges. To the west is Banthad mountain range which lies in the north-south direction, and to the south is part of Sangala Kiri mountain range. The higher grounds of the two mountain ranges are covered with rain forests, constituting an upstream portion of the catchment area. Further down from the Banthad mountain range, from the north to the south of the basin are undulating plains alternating with low hills. The area towards the east approaching the lake is a large flat plain, most of which are paddy fields. The north of the Songkhla lake is large wetlands called “Phru Kuan Kreng” which cover approximately 137 sq.km (include Thale Noi). The east of Songkhla lake, which lies between the lake and the sea, is a large flat plain.

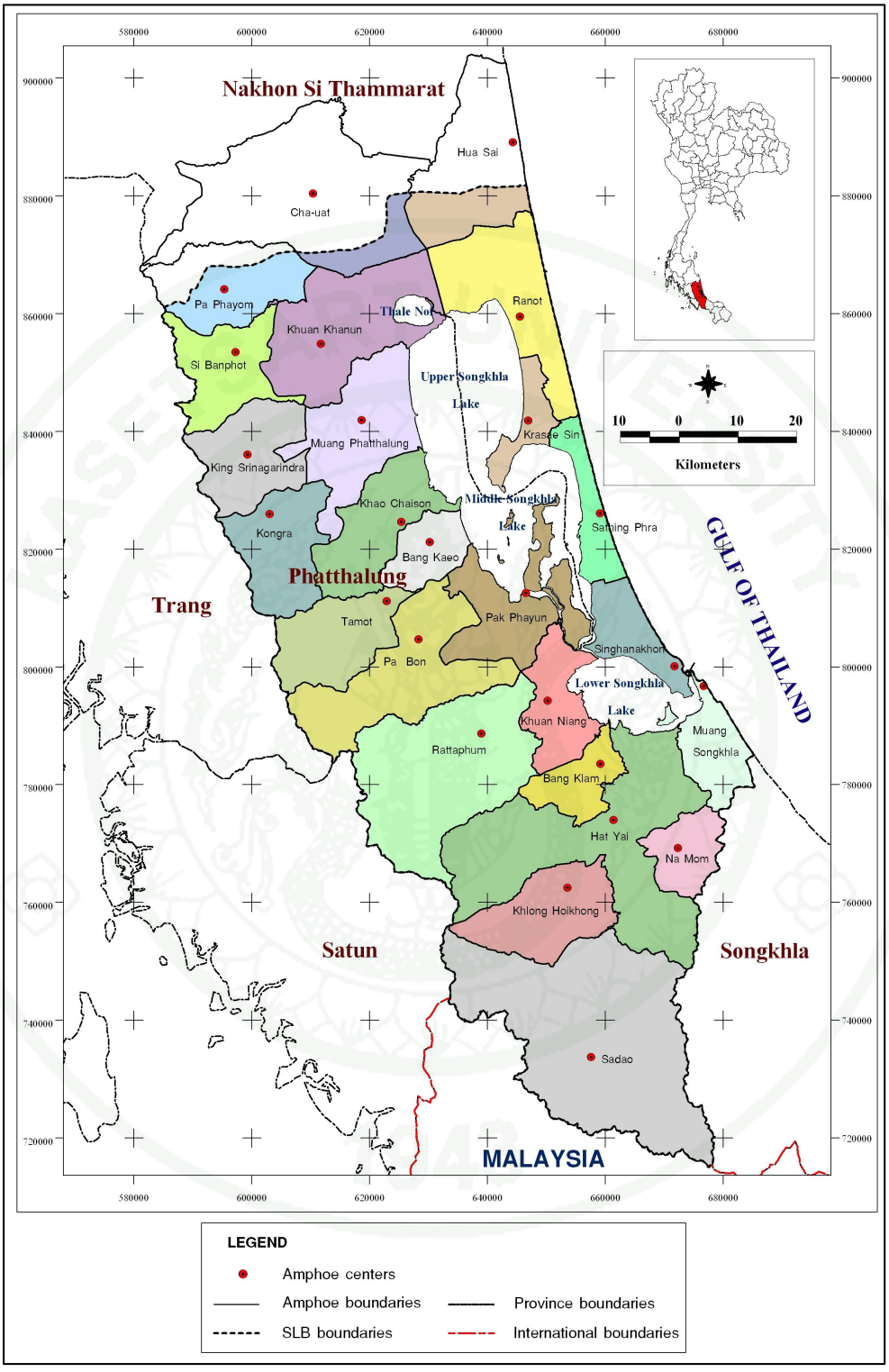


**Figure 1** Songkhla Lake Basin.

**Source**: Master Plan for Songkhla Lake Basin Development (2006).

Physically, the Songkhla lake can be divided into 4 parts, i.e., Thale Noi in the northern most of the Songkhla lake system, the Upper Songkhla Lake, the Middle Songkhla Lake and the Lower Songkhla Lake. The latter is connected to the Gulf of Thailand at Muang District, Songkhla Province. The characteristics of each part of Songkhla lake are as follow: (Office of Natural Resources and Environmental Policy and Planning, 2005)

(1) Thale Noi: Covering approximately 27 sq.km., Thale Noi lies at the northernmost part of the Songkhla Lake in Phattalung Province. It is approximately 1.2 m. deep. It connects with the Upper Songkhla Lake by 3 waterways: Klong Yuan, Klong Ban Klang and Klong Nang Riam. Thale Noi water is freshwater all year round.

(2) Upper Songkhla Lake (Thale Luang): Covering approximately 473 sq.km, the Upper Songkhla Lake extends from the southern part of Thale Noi to Tambon Ko Yai, Krasaesin District, Songkhla Province, and Ban Laem Jong Thanon, Pak Payoon District, Phattalung Province. It is approximately 2 m deep. Three main streams drain into the Upper Songkhla Lake: Klong Tha Nae, Klong Nathom and Klong Tha Madue. Mostly, its water is freshwater except in very dry years when saline water intrusion in the dry season may cause salinity rise as high as 10 psu.

(3) Middle Songkhla Lake (Thale Sab): Covering approximately 360 sq.km, the Middle Songkhla Lake extends from Tambon Ko Yai, Krasaesin District, Songkhla Province, to Tambon Pak Ro, Singha Nakhon District, Songkhla Province, It is approximately 2 m deep. There are several islands in the Middle Songkhla Lake, such as Ko Si–Ko Ha, Ko Mhak and Ko Nang Kam. It receives surface runoff from 3 main streams: Klong Phru Poh, Klong Pansai and Klong Pa Bon. The Middle Songkhla Lake connects with the Lower Songkhla Lake by two large channels: Klong Luang and Ao Tong Baen. Salinity of water in the Middle Songkhla Lake varies seasonally within the range of 0 - 20 psu.

(4) Lower Songkhla Lake (Thale Sab Songkhla): Covering approximately 182 sq.km, the Lower Songkhla Lake extends from Tambon Pak Ro, Singha Nakhon District, Songkhla Province, to the mouth of the Songkhla Lake which connects to the Gulf of Thailand. Most part of the Lower Songkhla Lake is approximately 1.5 m

deep, except the area near the mouth of the Lake which is about 12-14 m deep. Salinity of water in the Lower Songkhla Lake varies seasonally within the range of 23 - 30 psu.

The land area of the SLB (excluding 102 sq.km on islets) is divided by the Royal Irrigation Department into 12 sub-basins (Figure 2), including:

1) Klong Pa Payom Sub-basin (808 sq.km.)
2) Klong Thanae Sub-basin (353 sq.km.)
3) Klong Nathom Sub-basin (757 sq.km.)
4) Klong Tachiad Sub-basin (769 sq.km.)
5) Klong Pa Bon Sub-basin (329 sq.km.)
6) Klong Phru Poh Sub-basin (507 sq.km.)
7) Klong Rattaphum Sub-basin (625 sq.km.)
8) Klong U-Tapao Sub-basin (2,357 sq.km.)
9) East Coast Sub-basin 1 (536 sq.km.)
10) East Coast Sub-basin 2 (202 sq.km.)
11) East Coast Sub-basin 3 (137 sq.km.)
12) East Coast Sub-basin 4 (205 sq.km.)

Remark: Data shown in parentheses are sub-basin areas.

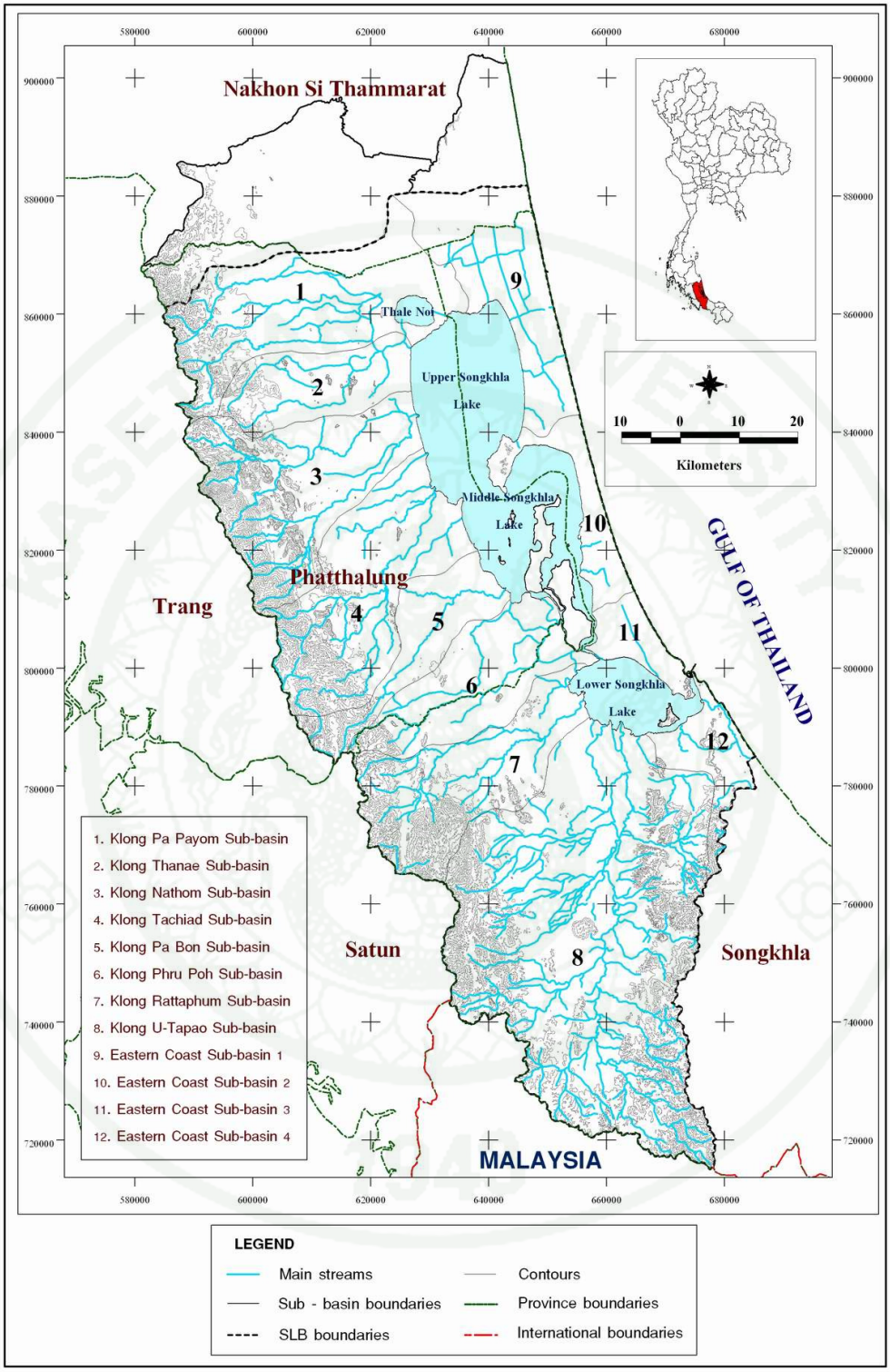


**Figure 2** Sub-basins in Songkhla Lake Basin system.

**Source:** ONEP (2005).

## 1.2 Climate and Meteorology

With influence of the southwest monsoon and the northeast monsoon, the SLB has only 2 seasons, i.e., rainy season and summer season.

1) Rainy season: extending from May to January which can be divided to 2 stages, i.e.

1.1) The first stage from May to September. This stage has influence from the southwest monsoon which causes slight rainfall.

1.2) The second stage from October to January. This stage has influence from the northeast monsoon which causes heavy rainfall. Normally, November is the month with maximum rainfall.

2) Summer season : extending from Febuary to April, this season has influence from the east wind with hot air, resulting in very hot weather. Usually, April is the hottest month.

Data on monthly rainfall in the SLB during 1980 - 2009 are shown in Table 1. Climatological data for the period 1980 - 2009 are shown in Appendix C.

## 1.3 Stream Runoff

ONEP (2005) evaluated stream runoff on the western part of the SLB by using Variable Infiltration Capacity 2 Layers (VIC-2L) model and precipitation-runoff model developed by University of Washington. VIC-2L model takes into consideration some important parameters, including landuse, altitude and main river network for evaluating stream runoff. The results are shown in Table 2.

**Table 1** Monthly rainfall in SLB from 1980-2009.

| Month | Rainfall (mm) | | |
|---|---|---|---|
| | Mean | Mean Rainy Day | Daily Max |
| January | 72.6 | 9 | 182.0 |
| Febuary | 48.6 | 5 | 353.6 |
| March | 59.0 | 6 | 148.2 |
| April | 76.5 | 8 | 67.4 |
| May | 123.8 | 13 | 193.2 |
| June | 99.1 | 12 | 86.0 |
| July | 92.7 | 12 | 99.5 |
| August | 110.7 | 13 | 91.0 |
| September | 130.3 | 15 | 110.2 |
| October | 250.0 | 20 | 150.8 |
| November | 533.2 | 22 | 521.8 |
| December | 431.2 | 20 | 286.0 |
| Annual | 169.0 | 13 | 521.8 |

**Sources:** Meteorological Development Bureau (2009).

**Table 2** Monthly Runoff in the west of SLB Subbasin.

| Mouth | Runoff ($x10^6$ $m^3$) | | | | | | | |
|---|---|---|---|---|---|---|---|---|
| | Pa Payom & Thanae | Nathom | Tachiad | Pa Bon | Phru Poh | Rattaphum | U-Tapao | Total |
| January | 57.65 | 15.45 | 41.92 | 8.00 | 11.43 | 17.40 | 51.77 | 203.61 |
| Febuary | 52.61 | 18.55 | 45.06 | 7.30 | 10.24 | 13.09 | 23.59 | 170.45 |
| March | 34.48 | 13.61 | 32.09 | 5.59 | 7.73 | 10.09 | 36.39 | 139.97 |
| April | 33.41 | 11.22 | 19.76 | 3.70 | 7.72 | 15.53 | 53.83 | 145.17 |
| May | 29.47 | 13.63 | 32.75 | 6.37 | 12.09 | 22.37 | 67.09 | 183.78 |
| June | 22.58 | 9.65 | 24.07 | 5.67 | 9.88 | 17.06 | 53.22 | 142.12 |
| July | 29.93 | 13.74 | 28.09 | 6.19 | 12.54 | 28.20 | 75.76 | 194.44 |
| August | 35.43 | 20.14 | 60.54 | 7.36 | 13.13 | 40.66 | 115.88 | 293.13 |
| September | 46.86 | 19.53 | 49.18 | 8.59 | 14.92 | 37.30 | 109.11 | 285.49 |
| October | 84.29 | 30.90 | 90.87 | 17.91 | 32.53 | 73.56 | 178.59 | 508.64 |
| November | 284.74 | 93.97 | 270.29 | 43.95 | 71.71 | 118.69 | 286.10 | 1,133.45 |
| December | 270.85 | 90.33 | 231.32 | 40.80 | 69.42 | 108.58 | 318.06 | 1,129.36 |
| Total | 946.28 | 350.72 | 925.92 | 161.44 | 273.33 | 502.53 | 1,369.38 | 4,529.60 |

**Sources :** ONEP (2005).

## 1.4 Existing Problems and Issues

ONEP (2005) summarized existing problems and issues in the SLB as follow (Figure 3):

(1) Steady decline of upstream forest : In the year 2002, the SLB had only 1,164 sq.km forest area, equivalent to 13.7% of the SLB area, in the upstream watershed.

(2) Steady decline of mangrove and peat swamp forest : In the year 2004, the SLB had only 150 sq.km mangrove and swamp forest, equivalent to 1.75% of the SLB area.

(3) Soil erosion and sedimentation in waterways and lake : Large portion of the SLB area has been facing erosion problem. Approximately 1.8 million rais, equivalent to 27.3% of the SLB area, has an erosion rate exceeding 2 tons/rai/year. Out of this, over 0.7 millions rais has an erosion rate exceeding 15 tons/rai/year, which is ranked very severe.

(4) Loss of rare and vulnerable species : Due to deterioration of various environmental conditions, several rare and vulnerable species are declining in number and likely to be disappearing, if no appropriate conservation measures are provided. These include: Nieuhof's walking catfish (*Prophagorus nieuhofii*), Pla Prom (*Thynnichthys thynnoides*), Pla Mein (*Osphronemus goramy*), Pla Toom (*Puntius bulu*), Pla Lampam (*Puntius schwanenfeldii*), as well as some aquatic animals living in the SLB, such as Otter (*Lutra spp.*), Painted Stork (*Mycteria leucocephaia*), and most importantly, Irrawaddi dolphin (*Orcaella brevirostris*).

(5) Inappropriate and unplanned land use : At present, paddy rice farming area has reduced to approximately one million rais, a decline of 30% during the past 10 years. Approximately 191,400 rais, or 3.6% of the SLB area, is facing acidic soil problem; approximately 20,400 rais, or 0.4 % of the SLB area, is facing saline soil problem.

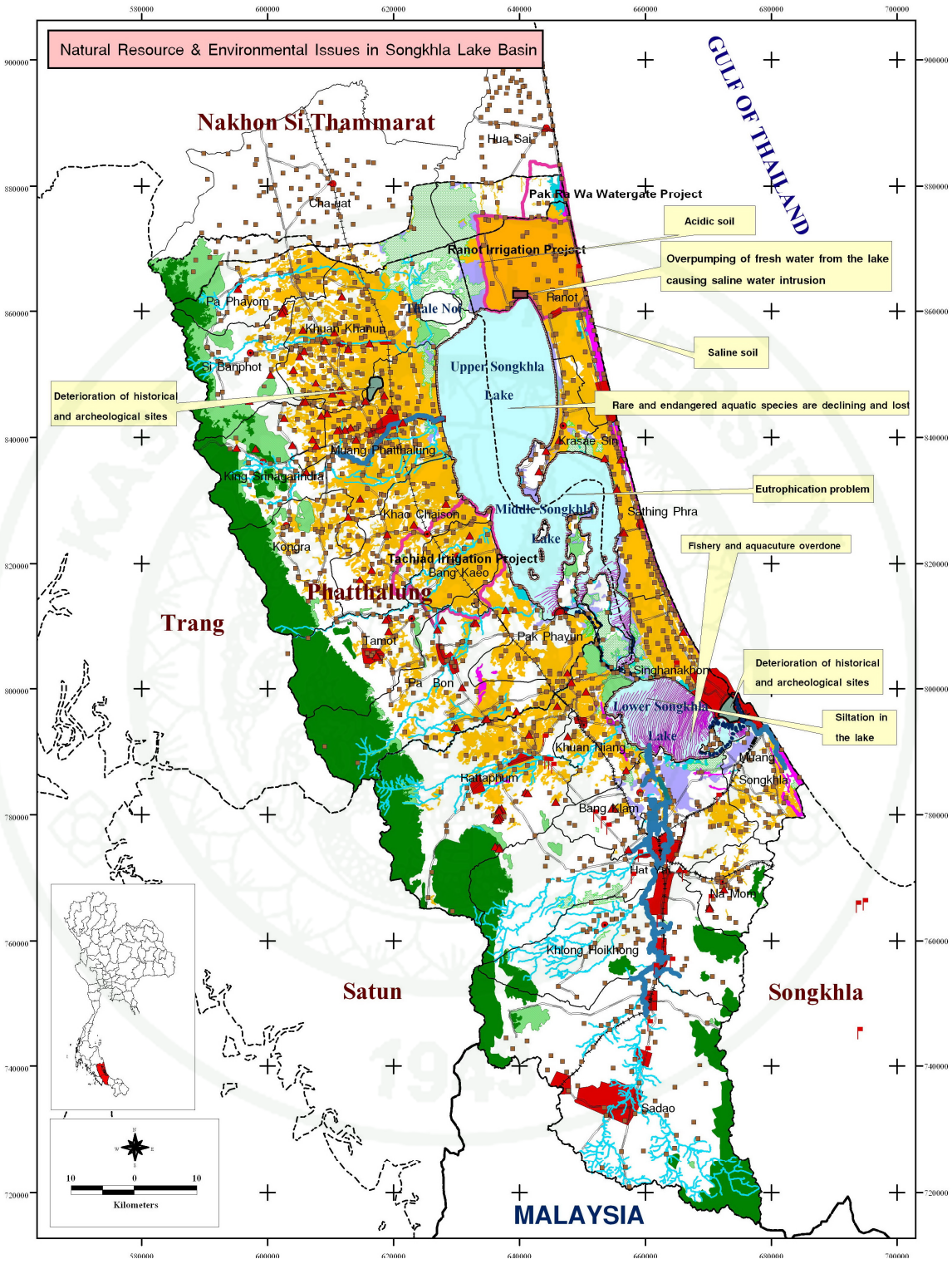


**Figure 3** Summary of SLB Problem and Issues.

**Source:** ONEP (2005).

(6) Lack of integrated water management : Total water demand in the SLB for various activities including domestic consumption, industrial use, irrigation, as well as ecological system is approximately 1,454 million $m^3$ per year, and has been gradually increasing. Thus, an effective mechanism for integrated water resource management is urgently needed.

(7) Freshwater over-pumping/saline intrusion : An average of 58 million $m^3$ of freshwater per year is extracted from the Songkhla Lake for irrigating paddy fields in Ranot District, Songkhla Province, and part of Huasai District, Nakhon Si Thammarat Province. At present, in the dry season, salinity can intrude to the northern most part of the Upper Songkhla Lake. In the severe dry season, salinity in the Upper Songkhla Lake can be as high as 10 psu.

(8) Groundwater over use : The safe yield for groundwater extraction from the Hat Yai Basin was estimated approximately 35 million $m^3$ per year, or about 96,000 $m^3$ per day. In the year 2004, about 75,600 $m^3$ per day of groundwater was extracted from the Hat Yai Basin, which was considered critical. Data in the year 2002 show that the areas where groundwater level lower than 8 m has expanded to cover about 103 sq.km, and continue expanding. This will affect groundwater resource on the basin : it will induce salinity intrusion to the point that groundwater becomes unusable.

(9) More severe flooding : Flood regimes in the SLB differ in different parts of the Basin. In the upstream and midstream zones, flash flood is usually associated with heavy rain and overland flow, whereas in the downstream zone inundation is usually caused by either prolonged impounding in lowland area or overflow from waterways.

(10) Over-capacity fishing : Fishery in the Songkhla Lake and Phru Kuan Kreng has recently undergone massive changes. Innovative and more efficient methods and fishing gears have been introduced. Many of them are destructive, leading to drastic deterioration and decline of aquatic fauna resources.

(11) Insufficient wastewater treatment facilities : There are only two central wastewater treatment plants in the SLB: one in Hat Yai City Municipality, another in Songkhla City Municipality. The service area, however, does not cover the total area of both municipalities. Only about 100,000 inhabitants, or 7% of total

population in the Basin (approximately 1.6 million population), are currently serviced by the existing facilities.

(12) Wastewater pollution problems : Major wastewater pollution sources comprise

*i. Domestic wastewater sources* which discharges approx. 100,000 $m^3$ per day, containing about 17,000 kg. BOD per day, most of which is generated from large communities, especially Hat Yai and Songkhla;

*ii. Industrial wastewater sources* most of which lie along main highways, having total BOD of approx. 3,000 kg. per day;

*iii. Wastewater from swine farms* which has total BOD of about 1,200 kg. per day;

*iv. Wastewater from shrimp farms* which widely fluctuates, with total BOD (considering only the portion which is discharged into the Songkhla Lake) in the range of 13,600-19,000 kg. per day. Apart from simple organic waste (BOD), this wastewater also discharges nutrients (nitrogen and phosphorus), which contribute to the eutrophication problem.

(13) Unsanitary solid waste management : Solid waste in the SLB is typically disposed of by landfill. Sanitary landfill, which is considered to be among a few appropriate methods for solid waste disposal, is found only in large municipalities, such as Hat Yai and Songkhla. In the remaining communities, solid waste is disposed of by simple (unsanitary) landfill, or open dumping.

(14) Deterioration water quality in wasterways and lake: Major wastewater sources are (i) domestic wastewater source; (ii) industrial wastewater source; (iii) wastewater from swine farms; and (iv) wastewater from shrimp farms. All these contribute to pollution problem in waterways and Songkhla Lake.

(15) Culture and local wisdom disregarded historical/archeological sites deteriorated: This is because no policy has been formulated to enhance public awareness to understand values of these resources, which in turn is due to lack of good management and probing intensive research.

(16) Lack of network of culture and historical/archeological sites and local wisdom : Networks in the form of associations, clubs, and foundations occasionally coordinate in joint-missions, but hardly in sustained and continuous

basis. Such loose coordination does not lend itself to long lasting relationship, empowerment, exchange of information, knowledge and experices; all of which are necessary in inheriting process of learning and development of culture & historical/ archeological sites and local wisdom.

(17) Lack of sustainable tourism promotion : The SLB is home to a large number of invalualble tourism resources, but lacking sufficient analyses and syntheses to assess their potentials and carrying capacities. Some of these problems include lack of coordination and cooperation between government agencies and local communities.

(18) Lack of effective management : Given centralization-style management which emphasizes individual ministerial and departmental missions, no organizations or agencies have been assigned direct responsibility for SLB development. Most decisions are still made by centralized agencies. There is thus an urgent need to establish the organization which is responsible for SLB management, which will provide venue for full public participation.

1.5 Sedimentation and Siltation in SLB

In the past, the Songkhla Lake was coastal area. After sand sediment transported and deposited between islands, the area was transformed to lake. After that, sediment from various canals has drained into the lake and deposited, making the lake shallower gradually. The sedimentation rate has been rapidly increasing. It is forecasted that the lake will be transformed to peat swamp and finally it will become land area in the future. Sediment entering the Songkhla Lake comes from 3 main sources, i.e.;

(1) Sediment from eroded coastline surrounding the lake under influence of tidal current and wind-driven wave.

(2) Sediment from surface runoff which occurs due to soil erosion.

(3) Sediment from decomposition of humus in the lake especially in Thale Noi which has lots of aquatic plants, such as water hyacinth. In the Upper Songkhla

Lake, there are lots of algae which will die when water salinity changes and deposition at the bed will occur.

Several researchers attempted to propose mathematical models for predicting sedimentation rate in the lake. However, the reported results were rather different. For examples: Chittrakarn *et al* (1996) determined the sedimentation rate in the lake by using isotope Cs-137 and reported that the sedimentation rate was 5-6 mm/year. John Taylor & Sons (1985) reported that the sedimentation rate was in the range of 0.1-0.4 mm/year. ONEP (2006) estimated that the sedimentation rate was about 0.04-0.19 mm/year (Figure 4). It can be seen that the rate analyzed by the isotope technique is 10 times higher than the rate obtained from rainfall-runoff relationship model. So, more detailed studies are still needed.

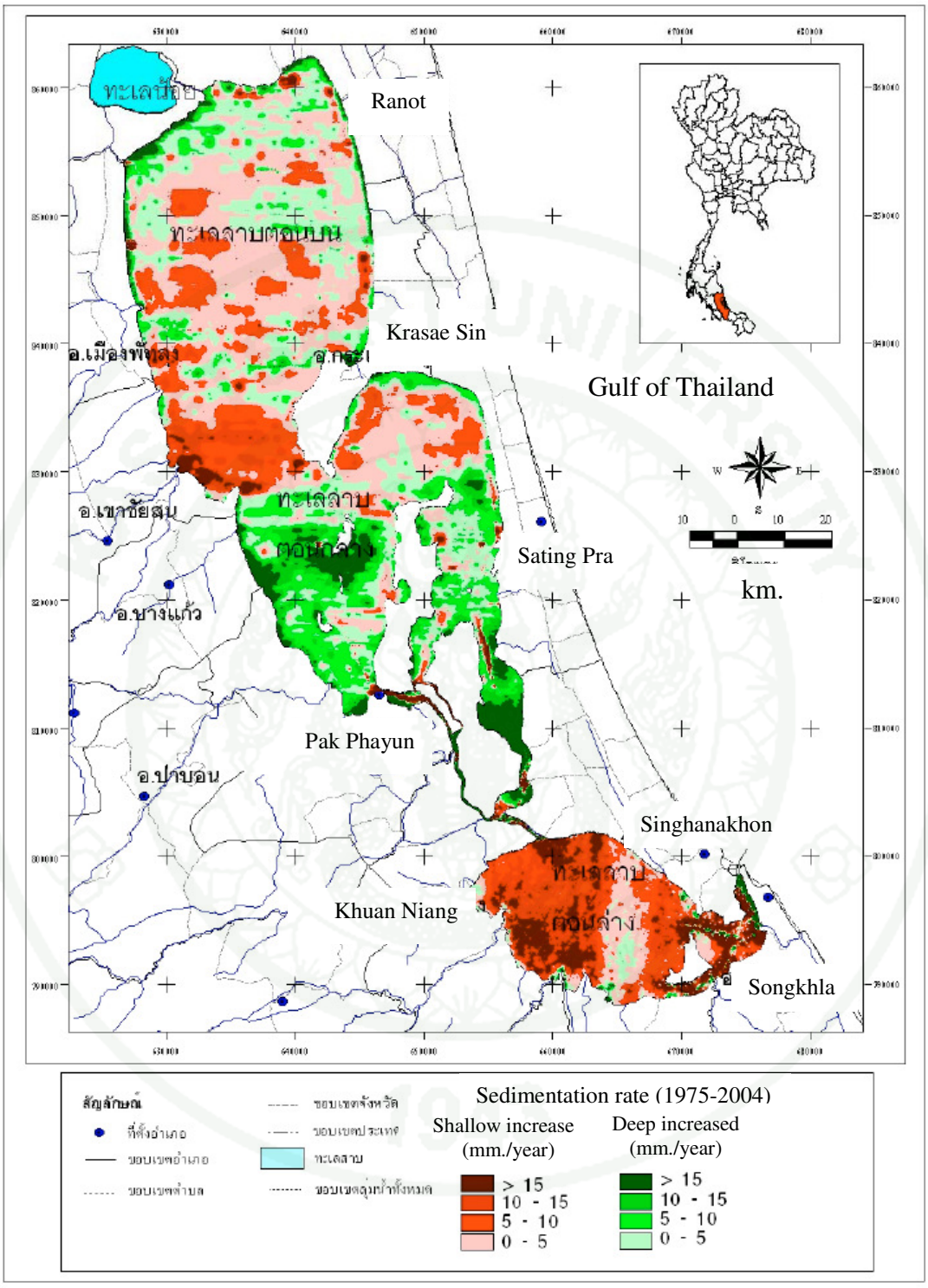


**Figure 4** Sedimentation rate in Songkhla Lake.

**Sources :** ONEP (2006).

## 2. Sediment Transport Process

Sediment transport in a water body affects its water uses. Continuous sediment deposition makes water body shallower and decrease in volume. On the contrary, if there exists a hydraulic structure which blocks sediment transport, deposition will occur at the front of that structure while erosion will occur at the back side. When eroded soil from the catchment area drains into water body, it will become suspended solid in water. The suspended solid of large size will settle to the bed near the coastline whereas small-size suspended solid may take several months for settling, so it can transport farther to downstream water body. When there exists strong storm which causes turbulent water current and waves, bedload sediment will resuspend to water column and becomes suspended sediment again. These complex natural phenomena make sediment dispersion calculation very difficult. However, in the past few decades, many researches have attempted to investigate various factors which affect sediment movement in water bodies and several models and empirical expressions have been proposed for sediment transport calculation.

### 2.1 Classification of sediment transport

Sediment transport can be classified into 2 major types, i.e., bedload transport and suspended load transport. For sediment transport in the sea, gravel (diameter up to 2 mm.) often transport along the bed, but for sandy (diameter between 0.06-2 mm.) will transport both along the bed and suspend. While the one that smaller than 0.06 mm. will often suspend with water current (Reeve *et al*., 2004).

If a round material is placed on horizontal surface, only small horizontal force will readily make it roll. However in the case of erodible boundary, the particles are not perfectly round and they lie on surface which is inherently rough and may not be horizontal, and particles are usually non-uniform in size. Thus, motion will occur only when the applied force is sufficient to overcome natural resistance to motion of the particle. At the interface, moving fluid will cause shear force, $\tau_c$, which implies that

proportionate force will be applied to the exposed surface of a particle by flowing water.

From many experiments, researchers found that if shear force was gradually increased, a point was reached at which particle movements could be observed at a number of small areas over the bed. A further small increase in $\tau_c$ was usually sufficient to generate a widespread sediment motion (of bedload type). This showed the "threshold of motion" and the associated critical shear stress ($\tau_{cr}$). After further increments in $\tau_c$, another point was reached at which the finer particles began to be swept up into the water current. This defines the inception of suspended load (Reeve *et al*., 2004).

## 2.2 Bedload sediment transport

### 2.2.1 Bed shear stress due to current flow

The general equation, total bed shear stress to depth mean velocity is given by

$$\tau_c = \rho C_D V_h^2 \tag{1}$$

where $\tau_c$ is total bed shear stress due to current flow;

$\rho$ is water density;

$C_D$ is coefficient of total shear stress;

$V_h$ is depth mean velocity.

The value of $C_D$ can be computed (Reeve *et al*., 2004) :

$$C_D = \left[ \frac{0.4}{1 + \ln(z_0 / h)} \right]^2 \tag{2}$$

where $z_0$ is roughness length;

$h$ is the depth of water.

Another important parameter involved in sediment movement along the bed of water body is 'shear velocity', $u^*$ which is related to shear stress as follows:

$$u^* = \sqrt{\tau_c / \rho} \tag{3}$$

For river flow, the skin friction bed shear stress can be simply related to the bed slope as follows :

$$\tau_c = \rho g h S_0 \tag{4}$$

where $\tau_c$ is total bed shear stress due to current flow;

$\rho$ is water density;

$g$ is acceleration due to gravity force;

$S_0$ is bed slope.

From equation (1) and (4), we obtain :

$$\rho C_D V_h^2 = \rho g h S_0 \tag{5}$$

From Manning equation, depth mean velocity is related to bed slope and hydraulic radius as follows:

$$V_h = \frac{1}{n} R^{2/3} S_0^{1/2} \tag{6}$$

where $n$ is Manning's coefficient;

$R$ is hydraulic radius.

By substituting $V_h$ into Eq. (5), we can find relationship between $C_D$ and Manning's coefficient ( $n$ ) as following

$$C_D = \frac{g n^2}{h^{1/2}} \tag{7}$$

However, under influence of tidal flow or ripple, bed shear stress is mainly dependent on bed roughness and ripple. The bed shear stress consists of 3 parts, i.e., (1) skin friction, 2) form drag due to dune and ripple of bedform, and (3) force from momentum transfer between sediment particles (Reeve *et al.*, 2004).

The skin friction shear stress can be calculated from an equation with the same format as Eq. (1) as follows :

$$\tau_s = \rho C_s V_h^2 \tag{8}$$

where $\tau_s$ is skin friction bed shear stress;

$C_s$ is coefficient of friction.

The value of $C_s$ can be computed from Eq. (2) by replacing $z_0$ with $z_{0S}$ which is calculated from:

$$z_{0S} = \frac{k_S}{30} \tag{9}$$

where $z_{0S}$ is skin friction roughness height;

$k_S$ Nikuradse roughness which is related to the size of sand as follows :

$$k_S = 2.5 D_{50} \tag{10}$$

in which $D_{50}$ is the mean sediment grain diameter of which the amount less than (or more than) $D_{50}$ is 50% by weight.

The water current-generated ripple will be formed on sandy bed with particle grain sizes up to about 0.8 mm. Their wavelength ($\lambda_r$) and wave height ($\Delta_r$) can be estimated form $\lambda_r = 1000\, D_{50}$ and $\Delta_r = \lambda_r / 7$, respectively. Typical average measured values are: $\lambda_r = 0.14$ m and $\Delta_r = 0.016$ m. Dunes and sand waves are much larger,

having dimensions ( $\lambda_s$, $\Delta_s$ ) which are dependent on both bed shear stress due to skin friction ( $\tau_{0s}$ ) and water depth ( $h$ ). Wavelengths are typically tens of meters and wave heights a few meters. Van Rijn (1984) has developed equation for calculation as follows:

$$\lambda_s = 7.3h \tag{11}$$

for $\tau_s < \tau_{cr}$ and $\tau_s > 26\tau_{cr}$ $\quad \Delta_s = 0$ (12)

for $\tau_{cr} < \tau_s < 26\tau_{cr}$ $\quad \Delta_s = 0.11h^{0.7} D_{50}^{0.3} \left(1 - e^{0.5T_s}\right)\left(25 - T_s\right)$ (13)

where $$T_s = \frac{\tau_s - \tau_{cr}}{\tau_{cr}} \tag{14}$$

in which $\tau_{cr}$ is critical shear stress that sediment begins to transport.

Bedform roughness height ( $z_{0F}$ ) is given by:

$$z_{0F} = \frac{a_r \Delta_s^2}{\lambda_s} \tag{15}$$

where $a_r$ is in the range 0.3-3 with a typical value of 1.0.

For sheet flow condition, further increase in $z_0$ arises due to turbulent momentum exchange between particles (as noted above). The bed shear stress can be calculated by replacing roughness length ( $z_0$ ) in Eq. (2) by $z_{0T}$ which is calculated from (Wilson, 1989):

$$z_{0T} = \frac{5\tau_s}{30g\left(\rho_s - \rho\right)} \tag{16}$$

Therefore, the total roughness length ( $z_{0C}$ ) can be calculated from:

$$z_{0C} = z_{0S} + z_{0F} + z_{0T} \tag{17}$$

The corresponding total drag coefficient can be calculated by replacing $z_0$ in Eq. (2) by $z_{0C}$. Then, the value of $C_D$ is used in Eq. (1) to estimate the total bed shear stress.

2.2.2 Bed shear stress due to waveforms

When there is wave at water surface, water will move in ellipse shape from surface to bed as shown in Figure 5. Sine wave at water surface can be substituted with following equation (Figure 6):

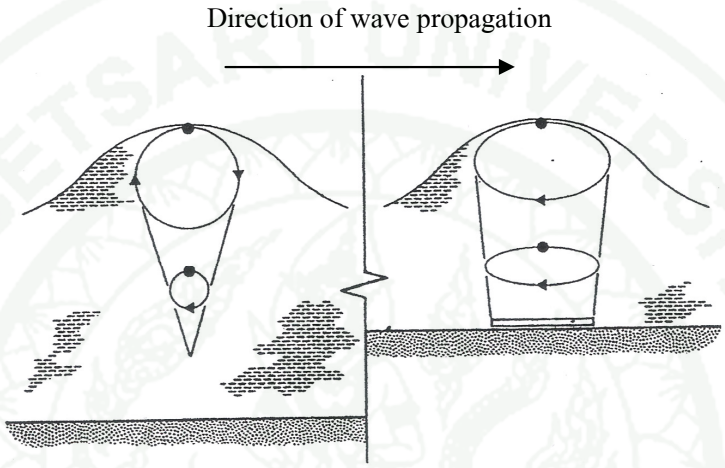


a) deep water circular orbits b) transitional water elliptical orbits

**Figure 5** Particle displacements for deep and transitional waves.

**Source** : Reeve *et al*. (2004).

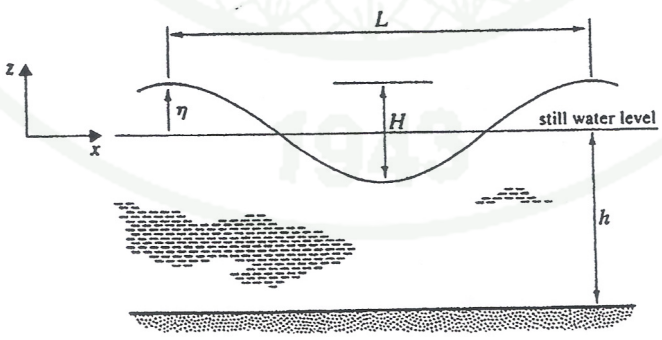


**Figure 6** Definition sketch for a sinusoidal wave.

**Source** : Reeve *et al*. (2004).

$$\eta = \frac{H}{2}\cos 2\pi\left(\frac{x}{L} - \frac{t}{\tau}\right) \quad (18)$$

where $\eta$ is water surface which varies with distances $x$ and time $t$, measureed from the mean level;

$H$ is wave height;

$L$ is wave length;

$\tau$ is time period.

Considering movement of a water particle at mean depth z measured from the mean level, it is found that it moves in circular orbits if water is deep (Figure 5a). However, for shallow water it will move in elliptical orbits (Figure 5b).

The velocity of a particle at a mean depth z below the still-water level can be determined from (Reeve *et al*., 2004):

$$u = \frac{\pi H}{T}\left[\frac{\cosh k(z+h)}{\sinh kh}\right]\cos\left\{2\pi\left(\frac{x}{L} - \frac{t}{T}\right)\right\} \quad (19)$$

where $k = \frac{2\pi}{L}$

At bed level, $z = -h$ so water velocity due to wave can be calculated from:

$$u_b = \frac{\pi H}{T.\sinh(kh)}\cos\left\{2\pi\left(\frac{x}{L} - \frac{t}{T}\right)\right\} \quad (20)$$

The bed shear stress due to the wave can be calculated from:

$$\tau_w = \frac{1}{2}\rho f_w u_b^{\,2} \quad (21)$$

where $\tau_w$ is bed shear stress due to waves;

$\rho$ is water density;

$u_b$ is water velocities at bed (due to wave);

$f_w$ is wave friction factor.

Soulsby (1999) proposed the formula to calculate $f_w$ as follows:

$$f_w = 1.39\left(\frac{A}{z_0}\right)^{-0.52} \tag{22}$$

where $z_0$ is roughness height. The parameter $A$ is wave orbital amplitude which can be calculated from:

$$A = \frac{u_b T}{2\pi} \tag{23}$$

In case of bed shear stress due to friction force, its value can be determined by replacing $z_0$ in Eq. (22) with $z_{0S}$ from Eq. (9)

$$f_{ws} = 1.39\left(\frac{A}{z_{os}}\right)^{-0.52} \tag{24}$$

where $z_{0S}$ is skin friction roughness length due to wave.

Substitute $f_w$ in Eq. (21) with $f_{ws}$, we obtain

$$\tau_{ws} = \frac{1}{2}\rho f_{ws} u_b^2 \tag{25}$$

where $\tau_{ws}$ is bed shear stress due to friction force from wave.

Waves generate ripples with wavelengths ($\lambda_r$) typically 1-2 times the wave orbital amplitude ($A = u_b T / 2\pi$) and wave height ($\Delta_r$) typically 0.1-0.2 times the wavelength. With the values of wavelengths ($\lambda_r$) and wave height ($\Delta_r$), the value of bed form roughness height ($z_{0f}$) can be calculated from Eq. (15) as the case of bed shear stress due to water current.

When add value of bed form roughness height ( $z_{0f}$ ) and skin friction roughness height that calculate from Eq. (9), we got the value of total roughness height result from wave $z_{0w}$ as follows:

$$z_{ow} = z_{0S} + z_{0f} \tag{26}$$

Substitute $z_0$ in Eq. (22) with $z_{0w}$, we can calculate $f_w$ and when substitute $f_w$ in Eq. (21), we can calculate total bed shear stress due to wave.

2.2.3 Bed shear stress due to currents and waves

When waves and currents occurred as the same time, they will affect to the total bed shear stress. However, the total bed shear stress cannot be equal summation of shear stress vector due to waves and currents. Soulsby (1995) has developed equation to calculate the mean of bed shear stress ( $\tau_m$ ) and maximum bed shear stress ( $\tau_{\max}$ ) due to currents and waves and currents as following:

$$\tau_m = \tau_c \left[ 1 + 1.2 \left( \frac{\tau_w}{\tau_c + \tau_w} \right)^{3.2} \right] \tag{27}$$

$$\tau_{\max} = \left[ \left( \tau_m + \tau_w \cos\phi \right)^2 + \left( \tau_w \sin\phi \right)^2 \right]^{\frac{1}{2}} \tag{28}$$

where $\tau_c$ is the bed shear stress due to current;

$\tau_w$ is the bed shear stress due to wave;

$\phi$ is the angle between the wave and the current.

2.2.4 Shields parameter

A close inspection of an erodible granular boundary would reval that some of the surface particles were more 'prominent' or 'exposed' (and therefore more prone to move) than others (Figure 7(b)). The external forces on this particle are due to the separated flow pattern (the lift and drag forces). Its resistance to motion is equal to $W'\tan\phi$ (where W' is the submerged self-weight $= \pi D^3 g(\rho_s - \rho)/6$ for a spherical particle with diameter *D*, density $\rho_s$ and $\phi$ is the angle of repose or internal friction). The number of prominent grains in a given surface area is related to the areal grain packing (area of grains/total area $A_p$). As the area of a particles is proportional to the square of the typical particle size ($D^2$), the number of exposed grains is a function of $A_p / D^2$. The shear stress at the interface, $\tau_0$, is equal to the sum of the horizontal forces acting on the individual particles, with the contribution due to prominent grains dominating; so the total force on each prominent grain in unit area may be expressed as:

$$F_D \propto \tau_0 \frac{D^2}{A_p} \tag{29}$$

where $F_D$ is the total force on each prominent grain in unit area;

$\tau_c$ is the total bed shear stress.

At the threshold of movement $\tau_0 = \tau_{CR}$, so

$$\tau_{CR} \frac{D^2}{A_p} \propto (\rho_s - \rho) g \frac{\pi D^3}{6} \tan\phi \tag{30}$$

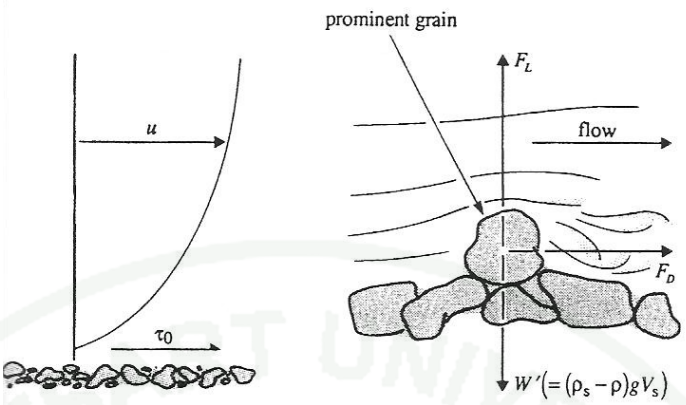


a) shear forces on granular bed. b) force on prominent grain.

**Figure 7** Fluid forces causing sediment movement.

**Source**: Reev *et al*. (2004).

This can be re-arranged to give a dimensionless relationship

$$\frac{\tau_{CR}}{(\rho_s-\rho)gD} \propto \frac{\pi A_p}{6}\tan\phi \tag{31}$$

The left-hand side of this Eq. (31) is the ratio of shear stress to gravity force which is known as Shields parameter ($\theta$), i.e.,

$$\theta = \frac{\tau}{(\rho_s-\rho)gD} \tag{32}$$

When $\tau_0 = \tau_{cr}$, this parameter becomes the critical Shields parameter, i.e.,

$$\theta_{cr} = \frac{\tau_{cr}}{(\rho_s-\rho)gD} \tag{33}$$

Shields (1936) showed that the critical shields parameter ($\theta_{cr}$) was related to a form of Reynolds number $R_e^* = \rho u^* D / \mu$, in which $u^*$ is shear velocity. Shields plotted the results of his experiments in the form of $\theta_{cr}$ against $R_e^*$, and proved that there was a well-defined band of results indicating the threshold of motion. The Shields threshold line has subsequently been expressed in a more convenient explicit form (Soulsby and Whitehouse, 1997), based on the use of a dimensionless particle size parameter, $D^*$, given by:

$$\theta_{cr} = \frac{0.3}{1+1.2D^*} + 0.055\left[1 - \exp\left(-0.02D^*\right)\right] \quad (34)$$

where $$D^* = \left[\frac{g(s-1)}{\nu^2}\right]^{\frac{1}{3}} D \quad (35)$$

in which $s = \rho_s / \rho$ and $\nu$ is kinematic viscosity of water = $\mu / \rho$

Eq. (33), (34) and (35) are used to determine the critical shear stress ($\tau_{cr}$) for any particle size ($D$) and specific gravity ($s$).

For a flat bed, if the bed skin friction shear stress ($\tau_{0s}$) is known, the value of Shields parameter can be calculated from:

$$\theta_s = \frac{\tau_{0s}}{g(\rho_s - \rho)D} \quad (36)$$

This can be used to determine the regime of sediment transport as follows (Reeve *et al*., 2004)

- If $\theta_s < \theta_{cr}$, no sediment transport will occur;
- If $\theta_{cr} \le \theta_s \le 0.8$, sediment transport will occur with ripples or dunes;
- If $\theta_s > 0.8$, sediment transport will occur as sheet flow with a flat bed;

- If $u_s^* \leq v_s$ there will not be any suspended sediment transport ($v_s$ is the particle fall speed)
- If $u_s^* > v_s$ suspended sediment transport will occur

For a sloping bed, the critical bed shear stress ($\tau_{\beta cr}$) may be more or less than the critical bed shear stress on a flat bed ($\tau_{cr}$). If the bed is inclined at an angle $\beta$, and the flow is at an angle $\psi$ to the upslope direction (Figure 8), the two shear stresses are related by the following equation (Reeve *et al*., 2004) :

$$\frac{\tau_{\beta CR}}{\tau_{CR}} = \frac{\cos\psi \sin\beta + \left(\cos^2\beta \tan^2\phi - \sin^2\psi \sin^2\beta\right)^{\frac{1}{2}}}{\tan\phi} \qquad (37)$$

where $\phi$ is internal friction or angle of repose of the sediment.

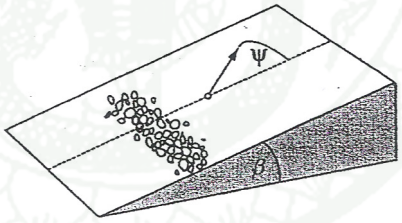


**Figure 8** Threshold of motion on a sloping bed.

**Source** : Soulsby (1997).

### 2.2.5 Bedload transport equations

To consider the influence of water current in many past decades, many researchers have tried to develop the equation to calculate the bedload sediment transport, mainly based on the results from Shields's work (1936). These equations often show the relationship between bedload sediment transport and Shields parameter as well as its critical value. A convenient way to express the resulting relationships is to use the dimensionless bedload transport rate factor ($\Phi$) given by:

$$\Phi = \frac{q_b}{\left[g(s-1)D^3\right]^{\frac{1}{2}}} \tag{38}$$

where $q_b$ is volumetric bedload transport rate per unit width, with units of $m^3/m/s$.

Bedload transport rate factor ($\Phi$) can be calculated from Shields parameter $\theta_s$ and $\theta_{cr}$, given by (Neilsen, 1992) :

$$\Phi = 12\theta_s^{\frac{1}{2}}\left(\theta_s - \theta_{cr}\right) \tag{39}$$

For deep area that has symmetric waves, the net bedload transport is zero. However, for steep waves in shallow water the wave motion becomes asymmetrical, in this case, the quantity of net bedload transport is not equal to zero. We can use Eq. (38) and (39) to determine the net transport by integration over a wave cycle.

Regarding influence of water current and wave, it is found that the wave provides a stirring mechanism of sediment and the water current helps build up sediment transport. To determine bedload sediment transport, integration over the wave cycle may be employed. However, due to non-liner interaction between wave and current, the instantaneous value of shear stress needs to be determined by the method given in topic 2.2.2.

## 2.3 Suspended sediment transport

### 2.3.1 Suspended sediment transport equation

Sediment is washed to river, lake and sea or sediment from any human activity such as mining, digging or filling around the coast. Some will flow with water current which is the movement in suspended condition before falling to bed. Sediment with small particle size may suspend in water for months. Even though, some also fall to bed. Under influence of water current and wave, some sediment may resuspended into water again, especially during storm with strong wind which causes wave and water current turbulent severely. Natural phenomenon like this is difficult to estimate for frequency to happen, route of storm, wind velocity and size of waves. So, it is very difficult to evaluate sediment transport rate. However, in normal weather that can estimate direction and velocity of water and size of wave, we can calculate the sediment transport rate in bedload and suspended conditions.

For suspended sediment transport, the basic equation which is used to calculate its dispersion is the mass balance equation. Three-dimensional mass balance equation in turbulent flow can be written as follows.

$$\frac{\partial c}{\partial t}+u\frac{\partial c}{\partial x}+v\frac{\partial c}{\partial y}+w\frac{\partial c}{\partial z}-\frac{\partial}{\partial x}\left(K_x\frac{\partial c}{\partial x}\right)-\frac{\partial}{\partial y}\left(K_y\frac{\partial c}{\partial y}\right)-\frac{\partial}{\partial z}\left(K_z\frac{\partial c}{\partial z}\right)-R+S=0 \quad (40)$$

where $c$ is suspended sediment concentration at *(x*, y, z) and at time *t*;

*u, v, w* are flow velocities at *(x*, y, z) in the *x*, *y*, and *z* directions respectively, at time *t*;

$K_x$, $K_y$ and $K_z$ are dispersion coefficients in the *x*, *y* and *z* directions, respectively;

*R* is suspended sediment generation rate per water volume and time;

*S* is suspended sediment decaying rate per water volume and time.

Each variable and parameter in mass balance equation for turbulent flow is not constant as in laminar flow. Therefore, Reynolds average is used which is a mean of variable and each parameter in defined time. This can reduce variation of variable and parameter.

The dispersion coefficient of suspended sediment dispersion is different from dispersion coefficient of soluble substance because the sediment particle is much larger than molecule of soluble substance. Thus, sediment dispersion will be likely from the variation of hydrodynamic dispersion than molecular diffusion. However, this dispersion coefficient can be approximated from model calibration with sediment concentrations obtained from field survey.

Term *R* in Eq. (40) is increasing rate of sediment particle in water such as occurring from adsorption on particle surface. This increases the weight of particle or the compound crystallization on suspended particle in water. Moreover, this also includes drainage of suspended sediment into water resources or some activities such as offshore mining or oil and natural gas extraction.

Term *S* in Eq. (40) is the rate of suspended particle decaying or separating from water per volume and time. This includes sedimentation and change by chemistry or biochemistry which causes change from suspended particle to other soluable compounds.

The sedimentation of suspended sediment in water is the main factor that makes it separate from water and change to bedload sediment. Consider small cube $\Delta x \Delta y \Delta z$ in water (Figure 9). The intensity of suspended particle at level z is equal to $c$ and at level $z + \Delta z$ is equal to $c + \frac{\partial c}{\partial z}\Delta z$. The rate that suspended sediment moves passing the surface area at level $z + \Delta z$ into the cube equals $v_s\left(c + \frac{\partial c}{\partial z}\Delta z\right)\Delta x \Delta y$, in which $v_s$ is terminal setting velocity of sediment while the rate that suspended

sediment moves passing the surface area at level $z$ out of the cube equals $v_s c\Delta x\Delta y$. Hence, the net rate of suspended sediment removed due to sedimentation equals:

$$v_s C\Delta x\Delta y - v_s\left\{C + \frac{\partial C}{\partial z}\Delta z\right\}\Delta x\Delta y = -v_s\frac{\partial C}{\partial z}\Delta x\Delta y\Delta z \qquad (41)$$

When divided by $\Delta x\Delta y\Delta z$, the suspended sediment particle separation rate per volume and time equals $-v_s\frac{\partial c}{\partial z}$

Then, the term $S$ in Eq. (40) can be separated into 2 parts as follows:

$$S = -v_s\frac{\partial C}{\partial z} + S_d \qquad (43)$$

where $-v_s\frac{\partial C}{\partial z}$ is rate of suspended particle decreasing due to sedimentation.

$S_d$ is rate of suspended particle decreasing due to other causes.

When substitute $S$ in Eq. (43) into mass balance equation (Eq. (40) and rearrange, we obtain suspended sediment transport equation as follows:

$$\frac{\partial c}{\partial t} + u\frac{\partial c}{\partial x} + v\frac{\partial c}{\partial y} + (w - v_s)\frac{\partial c}{\partial z} - \frac{\partial}{\partial x}\left(K_x\frac{\partial c}{\partial x}\right) - \frac{\partial}{\partial y}\left(K_y\frac{\partial c}{\partial y}\right) - \frac{\partial}{\partial z}\left(K_z\frac{\partial c}{\partial z}\right) - R + S_d = 0 \qquad (44)$$

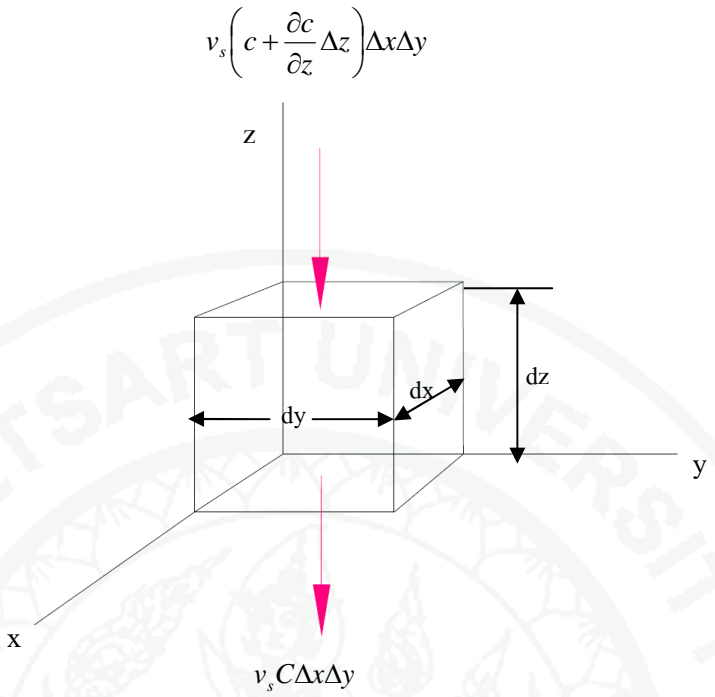


**Figure 9** Suspended sediment move pass small cube $\Delta x\Delta y\Delta z$.

Eq. (44) is a basic governing equation used to calculate suspended sediment transport in water. The quantity of suspended sediment is related to the quantity of bedload sediment. When suspended sediment settling to bed, it becomes bedload sediment and when bedload sediment resuspends into water column, with the influence of water current or surface wave, it becomes suspended sediment. Therefore, in calculating sediment transport it is necessary to calculate the bedload and suspended sediment transports at the same time.

### 2.3.2 Terminal settling velocity

Suspended sediment in water resources has density more than water density. While suspended sediment transport with water current, its will be settle to bed due to gravity forces. The forces consist of sediment weight, buoyancy force due to water pressure and drag force due to friction between sediment and water. The force due to sediment weight and buoyancy force can be calculated from:

$$F_I = g(\rho_s - \rho)V \quad (45)$$

where $F_I$ is sediment weight in water;

$\rho_s$ is sediment density;

$\rho$ is water density;

$g$ is gravitational acceleration;

$V$ is volume of sediment particle.

Drag force due to friction can be calculated from (Fair *et al*., 1968)

$$F_D = \frac{1}{2} C_D A_s \rho v_s^2 \quad (46)$$

when $F_D$ is drag force due to friction;

$C_D$ is drag coefficient;

$A_s$ is sediment profile in cross line with transport direction;

$v_s$ is settling velocity.

$C_D$ varies with flow condition which is indicated by the value of Reynolds number, $\boldsymbol{R}$ , of which:

$$\boldsymbol{R} = \frac{v_s D \rho}{\mu} \quad (47)$$

in which $\boldsymbol{R}$ is Reynolds number;

$D$ is sediment diameter;

$\mu$ is dynamic viscosity.

For sphere sediment, $C_D$ can be calculated from:

Stokes' law ($\boldsymbol{R} < 0.5$) : $$C_D = \frac{24}{\boldsymbol{R}} \quad (48)$$

Transition ($0.5 < \boldsymbol{R} < 2{,}000$) : $$C_D = \frac{24}{\boldsymbol{R}} + \frac{3}{\sqrt{\boldsymbol{R}}} + 0.34 \quad (49)$$

Newton's law ($2{,}000 < \boldsymbol{R}$): $$C_D = 0.4 \quad (50)$$

Terminal settling velocity, $v_s$, can be calculated by setting $F_I = F_D$ and then analyzing for $v_s$. The obtained result is:

$$v_s = \left\{ \frac{2g}{C_D A_s} \left( \frac{\rho_s - \rho}{\rho} \right) V \right\}^{1/2} \quad (51)$$

For sphere sediment which diameter $d$, volume $V = \frac{\pi D^3}{6}$ and $A_s = \frac{\pi D^2}{4}$, we obtain:

$$v_s = \left\{ \frac{4g}{3C_D} (s-1) D \right\}^{1/2} \quad (52)$$

where $s$ is specific gravity of sediment.

For Stokes' law ($\boldsymbol{R} < 0.5$) : terminal settling velocity, $v_s$, is calculated by:

$$v_s = \left( \frac{g(s-1)}{18\nu} \right) D^2 \quad (53)$$

where $\nu$ is kinematic viscosity of water.

For Newton's law (2,000 < ***R***): terminal settling velocity, $v_s$, is calculated by:

$$v_s = \left[3.3g(s-1)D\right]^{1/2} \tag{54}$$

2.3.3 Sediment resuspension

Disturbance due to water current or wave can make fine sediment resuspend to water column. If near-bed water velocity in a flume is gradually increased from rest, a range of conditions can be observed. First, particles remain on the bed at very low velocity. As velocity is increased, particles start to move close to the bottom, by a combination of rolling and saltating. For further increase, some small particles are "entrained" into suspension, i.e., they are resuspended (Garcia, 1999). Sediment resuspension in shallow, wind-exposed lades is caused by bottom shear stress associated with combination of near-bed wave orbital velocity, near-bed current velocity, and surface and internal seiches. Among them, the most important force to induce sediment resuspension in shallow water bodies is the bed shear stress exerted by surface wave (Luettich *et al*., 1990 ; Hawley *et al*., 2004 ; Mian and Yanful, 2004).

General formulas for determining sediment resuspension rate are empirical formula as follow;

1) For cohesive sediment : Metha *et al*., 1982 and Sanford and Maa, 2001 found that sediment resuspension rate can be calculated from;

$$E = \alpha\left[\frac{\tau_c - \tau_{cr}}{\tau_{cr}}\right]^m \qquad \text{for } \tau_c \geq \tau_{cr} \tag{55}$$

$$= 0 \qquad \text{for } \tau_c < \tau_{cr}$$

where E is sediment resuspension rate;

$\tau_c$ is total bed shear stress;

$\tau_{cr}$ is critical shear stress;

$\alpha$ is coefficient depending on bedload sediment characteristic;
= 0.8

$m$ is constant from calibration.
= 2 (Mian and Yanful, 2004)
= 1 (Hawley and Lesht (1992), Sanford and Halka (1993), Mei *et al*.,(1997), Sanford and Maa (2001), Gowland *et al*., (2007)

2. For non-cohesive sediment : Garcia and Parker (1991) considered sediment grain size that affected sediment resuspension rate as follow:

$$E = \frac{AZ_u^5}{1+\left(\frac{A}{0.3}\right)Z_u^5} \tag{56}$$

where

$$Z_u = \left(\frac{u*}{v_s}\right) f(\Re) \tag{57}$$

in which $E$ is sediment resuspension rate;

$A$ is constant = $1.3 \times 10^{-7}$;

$u*$ is shear velocity;

$v_s$ is terminal settling velocity;

$R$ is Reynolds number; determined from

$$R = \frac{1}{\nu}\sqrt{g\left(\frac{\rho_s}{\rho}-1\right)D^3} \tag{58}$$

where $\nu$ is kinematic viscosity;

$\rho_s$ is sediment density;

$\rho$ is water density;

$D$ is sediment diameter;

$g$ is gravitational acceleration.

For non-cohesive sediment which diameter ≥ 100 μm; Garcia and Parker (1993) use $f(R)$ as;

$$f(R) = 0.586\,R^{1.23} \qquad \text{for } 1 < R < 3 \qquad (59)$$

Chung *et al*., (2009) applied Garcia and Parker (1991) formula with fine sediment of which diameter ≤ 100 μm in Salton Sea. They found appropriate $f(R)$ for calculating sediment resuspension rate as follows;

$$f(R) = 0.076\,R^{3.75} \qquad \text{for } 0.4 < R < 1 \qquad (60)$$

3. The resuspension rate can be calculated by (Partheniades, 1965):

$$E_b = 0 \qquad \tau_b < \tau_{ce} \qquad (61)$$

$$E_b = M\left(\frac{\tau_b}{\tau_{ce}} - 1\right) \qquad \tau_b > \tau_{ce} \qquad (62)$$

where $\tau_b$ is bed shear stress (N/m$^2$);

$\tau_{ce}$ is critical shear stress for erosion (N/m$^2$);

$M$ is erodibility coefficient relating to sediment properties, the reported values are in the range of 0.00001-0.0004 kg/m$^2$/s (Van Rijn LC., 1989);

## 3. Finite Element Method

A mathematical model is developed to describe an engineering system. Some assumptions are made for simplification, finally a governing mathematical expression is developed to describe behavior of the system. This mathematical expression is usually in the form of differential equation. The finite element method is one of the most efficient numerical techniques which are used to fine the solutions of such equation. It requires division of the problem domain into many subdomains referred to as *elements*, therefore, the problem domain consists of many finite element patches.

### 3.1 Basic of the finite element method

The finite element method is a numerical approach by which differential equations are solved in an approximate manner. The major features of the finite element method can be concluded as follow (Huebner *et al*., 1995; Reddy, 2006; Lewis and Ward, 1991, Ottosen and Petersson, 1992).

1) The finite element method is an approximation approach that instead of seeking approximations that hold directly over a whole domain, the domain is divided into small simple regions, called element, for which a rather simple approximation is adopted. A variety of element shapes (such as line, triangle, quadrilateral, tetrahedral elements, etc.) may be used, and different element shapes can be employed in the same domain. Each element is viewed as an independent domain by itself.

2) Over each element, an approximation is performed to determine its individual property. For this means, the unknown variable within each element is represented by trial functions expressed in terms of interpolation functions and parameters at selective points, called nodes or nodal points. The algebraic relations among the nodal values of the solution are derived using the governing equations of the problem.

3) Having determined the property of all elements, a solution to the whole domain is replaced by an assemblage of these elements.

## 3.2 Advantages of the finite element method

Although there are several numerical methods that can be applied to the solution of this study, the finite element approach is used here because of the following advantages.

1) It is well-suited for problems involving complex geometries.

2) It can handle problems where field parameters vary with position within the domain.

3) It can be used for non-linear and/or time-varying problems.

4) Complex boundary conditions can be dealt with.

5) General computer programs to perform finite element calculations can be, and have been, developed.

6) Conventional numerical techniques can be used to solve the equations resulting from a finite element analysis.

7) Over several decades, the finite element method have been proved to be useful in the mathematical modeling and served as the computational basis of many computer-aided design packages.

## 3.3 Basic steps of the finite element method

The basic steps of the finite element method can be summarized as follow:

Step 1 : Discretize the continuum. The solution domain is divided into elements. Shape and type of every element within the domain are assigned in this step.

Step 2 : Select interpolation function. This step is to assign nodes to each element and then choose the interpolation function to represent the variation of the unknown variable over each element.

Step 3 : Find the element properties. Once the elements and their interpolation functions have been selected, the equations expressing the properties of the individual elements are then determined. Approaches used for this task will be discussed later. Note that, it is convenient for proceeding in other next steps to express the equations of each element in matrix form, termed element matrix.

Step 4 : Assemble the element properties. To find the properties of the whole solution domain, the element matrices are put together to form the matrix equations expressing the behavior of the entire system. A concept of this assemblage lies on the fact that the value of the variable at a node where elements are interconnected is the same for each element sharing that node (Huebner *et al*., 1995).

Step 5 : Apply boundary conditions. To obtain a unique solution of the problem, the derived system equations are then modified to satisfy the boundary conditions. At this step known values of the certain nodal variables are imposed into a set of the equations.

Step 6 : Solve the system of equations. The final step is the solution of a set of simultaneous equations, in matrix expressions, to find the unknown nodal values of the problem using matrix algebra.

## 3.4 Galerkin's Weighted Residual Method

In the finite element method, an approximation is required for the unknown function or parameter in deriving finite element equations. There are basically three different approaches for finding the approximate solution: the direct approach, the variational approach, and the weighted residual approach (Heubner, 1995). The third approach is found to be widely used to derive element properties.

The method of weighted residuals is an approximation approach by which unknown variables $\phi$ in the equation are replaced by approximation functions. This approximation function is often expressed as a series of $\phi_i$ and parameters $N_i$ (i = 1, 2,

…, n). Substitution of the approximation function into the governing equation results in an error function, called a residual, which is required to vanish in some average sense over the entire solution domain.

Suppose that the differential equation is expressed by

$$f(\phi) = 0 \tag{63}$$

When approximation function is substituted into Eq. (3), it turns out that

$$f(\phi_i, N_i) - f(\phi) = R = f(\phi_i, N_i) \tag{64}$$

where R is the residual or error that results from the approximation of $\phi$.

The method of weighted residuals seeks to determine the n parameters $\phi_i$ in such a way that the residual R over the entire solution domain is small. This is carried out by multiplying the residual R with weighting function $W_i$, taking the integral of this term over the entire domain, and setting to be zero. This can be expressed by

$$\int_{\Omega} RW_i d\Omega = 0 \tag{65}$$

The error distribution principle most often use to derive finite element equations is known as the Galerkin method (Heubner, 1995). By this method, the weighting functions $W_i$ are chosen to be the same as the parameter $N_i$ for i = 1, 2,…, n.

Suppose that the variable $\phi$ is replaced by a function $\tilde{\phi}$ expressed by

$$\tilde{\phi} = \sum_{i=1}^{n} N_i(\phi) a_i \tag{66}$$

The n equation of weighted residual integral are obtained as

$$\int_{\Omega} R N_i d\Omega = 0 \quad (i = 1, 2, \ldots, n) \qquad (67)$$

which can be solved for $\phi_i$ and the replace in Eq. (60) to determine function $\tilde{\phi}$ .

## 4. Related Researches

Estimation of sediment transport is very difficult because of physical factors such as water velocities, wind and wave. In order to estimate sediment transport accurately, all important factors should be considered. Several researches concerning sediment transport can be consolidated as follow;

### 4.1 Related researches on sediment transport model

Ribberink (1998) studied on bed-load transport for steady flows and unsteady oscillatory flows. The validity of a bed-load transport formula, based on the bed-shear concept of Meyer-Peter and Mueller, was investigated for steady unidirectional flows, oscillatory flows and oscillatory flows with superimposed net currents. The aim of the study was to develop a general bed-load transport concept for a wide range of flow and sediment conditions, as occurring in the marine coastal environment. The results of more than 150 laboratory experiments, including more than 75 recent bed-load transport measurements in oscillating water tunnels, were used for the study. For oscillatory flows, the time-dependent bed-load transport was treated in a 'quasi-steady' way and an equivalent Shields parameter was $\theta'_{eq}$ defined in order to enable a comparison between 'steady flow' and 'unsteady oscillatory flow' measurements. A good correlation was found between the non-dimensional transport parameter $\Phi_b$ and the non-dimensional excess bed-shear $\theta'_{eq} - \theta_c$ for different sets of oscillatory bed-load transport measurements. However, especially in the lower Shields regime, the oscillatory flow data show a clear deviation from an extensive set

of steady flow bed=load data. A good agreement between the (oscillatory floe and the steady flow) data sets could then be obtained by reducing the lower limit of the roughness height $k_s$ for oscillatory flows from the (steady flow) value $3\,D_{90}$ to $D_{50}$. Based on the obtained concept a generalized bed-load formula was derived for both flow types, including oscillatory flows and superimposed currents under an arbitrary angle. A verification, carried out with a set of (co-linear) oscillatory+superimposed current measurements, showed a good agreement between calculated and measured bed-load transport rates. Finally, the validity and limitations of the obtained bed-load model are discussed.

Velegrafis *et al*. (1999) studied on source, sink and resuspension of suspended particulate matter in the eastern English Channel. They were found seasonal observations on the nature and concentration of suspended particulate matter (SPM) are presented for a cross-section of the English Channel, between the Isel of Wight (UK) and Cotentin peninsula (France) i.e. the western boundary of the eastern English Channel. The highest concentrations of suspended material are found adjacent to the English coastline, whereas the offshore waters are associated with low concentrations. Seasonal variations in the concentration and nature of suspended material are identified, with highest concentrations in concentration and nature of suspended material are identified, with highest concentrations in winter. At this time, the suspended particles are characterized generally by peaked grain size spectra and an enrichment in coarse silt particles; in summer, the distributions are generally flat. The diatom communities found within the suspended matter indicate that material resuspended in the coastal zone and the estuarine environments is transported offshore. SPM fluxes (based upon the observed SPM concentrations and the output from a 2-D hydrodynamic model) from the western Channel through the Wight-Cotentin Section, ranged between 2 and $71 \times 10^6$ $ta^{-1}$ with a mean of around $20 \times 10^6 ta^{-1}$ over the observations (1994-1995). These fluxes are comparable to the order of magnitude and mean value reported as output though the Doves Strait. Therefore, it is possible that the eastern English Channel may be characterized as an area of fine-grained sediment 'bypass'. This interpretation is corroborated by: (a) the absence of

fine-grained sediment deposits over the area; and (b) correlation between the potential resuspension time of fine particles and the seabed sediment distribution.

Hakanson *et al*. (2004) studied on a dynamic compartment model to predict sedimentation and suspended particulate matter in coastal areas. They were found that a new dynamic mass-balance model for suspended particulate matter (SPM) and sedimentation in coastal areas handling all important fluxes of SPM to, from and within coastal areas, as such areas can be defined according to the topographical bottleneck method. The model is based on ordinary differential equations and the calculation time (d*t*) is one month to reflect seasonal variations. An important demand, related to the practical utility of the model, is that it should be driven by variables readily accessed from standard monitoring programs or maps. Added to the dynamic core model are several (static) empirical regressions for standard operational effect variables used in coastal management, such as the Secchi depth, the oxygen saturation in the deep water, and chlorophyll-a concentrations. The obligatory driving variables include four morphometric parameters (coastal area, section area, mean mean and mazimum depth), latitude (to predict surface water and deep water temperatures, stratification and mixing) and Secchi depth or SPM-concentrations in the sea outside the given coastal area. The model is based on four compartments: two water compartments (surface water and deep water;the separation between these two compartments is done not in the traditional manner from temperatures but form sedimentological criteria, as the water depth separating transportation areas from accumulation areas) and two sediment compartments (ET-areas, i.e., erosion and transportation areas where fine sediments are discontinuously being deposited, and A-areas, i.e., accumulation areas where fine sediments are continuously being deposited). The processes accounted for include inflow and outflow via surface and deep water, input from point sources, from primary production, form land uplift, sedimentation, burial (the transport of matter from surficial A-sediments to underlying sediments), resuspension, mizing and mineralization.The model has been validated with good results (the predictions of sedimentation are within the 95 % confidence limits of the empirical data used to validate the model) against data collected by sediment traps placed in 17 Baltic coastal areas of different character. The paper also

presents sensitivity and uncertainty tests of the model. The weakest part of the model condemns the sub-model to predict the ET-areas. Many of the structures in the model are general and have also been used with similar success for other types of aquatic systems (mainly lakes) and for other substances (mainly phosphoruss, radionuclides and metals). We also present approaches to indicate how the model could be modified for coastal areas other than those included in this study,e.g., for open coasts, estuaries or areas influenced by tidal variations.

Camenen and Larson (2004) studied on a general formula for non-cohesive bed load sediment transport. Based on the bed-shear concept of Meyer-peter and Muller, was developed and validated for steady flows, oscillatory flows, and combined steady and oscillatory flows. The bed load formula introduced in this study was examined using data from experimental and field measurements for a wide range of flows and sediment conditions, as occurring in river, coastal, and marine environments. More than 1000 steady and 500 oscillatory flow cases were used in the study. The relationship between the bed load transport and the total Shields parameter to the power 1.5 was first confirmed for the steady flows. An exponential factor to take in to account the effect of the critical Shields parameter was introduced. The proposed formula for the steady current was expanded and generalized to take into account the effects of oscillatory flows as well as oscillatory flows with a superimposed current at an arbitrary angle. The time-dependent bed load transport was treated in a 'quasi-steady' manner using the quadratic value of the instantaneous Shields parameter for the two half-periods of the wave (when the total instantaneous velocity $u$ is in the direction of the wave, $u > 0$, or in the opposite direction, $u < 0$). A good correlation was found between the bed load formula and the measurements for collinear oscillatory and steady flows when no phase-lag occurred in the experiments. However, a marked scatter was observed since the Shields parameter had to be estimated and not derived directly from measured data. Finally, the validity and limitations of the obtained bed load transport formula are discussed.

Heppner *et al*. (2005) studied on adding sediment transport to the integrated hydrology model (InHM) : Development and testing. They were found that the

addition of sediment transport algorithm to the comprehensive hydrologic-response model known as the Integrated Hydrology Model (InHM) is discussed. The first test of the sediment transport version of InHM is reported, using field data from a series of erosion experiments conducted by Gabet and Dunne [E. J. Gabet, T. Dunne, Sediment detachment by rain power, Water Resour Res 39 (2003) 1002]. The performance of the sediment transport component of InHM, in both calibration and validation phases, is judged to be successful, based upon quantitative statistical criteria. The ability to simulate sub-plot-scale interactions between surface water hydrology and rain-induced sediment transport with InHM is demonstrated. Sensitivity analysis reveals that the rainfall intensity exponent has a substantial impact on simulated sediment discharge.

Paphitis and Collins (2005) studied on sediment resuspension events within the (microtidal) coastal waters of Thermaikos Gulf, northern Greece. High-frequency flow, pressure and suspended sediment concentration (SSC) measurements are presented from the Paralia-Katerinis coastal area, in Thermaikos Gulf. The data were collected along a cross-shore transect, between the 6 and 12 m water depth contours. The relative importance of wave- and tidally-induced resuspension is examined. Resuspension events are shown to be dominated by wind-generated waves, especially under storm conditions. Some evidence is provided for tidal resuspension, but the overall impact of this process is minimal, compared to wave resuspension. Such resuspension, under storm conditions, increased the SSC levels in the waters of the nearshore zone to ~35 mg/l; this is a > 15-fold increase over the ambient level (1-2 mg/l) of turbidity.

You (2005) studied on fine sediment resuspension dynamics in a large semi-enclosed bay. A field study was conducted to investigate fine sediment resuspension dynamics in Moreton Bay, a large semi-enclosed bay, a large semi-enclosed bay situated in South East Queensland, Australia. One S4ADW current meter and three OBS sensors were used to collect the field data on tides, mean currents, waves and suspended sediment concentrations in a mean water depth of 6.1 m for about 3 weeks. Two small cleaning units were apecially designed to automatically clean the OBS

sensors several times every hour to avoid biological growth on the OBS sensors. Based on the collected field data, the main driving force for fine sediment resuspension is found to be the storm wind-waves generated locally in the Bay, not the tidal current or penetrated ocean swell. The critical wind-wave orbital velocity for sediment resuspension was determined to be $U_{rms}$ = 7 cm/s and the critical bed shear stress $\tau_{cr}$ = 0.083-0.095 Pa at this study site.

Warner *et al*. (2006) studied on development of a three-dimensional, regional, coupled wave, current, and sediment-transport model. They developed a three-dimensional numerical model that implements algorithms for sediment transport and evolution of bottom morphology in the coastal-circulation model Regional Ocean Modeling System (ROMS v3.0), and provides a two-way link between ROMS and the wave model Simulating Waves in the Nearshore (SWAN) via the Model-Coupling Toolkit. The coupled model is applicable for fluvial, estuarine, shelf, shelf, and nearshore (surfzone) environments. Three-dimensional radiation-stress terms have been included in the momentum equations, along with effects of a surface wave roller model. The sediment-transport algorithms are implemented for an unlimited number of user-defined non-cohesive sediment classes. Each class has attributes of grain diameter, density, settling velocity, critical stress threshold for erosion, and erodibility constant. Suspended-sediment transport in the water column is computed with the same advection-diffusion algorithm used for all passive tracers and an additional algorithm for vertical settling that is not limited by the CFL criterion. Erosion and deposition are based on flux formulations. A multi-level bed framework tracks the distribution of every size class in each layer and stores bulk properties including layer thickness, porosity, and mass, allowing computation of bed morphology and stratigraphy. Also tracked are bed-surface properties including active-layer thick, ripple geometry, and bed roughness. Bedload transport is calculated for mobile sediment classes in the top layer. Bottom-boundary layer submodels parameterize wave-current interactions that enhance bottom stresses and thereby facilitate sediment transport and increase bottom drag, creating a feedback to the circulation. The model

is demonstrated in a series of simple test cases and a realistic application in Massachusetts Bay.

Chao *et al*. (2008) studied on three-dimensional numerical modeling of cohesive sediment transport and wind wave impact in a shallow oxbow lake. It was observed that in some closed inland lakes sediment transport was dominated by wind-induced currents, and the sediment resuspension was primarily driven by wind-induced waves. This paper presents the development and application of a three-dimensional numerical model for simulating cohesive sediment transport in water bodies where wind-induced currents and waves are important. In the model, the bottom shear stresses induced by currents and waves were calculated, and the processes of resuspension (erosion), deposition, settling, etc. were considered. This model was first verified by a simple test case consisting of the movement of a non-conservative tracer in a prismatic channel with uniform flow, and the model output agreed well with the analytical solution. Then it was applied to Deed Hollow Lake, a small oxbow lake in Mississippi. Simulated sediment concentrations were compared with available field observations, with generally good agreement. The transport and resuspension processes of cohesive sediment due to wind-induced current and wave in Deep Hollow Lake were also discussed.

Li *et al.* (2008) studied on a two-phase numerical model for sediment transport prediction under oscillatory sheet flows. They predict sediment transport under oscilly sheet flow condition, especially for fine sand, is still a challenging research subject in coastal engineering. This paper describes a newly-developed numerical model based on two-phase theory with the use of a one-equation turbulence closure, and its applications in predicting fine sediment suspension in near-prototype oscillatory sheet flow conditions. Model results were compared with comprehensive laboratory measurements of flow velocity and sediment concentration under both symmetrical and asymmetrical oscillatory sheet flows from a large-scale water tunnel. Good agreements between the modelresults and measurements were achieved and the results demonstrated that the model is capable of reproducing detailed characteristics of sediment entrainment process in the sheet flow regime. The comparisons also

revealed the fact that the concentration peaks at flow reversal is associated with the strong vertical sediment transport flux in the pickup layer, which has been widely observed in many laboratory experiments. The effects of flow reversal events on total sediment transport were also discussed.

Liu and Huang (2009) studied on modeling sediment resuspension and transport induced by storm wind in Apalachicola Bay, USA. Based on the data analysis in this study, surface wind speed is highly correlated to the turbidity of water column, which result from sediment resuspension and transport in the Apalachicola Bay. In this paper, an application of a 3D sediment transport model to predict the wind-induced sediment transport in Apalachicola Bay is described. The sediment model is coupled with a 3D hydrodynamic module in the Environmental Fluid Dynamics Code (EFDC) model that provide information of estuarine circulation and salinity transport under normal temperature conditions. The hydrodynamic model was calibrated with field observations of water levels and salinity. The sediment transport model solves the transport equation with sources and sinks terms to describe sediment deposition and resuspension. The coupled hydrodynamic and sediment transport models were used to investigate wind-induced total suspended sediments (TSS) resuspension and transport in the bay. For the period June 1-July 30, 2005 two storm events with strong winds gave model results of TSS concentrations that compared well with the field observations. Model simulations reasonably reproduce the sudden increase of sediment concentrations during the storm events. Maximum sediment concentrations in the bay during the two storm events were 10 times or more than those in the pre-storm conditions. Spatial sediment transport from model simulations indicate active sediment resuspension and transport near areas of highly productive oyster beds. The model predictions of TSS and salinity can be used as inputs to an oyster dynamic model (Wang, H., Huang, W.,Harwell, M.,Edimiston, L.,Johnson, E., Hsieh, P., Milla, K., Christensen, J., Stewart, J., Liu, X., 2008. Modeling eastern oyster population dynamics in response to changing environment in Apalachicola Bay, Florida. Journal of Ecological Modeling 211, 77-89) to support the ecological study of oyster growth and mortality in the aquatic ecosystem of Apalachicola Bay.

The previous work that mentioned above mostly sediment transport model studied on only suspended sediment transport or bedload sediment transport. Mostly previous works were not emphasize sediment grain size and specific gravity which the important factor for sediment transport.

4.2 Related researches on sediment transport for Songkhla Lake

Sedimentation and siltation is an important problem in the Songkhla lake basin. Sediment transport has been investigated for more than ten years ago. The researchers attempted to determine sedimentation rate and sediment transport in the Songkhla Lake as follows:

In 1996, Chittrakarn *et al*. studied on the determination of sedimentation rate in Songkhla Lake Basin using isotope Cs-137. They found that althogether 50 bottom lake sediment cores were collected from the Songkhla Lake Basin. Sampling was performed using a sediment corer which has been designed and constructed at the Department of Physics, Faculty of Science. A GPS Trimble Navigator model Basic Plus was used for navigation to and positioning of the sampling locations. Each sediment core of 30-45 cm long was cut with 1 cm increment to prepare a number of specimen. Each was then measured the radioactivity of isotope $^{137}Cs$ using gamma-ray spectrometer. $^{137}Cs$ is an radioisotope produced from nuclear fission and found in the environment due to the fallout of fission products generated from explosion of atomic bombs in atmosphere in the past. The magnetic susceptibility of 850 specimens was measured using a high sensitivity Kappabridge. Plots of magnetic susceptibility-depth section of sediment cores show a variation of magnetic susceptibility with depths which is interpreted as a record of history of landuse in the catchment area of Songkhla Lake Basin. A closed correlation of susceptibility layers among sediment cores has been observed when using a Cs-137 age as a reference deposition age. Results of analysis of $^{137}Cs$ in all 50 sediment cores show that the average sedimentation rate of sediment in Songkhla Lake Basin determined from each is between 0.0-10.0 $\pm$ 0.2 mm/year, with an average value of 5.0 $\pm$ 0.2 mm/year.

Later in the year 1998, Chittrakarn *et al*. studied on the mathematical model for determination of sedimentation rate in Thalae Sap Songkhla. They found that the maximum stream flow velocity at Pak Prayoon straight is equal to 0.24 m/s and the suspended sediment concentration in Thale Luang is nearly constant with the range of 16-40 mg/L for all year round. In the middle of Songkhla Lake system, the suspended sediment concentration is strongly influenced by water salinity. The model works precisely for prediction the stream flow velocity and water level in the Songkhla Lake system. Results of modeling also indicated the tidal effect in the gulf of Thailand has a tiny influence to the circulation in Thale Luang. The stream flow velocity at the center of Thale Luang is equal to 0.02 m/s and 0.03 m/s in dry and wet seasons, respectively. Result of sediment transport (150 mg/L) modeling indicated that a noncohesive sediment such as sand and silt will deposit nearby the river estuarine within a radius of 0.5 km, while a cohesive sediment such as clay will diffuse and transport with a velocity of 1 km/day in Thale Luang and can escape to Thale Sap Songkhla. A result comparison between the oceanographic data analysis and modeling, and a study of sedimentation rate using isotope Cs-137 indicated that it is necessary to include other factors which may influence the sediment concentration in the modeling. Those factors are (1) summer strom in Thale Luang which occurs more frequently in a summer season, and (2) the effect due to the water salinity change of water in the middle Songkhla Lake.

Songrukkiat (2006) studied on evaluation of soil erosion in Songkhla Lake watershed by mathematical model. They use Morgan, Morgan and Finney 1984 (MMF) model and geographic information systems. The input data which were used in MMF model included factors of rain (R, Rn), soil (MS, BD, K), land use (C, A, RD, $E_t/E_0$) and geography. The results of soil loss from MMF model could be identified into 5 levels due to the degree of soil loss. Level 1 was very slight with 0-2 ton/rai/year, cover 4,425.001 rai or 92.25% of the total studied area. Level 2 was slight with 2-5 ton/rai/year, cover 210,729 rai or 4.39% of total studied area. Level 3 was moderate with 5-15 ton/rai/year, cover 147,919 rai or 3.08% of total studied area. Level 4 was severe with 15-20 ton/rai/year, cover 8,010 rai or 0.17% of total studied area. Level 5 was very severe with more than 20 ton/rai/year, cover 5,165 rai or

0.11% of total studied area. Moreover, the comparison between soil erosion by using MMF model and Universal Soil Loss Equation found that the area which were the same in the 5 levels of the degree of soil loss was 3,535,965 rai or 73.71% of total studied area. The amount of soil loss from the sub-watershed in the west of Songkhla Lake was 2,883,832 ton/year. The total amount of canal's suspended sediment that ended up to the west of Songkhla Lake was 247,248 ton/year. According to the overall study, it was found that the sediment delivery ratio of Songkhla Lake Watershed was 8.57%.

In 2006, ONEP calculated sedimentation rate in the SLB by using primary and secondary data from various sources as following:

(1) Water depth map in the Songkhla Lake (Upper Songkhla Lake, Middle Songkhla Lake and Lower Songkhla Lake) prepared by Marine Department in 1975.

(2) Water depth map in the Songkhla Lake (only Lower Songkhla Lake) prepared by Marine Department in 2002.

(3) Water depth map in the Songkhla Lake (only Upper Songkhla Lake and Middle Songkhla Lake) prepared by ONEP in 2004.

In this study, bedload sediment will increase $3.5x10^7$ $m^3$ and surface area of the lake reduced to 163 sq.km. Sedimentation rate was 8.12 mm./year. The result from this studied is similar to Isotope technique studied and it is possible when compares the result with sediment deposition rate in the Gulf of Thailand (0.85-2.98 mm/year).

From the previous works that mentioned above, it can be seen that in some previous works, researchers attempted to present many models for predicting the sedimentation rate in the lake. Chittrakarn *et al* (1996) determined the sedimentation rate in the lake by using isotope Cs-137 and reported that the sedimentation rate was 5-6 mm/year. Songkhla Lake Basin Study by John Talor & Sons (VKI, 1985) reported that the sedimentation rate was in the range of 0.1-0.4 mm/year. ONEP (2006) estimated that the sedimentation rate was about 0.04-0.19 mm/year. However, the accurate prediction of sediment transport is still not clear.

The rate from isotope technique is 10 times higer than the rate from rainfall-runoff relationship model.

Therefore, we attempted to develop appropriate sediment transport model by consider sediment grain size and specific gravity because they are important parameters which affect sediment settling velocity in water column and also affect the rate of resuspension of bedload sediment from the bottom. In addition, we develop a sediment transport model with consisting of suspended sediment transport and bedload transport model which are linked to each other.

# MATERIALS AND METHODS

Materials and methods for develop sediment transport model are follow:

## Materials

Materials are separate into 2 types i.e.

1) Materials for experiments;

1.1) Suspended solids analysis, is required, and in addition :

1.1.1 Glass-fiber filter paper.

1.1.2 Filtration apparatus : One of the following, suitable for the filter paper selected.

1.1.3 Membrane filter funnel.

1.1.4 Gooch crucible, 25-mL to 40 mL capacity, with Gooch crucible.

1.1.5 Filtration apparatus with reservoir and coarse (40- to 60-μm) fritted disk as filter support.

1.1.6 Suction flask, of sufficient capacity for sample size selected.

1.1.7 Drying oven, for operation at 180+2$^{o}$C.

1.1.8 Desiccator, provided with a desiccant a color indicator of moisture concentration or an instrumental indicator.

1.2) Particle size analysis : Particle size analyzer, LS 13320 model. Beckman Coulter Inc., range 0.04 to 2000 μm.

2) Materials for computer procedure.

2.1) Personal computer (PC) or Notebook computer, Intel® Core(TM) 2Duo CPU P7350 @ 2.0 GHz, 320 80 GB, RAM 4.00 GB, 32-bit Operation System.

2.2) Software Microsoft Window XP.

2.3) Software Program MATLAB 7.6.0.

2.4) Hydrodynamic data of the Songkhla Lake including flow velocity and water depth.

2.5) Printer.

## Methods

1. Experiments methods

1.1 Collect information and data of the study area, the Songkhla lake basin. Conduct water sampling for total suspended solids and particle size analysis.

1.2 Analyze for the total suspended solids (TSS) following the Standard Methods for the Examination of Water and Wastewater (APHA, WEF, AWWA, 1995).

1.3 Analyze for particle size distribution by using Particle size Analyzer, LS 13320 model. Beckman Coulter Inc., range 0.04 to 2000 μm.

2. Computer procedures

2.1 Determine the basic equations of sediment transport. In this study, the governing equations used for developing the sediment transport model are three-dimensional mass balance equation for suspended sediment transport model and two-dimensional mass balance equation for bedload sediment transport model.

2.2 Formulating sediment transport models by using finite element method with Galerkin's weighted residual technique.

2.3 Select element configurations for the Songkhla lake. The hexahedral elements are used for the three-dimensional suspended sediment transport model and the bilinear quadrilateral elements are used for the two-dimensional bedload transport model. The total area of 1,042 $km^2$ of Songkhla lake is divided into 414 hexahedral elements with 880 nodal points. The bottom boundary of the lake projected on a horizontal plane is divided into 138 quadrilateral elements with 220 nodal points.

2.4 Assign boundary condition and initial condition. For suspended sediment concentrations at the beginning of simution time are the data from field samplings and analyses. For bedload sediment at the beginning simulation time, the concentrations are set to zero.

2.5 MATLAB 7.6.0 is used to write computer program.

2.6 The developed models are verified by applying to a simple problem, dispersion in a uniform channel, and comparing the results with analytical solutions, to test their accuracy and reliability

2.7 Apply the developed sediment transport models to the Songkhla lake.

# RESULTS AND DISCUSSION

## 1. Concept of Model Development

Sediment transport in a water body can be classified as bedload sediment transport and suspended sediment transport. Factors on sediment characteristics which are size, shape, specific gravity, and bed conditions such as roughness and ripple affect sediment transport pattern. However, the effects of these factors on bedload and suspended sediment transport rates are different. Therefore, we have to calculate bedload and suspended sediment transport rates separately. Anyhow, relationship between bedload and suspended sediment transports must be considered. The settling rate of suspended sediment to the bed is the sink term of the suspended sediment transport model while it is the source term of the bedload transport model. On the other hand, the rate of resuspension of bedload sediment caused by currents and waves is the sink term of the bedload transport model while it is the source term of the suspended sediment transport model.

Terminal setting velocity of sediment affects suspended sediment distribution in water and sediment concentration will vary with water depth. It is necessary to use three dimensional model to determine suspended sediment transport in the Songkhla lake. Regarding to the character of bed in water resources, they are usually not smooth and water depth varies depending on geology, velocity and direction of water current. With this condition, the finite difference method, which rectangular grids is not suitable. Therefore, the finite element method which is suitable for natural water bodies with irregular boundaries, is used in this study.

Here, we choose to use the finite element model to determine sediment transport by separating into two parts. The first one is the three dimensional model for determining suspended sediment transport (SST) and the second one is the two dimensional model for determining bedload sediment transport (BLT). The study area

of bedload sediment transport is the bottom boundary of the suspended sediment transport model projected onto a horizontal plane as shown in Figure 10.

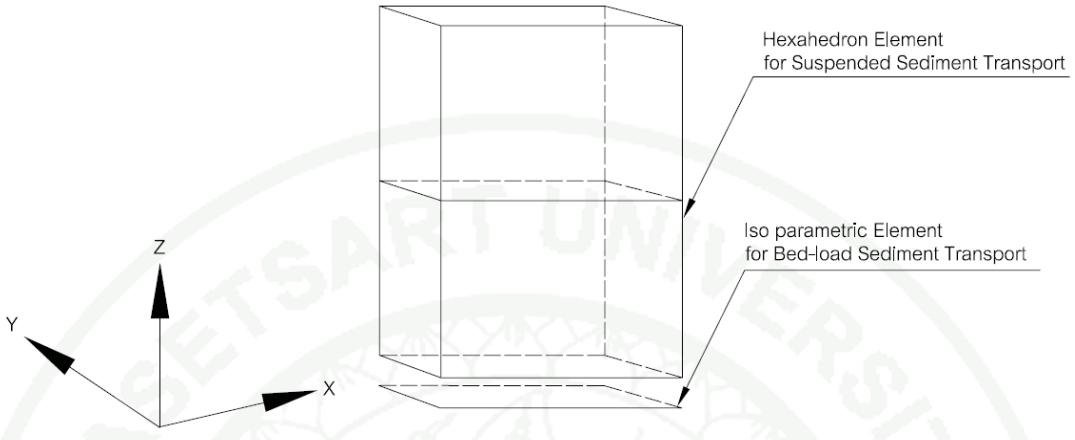


**Figure 10** Types of elements used in the developed sediment transport model.

## 2. Model Formulation

The formulated sediment transport model consists of 2 interrelated models, i.e. 1) suspended sediment transport (SST) model and 2) bedload sediment transport (BLT) model. These two models must be run together using the rate of sediment settling as a sink term of the SST model and as a source term of the BLT model. On the other hand, the rate of bedload resuspension is considered as a sink term of the BLT model and as a source term of the SST model.

As previously mentioned, the important factors affecting sediment transport are sediment settling velocity and resuspension rate, both of which depend on sediment grain size ($D$) and specific gravity ($s$). In this study, inflow sediment loads from various sources are divided into three groups based on their grain size ($D$) and specific gravity ($s$). The developed models are applied to estimate the transport of sediment in each group. Then, the total suspended sediment concentration and bedload sediment are computed from

$$c_{s,total}(x,y,z,t) = \sum_j \sum_k c^{jk}(x,y,z,t) \tag{68}$$

and

$$c_{b,total}(x, y, t) = \sum_j \sum_k c_b^{jk}(x, y, t) \quad (69)$$

in which

$c_{s,total}(x,y,z,t)$ is total suspended sediment concentration at $(x,y,z)$ at time $t$;

$c^{jk}(x,y,z,t)$ is concentration of suspended sediment with grain size $D_j$ and specific gravity $s_k$ at $(x,y,z)$ at time $t$;

$c_{b,total}(x,y,z,t)$ is the amount of bedload sediment at $(x,y)$ at time $t$;

$c_b^{jk}(x, y, t)$ is amount of bedload sediment with grain size $D_j$ and specific gravity $s_k$ at $(x,y)$ at time $t$.

2.1 Suspended sediment transport model

2.1.1 Suspended sediment transport equation

The basic equation to calculate three dimensional suspended sediment transport model i.e. suspended sediment mass balance equation (Eq. (40)). One of the main factor that affects suspended sediment transport is terminal settling velocity ($v_s$). It is known that suspended sediment having low terminal settling velocity will transport farther than suspended sediment having high terminal settling velocity.

As mentioned above, terminal settling velocity ($v_s$) depends on sediment grain size $D_j$ and specific gravity $s_k$, so sediment transport simulation using the mean values of sediment grain size, $D_{50}$, and specific gravity, $s_k$, cannot provide accurate results. Therefore, in this study the sediment particles are divided into groups based on their size and specific gravity by using data on grain size distribution obtained from field sampling and analysis. The sediment load discharged into the water body is also divided into the corresponding groups taken into consideration their percentages in the inflow sediment.

From this concept, we can adjust suspended sediment mass balance equation to the three-dimensional mass transport equation for sediment with grain size $D_j$ and specific gravity $s_k$ as follows;

$$\frac{\partial c^{jk}}{\partial t}+u\frac{\partial c^{jk}}{\partial x}+v\frac{\partial c^{jk}}{\partial y}+\left(w-v_s^{jk}\right)\frac{\partial c^{jk}}{\partial z}-\frac{\partial}{\partial x}\left(K_x\frac{\partial c^{jk}}{\partial x}\right)-\frac{\partial}{\partial y}\left(K_y\frac{\partial c^{jk}}{\partial y}\right)-\frac{\partial}{\partial z}\left(K_z\frac{\partial c^{jk}}{\partial z}\right)-R^{jk}+S_d^{jk}=0 \tag{70}$$

where

$c^{jk}$ is suspended sediment concentration at $(x,y,z)$ at time $t$;

$u, v, w$ are flow velocities at $(x,y,z)$ in the $x$, $y$ and $z$ directions respectively at time $t$;

$v_s^{jk}$ is terminal settling velocity of sediment with grain size $D_j$ and specific gravity $s_k$;

$K_x, K_y, K_z$ are dispersion coefficients in the $x$, $y$ and $z$ directions, respectively;

$R^{jk}$ is sources of suspended sediment;

$S_d^{jk}$ is suspended particles decaying rate.

2.1.2 Use of the finite element method and Galerkin's weighted residual technique

In the weighted residual method the variable $c^{jk}$ in the mass balance equation is replaced by an approximate function $\hat{c}^{jk}$ which is written in terms of the nodal concentrations as follows:

$$\hat{c}^{jk}=\sum_{i=1}^{n}N_iC_i^{jk}=\boldsymbol{N}^{\boldsymbol{T}}\boldsymbol{C}^{jk} \tag{71}$$

The error or residual which occurs from this approximation is multiplied with a weighting function $w_f$ and the integral of the product over the whole study domain is set to zero. This results in the following weighted residual equation;

$$\iiint_{\Omega} w_f \left\{ \frac{\partial \hat{c}^{jk}}{\partial t} + u\frac{\partial \hat{c}^{jk}}{\partial x} + v\frac{\partial \hat{c}^{jk}}{\partial y} + \left(w - v_s^{jk}\right)\frac{\partial \hat{c}^{jk}}{\partial z} - \frac{\partial}{\partial x}\left(K_x \frac{\partial \hat{c}^{jk}}{\partial x}\right) - \frac{\partial}{\partial y}\left(K_y \frac{\partial \hat{c}^{jk}}{\partial y}\right) - \frac{\partial}{\partial z}\left(K_z \frac{\partial \hat{c}^{jk}}{\partial z}\right) - R^{jk} + S_d^{jk} \right\} dV = 0 \quad (72)$$

From the integration by parts principle, Eq. (72) can be adjusted as;

$$\iiint_{\Omega} w_f \left\{ \frac{\partial \hat{c}^{jk}}{\partial t} + u\frac{\partial \hat{c}^{jk}}{\partial x} + v\frac{\partial \hat{c}^{jk}}{\partial y} + \left(w - v_s^{jk}\right)\frac{\partial \hat{c}^{jk}}{\partial z} - R^{jk} + S_d^{jk} \right\} dV$$

$$+ \iiint_{\Omega} \left\{ K_x \frac{\partial w_f}{\partial x}\frac{\partial \hat{c}^{jk}}{\partial x} + K_y \frac{\partial w_f}{\partial y}\frac{\partial \hat{c}^{jk}}{\partial y} + K_z \frac{\partial w_f}{\partial z}\frac{\partial \hat{c}^{jk}}{\partial z} \right\} dV$$

$$- \iiint_{\Omega} \left\{ \frac{\partial}{\partial x}\left( w_f K_x \frac{\partial \hat{c}^{jk}}{\partial x} \right) + \frac{\partial}{\partial y}\left( w_f K_y \frac{\partial \hat{c}^{jk}}{\partial y} \right) + \frac{\partial}{\partial z}\left( w_f K_z \frac{\partial \hat{c}^{jk}}{\partial z} \right) \right\} dV = 0 \quad (73)$$

By using Divergence Theorem, the last volume integral in Eq.(73) can be replaced by surface integral as follows:

$$\iiint_{\Omega} \left\{ \frac{\partial}{\partial x}\left( w_f K_x \frac{\partial \hat{c}^{jk}}{\partial x} \right) + \frac{\partial}{\partial y}\left( w_f K_y \frac{\partial \hat{c}^{jk}}{\partial y} \right) + \frac{\partial}{\partial z}\left( w_f K_z \frac{\partial \hat{c}^{jk}}{\partial z} \right) \right\} dV$$

$$= \iint_{S} w_f \left\{ \left( K_x \frac{\partial \hat{c}^{jk}}{\partial x} \right)\bar{i} + \left( K_y \frac{\partial \hat{c}^{jk}}{\partial y} \right)\bar{j} + \left( K_z \frac{\partial \hat{c}^{jk}}{\partial z} \right)\bar{k} \right\} . \boldsymbol{n}\, dA \quad (74)$$

in which

$\bar{i}, \bar{j}, \bar{k}$ are unit vectors in the *x, y* and *z* directions, respectively;

***n*** is unit vector normal to the domain boundary with direction outward from the study domain.

The term $\left\{ \left( K_x \frac{\partial \hat{c}^{jk}}{\partial x} \right)\bar{i} + \left( K_y \frac{\partial \hat{c}^{jk}}{\partial y} \right)\bar{j} + \left( K_z \frac{\partial \hat{c}^{jk}}{\partial z} \right)\bar{k} \right\} . \boldsymbol{n}$ can be replaced by the sediment influx rate per unit area of the boundary. Then, Eq.(74) can be written as:

$$\iint_S w_f \left\{ \left( K_x \frac{\partial \hat{c}^{jk}}{\partial x} \right) \bar{i} + \left( K_y \frac{\partial \hat{c}^{jk}}{\partial y} \right) \bar{j} + \left( K_z \frac{\partial \hat{c}^{jk}}{\partial z} \right) \bar{k} \right\} . \boldsymbol{n} dA = \iint_S w_f q_n^{jk} dA \qquad (75)$$

where $q_n^{jk}$ is the influx rate per unit area of sediment with grain size $D_j$ and specific gravity $s_k$.

Therefore, the Eq. (73) can be written as

$$\iiint_\Omega w_f \left\{ \frac{\partial \hat{c}^{jk}}{\partial t} + u \frac{\partial \hat{c}^{jk}}{\partial x} + v \frac{\partial \hat{c}^{jk}}{\partial y} + \left( w - v_s^{jk} \right) \frac{\partial \hat{c}^{jk}}{\partial z} - R^{jk} + S_d^{jk} \right\} dV$$

$$+ \iiint_\Omega \left( K_x \frac{\partial w_f}{\partial x} \frac{\partial \hat{c}^{jk}}{\partial x} \right) + \left( K_y \frac{\partial w_f}{\partial y} \frac{\partial \hat{c}^{jk}}{\partial y} \right) + \left( K_z \frac{\partial w_f}{\partial z} \frac{\partial \hat{c}^{jk}}{\partial z} \right) dV - \iint_S w_f q_n^{jk} dA = 0 \qquad (76)$$

For the suspended sediment transport model, boundary area can be classified into three types as

*1) Water Surface area ($S_w$)* is part that is not touch bed and no sediment influx through this boundary; $q_n = 0$

*2) Bed area ($S_b$)* is bottom boundary of water resources that has sediment deposition. Besides influence from water current and surface wave, causes some sediment resuspension. Sediment resuspension rate in *jk* group per area unit is equal to $q_{br}^{jk}$ due to bedload sediment concentration that deposits for long time is not used to be boundary condition, but we consider sediment resuspension rate instead. In addition also consider that bedload boundary, terminal setting velocity of sediment remain the same. Sediment setting velocity is important factor that affect to suspend sediment transport away from water sources. Therefore, to set bedload boundary area should have some slight distance from the bed with setting velocity of sediment does not change. However, Soulsby (1997) and Reeve *et al*. (2004) reported distance from

bed that affect to terminal setting velocity rate of sediment are only not too many centimeters.

*3) Coastal area and river profile that connect to water sources ($S_s$)* : Boundary area around coastal. It is the part that sediment drains into water sources. Some suspend sediment is transported with water current that flows in the canals connecting to the studied area and some sediment drains into the water source along coastines. In addition, some sediment occurs from bank erosion. The sediment flow rate per unit of boundary area is equal to $q_s^{jk}$ which is evaluated from field survey.

From boundary area classification mentioned above, Eq. (76) can be adjusted to;

$$\iiint_{\Omega} w_f \left\{ \frac{\partial \hat{c}^{jk}}{\partial t} + u\frac{\partial \hat{c}^{jk}}{\partial x} + v\frac{\partial \hat{c}^{jk}}{\partial y} + \left(w - v_s^{jk}\right)\frac{\partial \hat{c}^{jk}}{\partial z} - R^{jk} + S_d^{jk} \right\} dV$$

$$+ \iiint_{\Omega} \left\{ K_x \frac{\partial w_f}{\partial x}\frac{\partial \hat{c}^{jk}}{\partial x} + K_y \frac{\partial w_f}{\partial y}\frac{\partial \hat{c}^{jk}}{\partial y} + K_z \frac{\partial w_f}{\partial z}\frac{\partial \hat{c}^{jk}}{\partial z} \right\} dV - \iint_{Sb} w_f q_r^{jk} dA - \iint_{Ss} w_f q_s^{jk} dA = 0 \qquad (77)$$

In the Galerkin's method, the shape functions or interpolation functions $N_i$ ($i$ = 1,2,..n) are used as weighting function $w_f$. This results in the following weighted residual equation:

$$\iiint_{\Omega} N_i \left\{ \frac{\partial \hat{c}^{jk}}{\partial t} + u\frac{\partial \hat{c}^{jk}}{\partial x} + v\frac{\partial \hat{c}^{jk}}{\partial y} + \left(w - v_s^{jk}\right)\frac{\partial \hat{c}^{jk}}{\partial z} - R^{jk} + S^{jk} \right\} dV$$

$$+ \iiint_{\Omega} \left\{ K_x \frac{\partial N_i}{\partial x}\frac{\partial \hat{c}^{jk}}{\partial x} + K_y \frac{\partial N_i}{\partial y}\frac{\partial \hat{c}^{jk}}{\partial y} + K_z \frac{\partial N_i}{\partial z}\frac{\partial \hat{c}^{jk}}{\partial z} \right\} dV$$

$$- \iint_{Sb} N_i q_b^{jk} dA - \iint_{Ss} N_i q_s^{jk} dA = 0 \qquad (i=1,2,..n) \qquad (78)$$

Which can be written in matrix form as:

$$\iiint_{\Omega} \boldsymbol{N}\left\{\frac{\partial \hat{c}^{jk}}{\partial t}+u\frac{\partial \hat{c}^{jk}}{\partial x}+v\frac{\partial \hat{c}^{jk}}{\partial y}+\left(w-v_s^{jk}\right)\frac{\partial \hat{c}^{jk}}{\partial z}-R^{jk}+S_d^{jk}\right\}dV$$
$$+\iiint_{\Omega}\left\{K_x\frac{\partial \boldsymbol{N}}{\partial x}\frac{\partial \hat{c}^{jk}}{\partial x}+K_y\frac{\partial \boldsymbol{N}}{\partial y}\frac{\partial \hat{c}^{jk}}{\partial y}+K_z\frac{\partial \boldsymbol{N}}{\partial z}\frac{\partial \hat{c}^{jk}}{\partial z}\right\}dV$$
$$-\iint_{Sb} q_r^{jk}\boldsymbol{N}dA-\iint_{Ss} q_s^{jk}\boldsymbol{N}dA=\boldsymbol{0} \qquad (79)$$

Besides function $\hat{c}^{jk}$, flow velocities *u, v, w* can be written in terms of their nodal values in the similar form. After substituting into Eq. (79), we obtain:

$$u=\sum_{i=1}^{n} N_i U_i=\boldsymbol{N^T U} \qquad (80)$$

$$v=\sum_{i=1}^{n} N_i V_i=\boldsymbol{N^T V} \qquad (81)$$

$$w=\sum_{i=1}^{n} N_i W_i=\boldsymbol{N^T W} \qquad (82)$$

where $U_i, V_i, W_i$ are the flow velocity in x, y, and z directions, respectively at node *i*;

$\boldsymbol{U}, \boldsymbol{V}, \boldsymbol{W}$ are the matrices of $U_i, V_i, W_i$.

When put into Eq. (79), we got weighting residual equation as following:

$$\iiint_{\Omega} \boldsymbol{N}\left\{\frac{\partial\left(\boldsymbol{N^T C}^{jk}\right)}{\partial t}+\boldsymbol{N^T U}\frac{\partial\left(\boldsymbol{N^T C}^{jk}\right)}{\partial x}+\boldsymbol{N^T V}\frac{\partial\left(\boldsymbol{N^T C}^{jk}\right)}{\partial y}+\boldsymbol{N^T W}\frac{\partial\left(\boldsymbol{N^T C}^{\mathbf{jk}}\right)}{\partial z}-v_s^{jk}\frac{\partial\left(\boldsymbol{N^T C}^{jk}\right)}{\partial z}-R^{jk}+S_d^{jk}\right\}dV$$
$$+\iiint_{\Omega}\left\{K_x\frac{\partial \boldsymbol{N}}{\partial x}\frac{\partial\left(\boldsymbol{N^T C}^{jk}\right)}{\partial x}+K_y\frac{\partial \boldsymbol{N}}{\partial y}\frac{\partial\left(\boldsymbol{N^T C}^{jk}\right)}{\partial y}+K_z\frac{\partial \boldsymbol{N}}{\partial z}\frac{\partial\left(\boldsymbol{N^T C}^{jk}\right)}{\partial z}\right\}dV-\iint_{Sb} q_r^{jk}\boldsymbol{N}dA-\iint_{Ss} q_s^{jk}\boldsymbol{N}dA=\boldsymbol{0}$$

(83)

Because matrix $\boldsymbol{C}^{jk}$, $\boldsymbol{U}$, $\boldsymbol{V}$, $\boldsymbol{W}$ are matrix of variable and parameter at nodal that is already assigned position. So it will not vary with $x$, $y$, $z$ distances and matrix $\boldsymbol{N}$ will not vary with time. Therefore Eq.(83) can be adjusted as follows:

$$\iiint_{\Omega} \boldsymbol{N}\boldsymbol{N}^{\boldsymbol{T}} dV \frac{\partial \boldsymbol{C}^{jk}}{\partial t} + \left[ \iiint_{\Omega} \boldsymbol{N}\boldsymbol{N}^{\boldsymbol{T}} \boldsymbol{U} \frac{\partial \boldsymbol{N}^{\mathbf{T}}}{\partial x} dV + \iiint_{\Omega} \boldsymbol{N}\boldsymbol{N}^{\boldsymbol{T}} \boldsymbol{V} \frac{\partial \boldsymbol{N}^{\boldsymbol{T}}}{\partial y} dV \right.$$
$$+ \iiint_{\Omega} \boldsymbol{N}\boldsymbol{N}^{\boldsymbol{T}} \boldsymbol{W} \frac{\partial \boldsymbol{N}^{\boldsymbol{T}}}{\partial z} dV - \iiint_{\Omega} v_s^{jk} \boldsymbol{N} \frac{\partial \boldsymbol{N}^{\boldsymbol{T}}}{\partial z} dV + \iiint_{\Omega} K_x \frac{\partial \boldsymbol{N}}{\partial x} \frac{\partial \boldsymbol{N}^{\boldsymbol{T}}}{\partial x} dV$$
$$\left. + \iiint_{\Omega} K_y \frac{\partial \boldsymbol{N}}{\partial y} \frac{\partial \mathbf{N}^{\mathbf{T}}}{\partial y} dV + \iiint_{\Omega} K_z \frac{\partial \boldsymbol{N}}{\partial z} \frac{\partial \boldsymbol{N}^{\boldsymbol{T}}}{\partial z} dV \right] \boldsymbol{C}^{jk} - \iiint_{\Omega} R^{jk} \boldsymbol{N} dV + \iiint_{\Omega} S_d^{jk} \boldsymbol{N} dV$$
$$- \iint_{Sb} q_r^{jk} \boldsymbol{N} dA - \iint_{Ss} q_s^{jk} \boldsymbol{N} dA = 0 \qquad (84)$$

which can be written in a compact form as:

$$\boldsymbol{M} \frac{d\boldsymbol{C}^{jk}}{dt} + \left[ \boldsymbol{M}_{wx} + \boldsymbol{M}_{wy} + \boldsymbol{M}_{wz} - \boldsymbol{M}_{vs} + \boldsymbol{M}_{kx} + \boldsymbol{M}_{ky} + \boldsymbol{M}_{kz} \right] \boldsymbol{C}^{jk} - \boldsymbol{M}_r + \boldsymbol{M}_s - \boldsymbol{M}_{qb} - \boldsymbol{M}_{qs} = 0 \qquad (85)$$

in which

$$\boldsymbol{M} = \iiint_{\Omega} \boldsymbol{N}\boldsymbol{N}^{\boldsymbol{T}} dV \qquad (86)$$

$$\boldsymbol{M}_{ux} = \iiint_{\Omega} \boldsymbol{N}\boldsymbol{N}^{\boldsymbol{T}} \boldsymbol{U} \frac{\partial \boldsymbol{N}^{\boldsymbol{T}}}{\partial x} dV \qquad (87)$$

$$\boldsymbol{M}_{vy} = \iiint_{\Omega} \boldsymbol{N}\boldsymbol{N}^{\boldsymbol{T}} \boldsymbol{V} \frac{\partial \boldsymbol{N}^{\boldsymbol{T}}}{\partial y} dV \qquad (88)$$

$$\boldsymbol{M}_{wz} = \iiint_{\Omega} \boldsymbol{N}\boldsymbol{N}^{\boldsymbol{T}} \boldsymbol{W} \frac{\partial \boldsymbol{N}^{\boldsymbol{T}}}{\partial z} dV \qquad (89)$$

$$\boldsymbol{M}_{vs} = \iiint_{\Omega} v_s^{jk} \boldsymbol{N} \frac{\partial \boldsymbol{N}^{\boldsymbol{T}}}{\partial z} dV \qquad (90)$$

$$\boldsymbol{M}_{kx} = \iiint_{\Omega} K_x \frac{\partial \boldsymbol{N}}{\partial x} \frac{\partial \boldsymbol{N}^{\boldsymbol{T}}}{\partial x} dV \qquad (91)$$

$$\boldsymbol{M_{ky}} = \iiint_{\Omega} K_y \frac{\partial \boldsymbol{N}}{\partial y} \frac{\partial \boldsymbol{N^T}}{\partial y} dV \quad (92)$$

$$\boldsymbol{M_{kz}} = \iiint_{\Omega} K_z \frac{\partial \boldsymbol{N}}{\partial z} \frac{\partial \boldsymbol{N^T}}{\partial z} dV \quad (93)$$

$$\boldsymbol{M_r} = \iiint_{\Omega} R^{jk} \boldsymbol{N} dV \quad (94)$$

$$\boldsymbol{M_s} = \iiint_{\Omega} S_d^{jk} \boldsymbol{N} dV \quad (95)$$

$$\boldsymbol{M_{qb}} = \iint_{Sb} q_r^{jk} \boldsymbol{N} dA \quad (96)$$

$$\boldsymbol{M_{qs}} = \iint_{Ss} q_s^{jk} \boldsymbol{N} dA \quad (97)$$

In finite element method, volume of the studied area are divided into elements. In this study, three-dimensional elements are used. Variable and parameter of each element are present to function of each node of the element. The integral over the whole study area is equal to summarize of integral over each element. We can substitute system matrix with union of element matrices as follow:

$$\boldsymbol{M} = \bigcup_{e=1}^{m} \boldsymbol{M}^e = \bigcup_{e=1}^{m} \left\{ \iiint_{V^e} \boldsymbol{N}^e \boldsymbol{N}^{eT} dV \right\} \quad (98)$$

$$\boldsymbol{M_{ux}} = \bigcup_{e=1}^{m} \boldsymbol{M}_{ux}^e = \bigcup_{e=1}^{m} \left\{ \iiint_{V^e} \boldsymbol{N}^e \boldsymbol{N}^{eT} \boldsymbol{U}^e \frac{\partial \boldsymbol{N}^{eT}}{\partial x} dV \right\} \quad (99)$$

$$\boldsymbol{M_{vy}} = \bigcup_{e=1}^{m} \boldsymbol{M}_{vy}^e = \bigcup_{e=1}^{m} \left\{ \iiint_{V^e} \boldsymbol{N}^e \boldsymbol{N}^{eT} \boldsymbol{V}^e \frac{\partial \boldsymbol{N}^{eT}}{\partial y} dV \right\} \quad (100)$$

$$\boldsymbol{M_{wz}} = \bigcup_{e=1}^{m} \boldsymbol{M}_{wz}^e = \bigcup_{e=1}^{m} \left\{ \iiint_{V^e} \boldsymbol{N}^e \boldsymbol{N}^{eT} \boldsymbol{W}^e \frac{\partial \boldsymbol{N}^{eT}}{\partial z} dV \right\} \quad (101)$$

$$\boldsymbol{M_{vs}} = \bigcup_{e=1}^{m} \boldsymbol{M}_{vs}^e = \bigcup_{e=1}^{m} \left\{ \iiint_{V^e} v_s^{jk} \boldsymbol{N}^e \frac{\partial \boldsymbol{N}^{eT}}{\partial z} dV \right\} \quad (102)$$

$$\boldsymbol{M_{kx}} = \bigcup_{e=1}^{m} \boldsymbol{M}_{kx}^{e} = \bigcup_{e=1}^{m} \left\{ \iiint_{V^e} K_x \frac{\partial \boldsymbol{N}^{e}}{\partial x} \frac{\partial \boldsymbol{N}^{eT}}{\partial x} dV \right\} \tag{103}$$

$$\boldsymbol{M_{ky}} = \bigcup_{e=1}^{m} \boldsymbol{M}_{ky}^{e} = \bigcup_{e=1}^{m} \left\{ \iiint_{V^e} K_y \frac{\partial \boldsymbol{N}^{e}}{\partial y} \frac{\partial \boldsymbol{N}^{eT}}{\partial y} dV \right\} \tag{104}$$

$$\boldsymbol{M_{kz}} = \bigcup_{e=1}^{m} \boldsymbol{M}_{kz}^{e} = \bigcup_{e=1}^{m} \left\{ \iiint_{V^e} K_z \frac{\partial \boldsymbol{N}^{e}}{\partial z} \frac{\partial \boldsymbol{N}^{eT}}{\partial z} dV \right\} \tag{105}$$

$$\boldsymbol{M_{r}} = \bigcup_{e=1}^{m} \boldsymbol{M}_{r}^{e} = \bigcup_{e=1}^{m} \left\{ \iiint_{V^e} R^{jk\,e} \boldsymbol{N}^{e} dV \right\} \tag{106}$$

$$\boldsymbol{M_{s}} = \bigcup_{e=1}^{m} \boldsymbol{M}_{s}^{e} = \bigcup_{e=1}^{m} \left\{ \iiint_{V^e} S_d^{jk\,e} \boldsymbol{N}^{e} dV \right\} \tag{107}$$

$$\boldsymbol{M_{qb}} = \bigcup_{e=1}^{m_b} \boldsymbol{M}_{qb}^{e} = \bigcup_{e=1}^{m_b} \left\{ \iint_{S_b^e} q_r^{jk\,e} \boldsymbol{N}^{e} dA \right\} \tag{108}$$

$$\boldsymbol{M_{qs}} = \bigcup_{e=1}^{m_s} \boldsymbol{M}_{qs}^{e} = \bigcup_{e=1}^{m_s} \left\{ \iint_{S_s^e} q_s^{jk\,e} \boldsymbol{N}^{e} dA \right\} \tag{109}$$

The superscript "*e*" above the matrix symbol means element matrix of the $e^{th}$ element. Superscript "*e*" above on $R^{jk}$, $S_d^{jk}$, $q_r^{jk}$ and $q_s^{jk}$ are average of each parameter in the $e^{th}$ element. The total number of elements is *m*. The numbers of elements the boundaries $S_b$ and $S_s$ are $m_b$ and $m_s$, respectively.

The appropriate element configuration for suspended sediment transport model is the hexahedral element, due to its easy to adapt with water resource condition. The matrices obtained from assempling element matrices are called system matrices. Eq (85) is called "Finite element equation".

Eq. (85) is a set of first order differential equations, in which initial conditions are necessary for calculating $\boldsymbol{C}^{jk}$ at various time. Here, we set sediment concentrations with size $D_j$ and specific gravity $s_k$ at each node at $t = t_0$ as follow:

$$\boldsymbol{C}^{jk}(t_0) = \boldsymbol{C}_{\boldsymbol{0}}^{\boldsymbol{jk}} \tag{110}$$

From Eq. (85), we can be written in a compact form as:

$$\boldsymbol{M}\frac{d\boldsymbol{C}^{jk}}{dt} + \boldsymbol{P}\boldsymbol{C}^{jk} - \boldsymbol{Q} = \boldsymbol{0} \tag{111}$$

in which

$$\boldsymbol{P} = \boldsymbol{M}_{ux} + \boldsymbol{M}_{vy} + \boldsymbol{M}_{wz} - \boldsymbol{M}_{vs} + \boldsymbol{M}_{kx} + \boldsymbol{M}_{ky} + \boldsymbol{M}_{kz} \tag{112}$$

and

$$\boldsymbol{Q} = \boldsymbol{M}_{r} - \boldsymbol{M}_{s} + \boldsymbol{M}_{qb} + \boldsymbol{M}_{qs} \tag{113}$$

2.1.3 Hexahedral finite element

In this study, we use hexahedral elements in the three-dimensional model. The natural coordinate system for the hexahedral element shown in Figure 11.

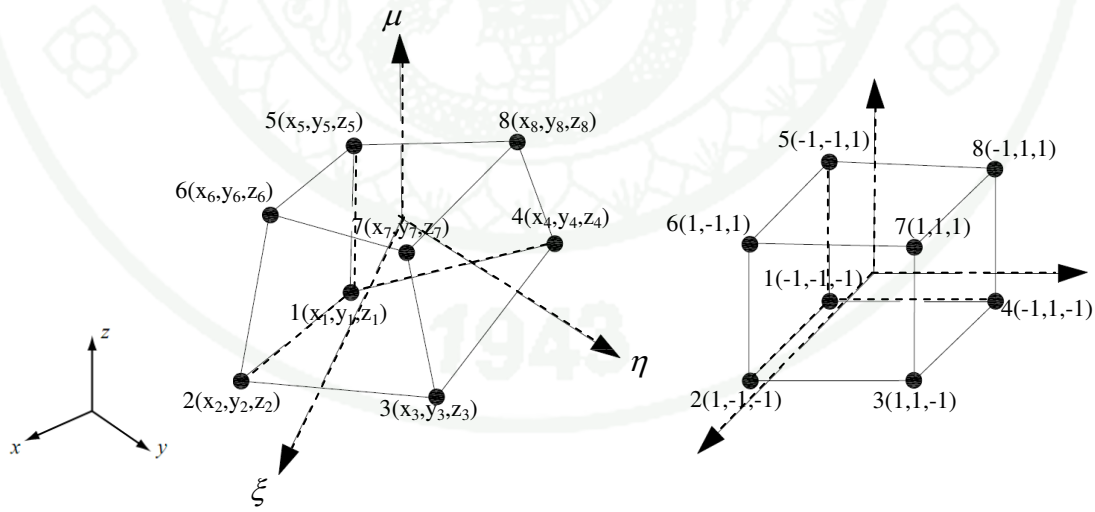


(a) Global system (b) Local system

**Figure 11** The 8-nodes hexahedron and the natural coordinates $\xi$, $\eta$ and $\mu$.

The hexahedral coordinates of the corners are

| node | $\xi$ | $\eta$ | $\mu$ |
|---|---|---|---|
| 1 | -1 | -1 | -1 |
| 2 | +1 | -1 | -1 |
| 3 | +1 | +1 | -1 |
| 4 | -1 | +1 | -1 |
| 5 | -1 | -1 | +1 |
| 6 | +1 | -1 | +1 |
| 7 | +1 | +1 | +1 |
| 8 | -1 | +1 | +1 |

The shape functions are (Polesky, S. P., *et al*., 1992)

$$N_1^{(e)} = \frac{1}{8}(1-\xi)(1-\eta)(1-\mu) \tag{114}$$

$$N_2^{(e)} = \frac{1}{8}(1+\xi)(1-\eta)(1-\mu) \tag{115}$$

$$N_3^{(e)} = \frac{1}{8}(1+\xi)(1+\eta)(1-\mu) \tag{116}$$

$$N_4^{(e)} = \frac{1}{8}(1-\xi)(1+\eta)(1-\mu) \tag{117}$$

$$N_5^{(e)} = \frac{1}{8}(1-\xi)(1-\eta)(1+\mu) \tag{118}$$

$$N_6^{(e)} = \frac{1}{8}(1+\xi)(1-\eta)(1+\mu) \tag{119}$$

$$N_7^{(e)} = \frac{1}{8}(1+\xi)(1+\eta)(1+\mu) \tag{120}$$

$$N_8^{(e)} = \frac{1}{8}(1-\xi)(1+\eta)(1+\mu) \tag{121}$$

These eight formulas can be summarized in a single expression :

$$N_i^{(e)} = \frac{1}{8}(1+\xi\xi_i)(1+\eta\eta_i)(1+\mu\mu_i) \tag{122}$$

where $\xi_i$, $\eta_i$ and $\mu_i$ denote the coordinates of the $i^{th}$ node.

Isoparametric hexahedral element is element which coordinates and parameter can be written in term of the value of each node with same function.

Where *u* is function of *x y* and *z* as

$$u = a_1 + a_2 x + a_3 y + a_4 z + a_5 xy + a_6 yz + a_7 xz + a_8 xyz \tag{123}$$

*u* at node i is equal to

$$u = a_1 + a_2 x_i + a_3 y_i + a_4 z_i + a_5 x_i y_i + a_6 y_i z_i + a_7 x_i z_i + a_8 x_i y_i z_i \tag{124}$$

The coefficients $a_1$ to $a_8$ can be expressed in terms of the values of the *u*-component of displacement at the eight node points by evaluating at the nodes and solving the resulting equations. The displacement functions are required in the form

$$u = \sum_{i=1}^{8} N_i u_i , \qquad v = \sum_{i=1}^{8} N_i v_i , \qquad w = \sum_{i=1}^{8} N_i w_i \tag{125}$$

Since

$$u = N_1 u_1 + N_2 u_2 + N_3 u_3 + N_4 u_4 + N_5 u_5 + N_6 u_6 + N_7 u_7 + N_8 u_8 \tag{126}$$

$$u = \sum_{i=1}^{n} N_i u_i \tag{127}$$

We can write *u* in terms of $\xi$, $\eta$ and $\mu$ as

$$u = a_1 + a_2 \xi + a_3 \eta + a_4 \mu + a_5 \xi\eta + a_6 \eta\mu + a_7 \xi\mu + a_8 \xi\eta\mu \tag{128}$$

We write the Cartesian coordinates (*x*, *y*, *z*) in the term of the local coordinates $(\xi, \eta, \mu)$ defined by

$$x = x(\xi, \eta, \mu), \qquad y = y(\xi, \eta, \mu), \qquad z = z(\xi, \eta, \mu) \tag{129}$$

Interpolation function and derivatives of local coordinates can be written as

$$\underline{N} = N(\xi,\eta,\mu) = \{N_1, N_2, .....\} \tag{130}$$

$$N_{,\xi} = \frac{\partial N}{\partial \xi} = \left\{\frac{\partial N_1}{\partial \xi}, \frac{\partial N_2}{\partial \xi}, .....\right\} \tag{131}$$

$$N_{,\eta} = \frac{\partial N}{\partial \eta} = \left\{\frac{\partial N_1}{\partial \eta}, \frac{\partial N_2}{\partial \eta}, .....\right\} \tag{132}$$

$$N_{,\mu} = \frac{\partial N}{\partial \mu} = \left\{\frac{\partial N_1}{\partial \mu}, \frac{\partial N_2}{\partial \mu}, .....\right\} \tag{133}$$

Normally, the element matrices will have derivatives of Local coordinates, which transform derivatives between Local coordinates and Cartesian coordinates from formulas as

$$\frac{\partial N}{\partial x} = \frac{\partial N}{\partial \xi}.\frac{\partial \xi}{\partial x} + \frac{\partial N}{\partial \eta}.\frac{\partial \eta}{\partial x} + \frac{\partial N}{\partial \mu}.\frac{\partial \mu}{\partial x} \tag{134}$$

$$\frac{\partial N}{\partial y} = \frac{\partial N}{\partial \xi}.\frac{\partial \xi}{\partial y} + \frac{\partial N}{\partial \eta}.\frac{\partial \eta}{\partial y} + \frac{\partial N}{\partial \mu}.\frac{\partial \mu}{\partial y} \tag{135}$$

$$\frac{\partial N}{\partial z} = \frac{\partial N}{\partial \xi}.\frac{\partial \xi}{\partial z} + \frac{\partial N}{\partial \eta}.\frac{\partial \eta}{\partial z} + \frac{\partial N}{\partial \mu}.\frac{\partial \mu}{\partial z} \tag{136}$$

To consider $N(x, y, z)$ and find its derivatives in term $N(\xi,\eta,\mu)$. Then calculate backwards as

$$\begin{bmatrix} \frac{\partial N}{\partial x} \\ \frac{\partial N}{\partial y} \\ \frac{\partial N}{\partial z} \end{bmatrix} = \begin{bmatrix} \frac{\partial x}{\partial \xi} & \frac{\partial y}{\partial \xi} & \frac{\partial z}{\partial \xi} \\ \frac{\partial x}{\partial \eta} & \frac{\partial y}{\partial \eta} & \frac{\partial z}{\partial \eta} \\ \frac{\partial x}{\partial \mu} & \frac{\partial y}{\partial \mu} & \frac{\partial z}{\partial \mu} \end{bmatrix} \begin{bmatrix} \frac{\partial N}{\partial x} \\ \frac{\partial N}{\partial y} \\ \frac{\partial N}{\partial z} \end{bmatrix} = \underline{J} \begin{bmatrix} \frac{\partial N}{\partial x} \\ \frac{\partial N}{\partial y} \\ \frac{\partial N}{\partial z} \end{bmatrix} \tag{137}$$

Then, we got

$$\mathrm{J}=\frac{\partial(x,y,z)}{\partial(\xi,\eta,\mu)}=\begin{bmatrix}\frac{\partial x}{\partial\xi} & \frac{\partial y}{\partial\xi} & \frac{\partial z}{\partial\xi}\\ \frac{\partial x}{\partial\eta} & \frac{\partial y}{\partial\eta} & \frac{\partial z}{\partial\eta}\\ \frac{\partial x}{\partial\mu} & \frac{\partial y}{\partial\mu} & \frac{\partial z}{\partial\mu}\end{bmatrix} \tag{138}$$

J is called the Jacobian matrix of ($x$,$y$,$z$) with repect to $(\xi,\eta,\mu)$. In the finite element literature, matrices J and $\mathrm{J}^{-1}$ are called simply the Jacobian and inverse Jacobian, respectively.

Then

$$\begin{Bmatrix}\frac{\partial N^T}{\partial x}\\ \frac{\partial N^T}{\partial y}\\ \frac{\partial N^T}{\partial z}\end{Bmatrix}=\mathrm{J}^{-1}\begin{Bmatrix}\frac{\partial N^T}{\partial\xi}\\ \frac{\partial N^T}{\partial\eta}\\ \frac{\partial N^T}{\partial\mu}\end{Bmatrix} \tag{139}$$

$$\begin{bmatrix}\frac{\partial u}{\partial x}\\ \frac{\partial u}{\partial y}\\ \frac{\partial u}{\partial z}\end{bmatrix}=\mathrm{J}^{-1}\begin{bmatrix}\frac{\partial u}{\partial\xi}\\ \frac{\partial u}{\partial\eta}\\ \frac{\partial u}{\partial\mu}\end{bmatrix}=\mathrm{J}^{-1}\begin{bmatrix}\frac{\partial N^T}{\partial\xi}\\ \frac{\partial N^T}{\partial\eta}\\ \frac{\partial N^T}{\partial\mu}\end{bmatrix}\underline{u} \tag{140}$$

So, the derivative of $u$ with respect to and $\xi,\eta$ and μ the derivative of $u$ with respect to $x$, $y$ and $z$ can be calculated by Eq.(139) and Eq.(140) respectively.

$$\begin{Bmatrix} \frac{\partial u}{\partial \xi} \\ \frac{\partial u}{\partial \eta} \\ \frac{\partial u}{\partial \mu} \end{Bmatrix} =$$

$$\begin{pmatrix} -\frac{1}{8}(1-\eta)(1-\mu) & \frac{1}{8}(1-\eta)(1-\mu) & \frac{1}{8}(1+\eta)(1-\mu) & -\frac{1}{8}(1+\eta)(1-\mu) & -\frac{1}{8}(1-\eta)(1+\mu) & \frac{1}{8}(1-\eta)(1+\mu) & \frac{1}{8}(1+\eta)(1+\mu) & -\frac{1}{8}(1+\eta)(1+\mu) \\ -\frac{1}{8}(1-\xi)(1-\mu) & -\frac{1}{8}(1+\xi)(1-\mu) & \frac{1}{8}(1+\xi)(1-\mu) & \frac{1}{8}(1-\xi)(1-\mu) & -\frac{1}{8}(1-\xi)(1+\mu) & -\frac{1}{8}(1+\xi)(1+\mu) & \frac{1}{8}(1+\xi)(1+\mu) & \frac{1}{8}(1-\xi)(1+\mu) \\ -\frac{1}{8}(1-\xi)(1-\eta) & \frac{1}{8}(1+\xi)(1-\eta) & -\frac{1}{8}(1+\xi)(1+\eta) & -\frac{1}{8}(1-\xi)(1+\eta) & \frac{1}{8}(1-\xi)(1-\eta) & \frac{1}{8}(1+\xi)(1-\eta) & \frac{1}{8}(1+\xi)(1+\eta) & \frac{1}{8}(1-\xi)(1+\eta) \end{pmatrix}$$

$$* \begin{bmatrix} u_{n1} \\ u_{n2} \\ u_{n3} \\ u_{n4} \\ u_{n5} \\ u_{n6} \\ u_{n7} \\ u_{n8} \end{bmatrix} = \mathrm{B}^{*} u^{n} \qquad (141)$$

$$\begin{Bmatrix} \frac{\partial u}{\partial x} \\ \frac{\partial u}{\partial y} \\ \frac{\partial u}{\partial z} \end{Bmatrix} = \mathrm{J}^{-1}\mathrm{B}^{*} u^{n} = \mathrm{B}u^{n} \qquad (142)$$

where $\mathrm{B} = \mathrm{J}^{-1}\mathrm{B}^{*}$

The relationship between *x-y-z* coordinate and $\xi - \eta - \mu$ coordinate can be expressed by using Jacobian.

$$\mathrm{J}=\begin{Bmatrix}\frac{\partial x}{\partial \xi} & \frac{\partial y}{\partial \xi} & \frac{\partial z}{\partial \xi}\\ \frac{\partial x}{\partial \eta} & \frac{\partial y}{\partial \eta} & \frac{\partial z}{\partial \eta}\\ \frac{\partial x}{\partial \mu} & \frac{\partial y}{\partial \mu} & \frac{\partial z}{\partial \mu}\end{Bmatrix}=\mathrm{B}^{*}\begin{bmatrix}x_1 & y_1 & z_1\\ x_2 & y_2 & z_2\\ x_3 & y_3 & z_3\\ x_4 & y_4 & z_4\\ x_5 & y_5 & z_5\\ x_6 & y_6 & z_6\\ x_7 & y_7 & z_7\\ x_8 & y_8 & z_8\end{bmatrix}=\begin{bmatrix}J_{11} & J_{12} & J_{13}\\ J_{21} & J_{22} & J_{23}\\ J_{31} & J_{32} & J_{33}\end{bmatrix} \tag{143}$$

If $|\mathrm{J}|$ is determinant of J, we got

$$|\mathrm{J}|=\frac{\partial x}{\partial \xi}\cdot\frac{\partial y}{\partial \eta}\cdot\frac{\partial z}{\partial \mu}+\frac{\partial y}{\partial \xi}\cdot\frac{\partial z}{\partial \eta}\cdot\frac{\partial x}{\partial \mu}-\frac{\partial x}{\partial \mu}\cdot\frac{\partial y}{\partial \eta}\cdot\frac{\partial z}{\partial \xi}-\frac{\partial y}{\partial \mu}\cdot\frac{\partial z}{\partial \eta}\cdot\frac{\partial x}{\partial \xi} \tag{144}$$

in which $|\mathrm{J}|=J_{11}J_{22}J_{33}+J_{12}J_{23}J_{31}-J_{13}J_{22}J_{31}-J_{11}J_{23}J_{32}$

Eq. (142) can be rewritten as

$$\begin{bmatrix}\frac{\partial u}{\partial x}\\ \frac{\partial u}{\partial y}\\ \frac{\partial u}{\partial z}\end{bmatrix}=\mathrm{B}\quad u^{n} \tag{145}$$

Where $\mathrm{B}=\mathrm{J}^{-1}\quad \mathrm{B}^{*}$

The difference volume (*dV*) can be defind in term $d\xi,d\eta,d\mu$ as

$$dV=\left(absolute\quad value\quad of\quad |\mathrm{J}|\right)d\xi d\eta d\mu \tag{146}$$

By transforming isoparametric hexahedral element as mentioned above, we can easily calculate element matrices by using the numerical integration method with the Gauss-Legendre integration as:

$$\iiint_{\Omega}(x,y,z)dxdydz=\iiint_{\Omega}f(\xi,\eta,\mu)d\xi\partial\eta\partial\mu=\int_{-1}^{1}\int_{-1}^{1}\int_{-1}^{1}f(\xi,\eta,\mu)\left|\mathrm{J}(\xi,\eta,\mu)\right|d\xi d\eta d\mu$$

$$=\sum_{i=1}^{m}\sum_{j=1}^{n}\sum_{k=1}^{l}W_iW_jW_kf(\xi_i,\eta_j,\mu_k)\left|\mathrm{J}(\xi_i,\eta_j,\mu_k)\right| \qquad (147)$$

where

| | |
|---|---|
| *m, n, l* | are number of Gauss Points; |
| $W_i$, $W_j$, $W_k$ | are weights of Gauss Points at $i$ = 1, 2, 3….8; $j$ = 1, 2, 3….8; and $k$ = 1, 2, 3….8; |
| $\xi_i,\eta_i,\mu_i$ | are Gauss Points Locations; |
| $\left\|\mathrm{J}(\xi_i,\eta_i,\mu_i)\right\|$ | are determinant of Jacobian matrix. which $\left\|\mathrm{J}\right\|=J_{11}J_{22}J_{33}+J_{12}J_{23}J_{31}-J_{13}J_{22}J_{31}-J_{11}J_{23}J_{32}$ |

In a case of hexahedral element with $m = n = 2$, weights of Gauss points $W_i$ = 1, $W_j$ = 1, $W_k$ = 1 and Gauss point locations are:

$$\begin{bmatrix}\xi_1&\eta_1&\mu_1\\ \xi_2&\eta_2&\mu_2\\ \xi_3&\eta_3&\mu_3\\ \xi_4&\eta_4&\mu_4\\ \xi_5&\eta_5&\mu_5\\ \xi_6&\eta_6&\mu_6\\ \xi_7&\eta_7&\mu_7\\ \xi_8&\eta_8&\mu_8\end{bmatrix}=\begin{bmatrix}1/\sqrt{3}&-1/\sqrt{3}&-1/\sqrt{3}\\ -1/\sqrt{3}&-1/\sqrt{3}&-1/\sqrt{3}\\ -1/\sqrt{3}&1/\sqrt{3}&-1/\sqrt{3}\\ 1/\sqrt{3}&1/\sqrt{3}&-1/\sqrt{3}\\ -1/\sqrt{3}&-1/\sqrt{3}&1/\sqrt{3}\\ 1/\sqrt{3}&-1/\sqrt{3}&1/\sqrt{3}\\ -1/\sqrt{3}&1/\sqrt{3}&1/\sqrt{3}\\ 1/\sqrt{3}&1/\sqrt{3}&1/\sqrt{3}\end{bmatrix} \qquad (148)$$

Eq.(111) is a set of equations for computing distribution of suspended sediment at various nodal points in the study domain. This will be computed alternately with a set of equations for bedload transport which is described below:

2.2 Bedload sediment transport model

Most studies concerning transport of bedload sediment transport utilize relationship between bedload movement and Shields parameter. In the past few decades, several bedload transport equations have been proposed (Reeve *et al*, 2004). A dimensionless parameter called 'bedload transport rate factor' ($\Phi$) has been used to relate the rate of bedload transport with particle grain size ($D$) and specific gravity ($s$). The relationship is as follows:

$$\Phi = \frac{q_b}{[g(s-1)D^3]^{1/2}} \tag{149}$$

in which $q_b$ is the rate of bedload transport per unit width.

The parameter $\Phi$ can be computed from Shields parameter $\theta_s$ and critical Shields parameter $\theta_{cr}$ as follows (Neilson, 1992)

$$\Phi = 12\theta_s^{1/2}(\theta_s - \theta_{cr}) \tag{150}$$

Shields parameter $\theta_s$ and critical Shields parameter $\theta_{cr}$ are expressed by (Reeve *et al*, 2004):

$$\theta_s = \tau/(\rho_s - \rho)gD \tag{151}$$

and

$$\theta_{cr} = \tau_{cr}/(\rho_s - \rho)gD \tag{152}$$

in which

$\tau$ is bed shear stress which is related to current velocity, wave action and water depth;

$\tau_{cr}$ is critical bed shear stress over which bedload transport will occur;

$\rho_s$ is particle density;

$\rho$ is water density;

$D$ is grain size diameter.

It can be seen that the grain size diameter and specific gravity of particles affect the value of bedload transport rate factor ( $\Phi$ ) and the rate of bedload transport rate per unit width $q_b$ . Therefore, in this study the total bedload sediment is divided into groups based on their diameter and specific gravity. The model is developed to simulate transport of each group of bedload sediment. Then, the amount of various groups is combined to obtain the total bed load per unit area at an identified location.

For particles with grain size diameter $D_j$ and specific gravity $s_k$, the mass balance equation for bedload transport can be written as:

$$\frac{\partial s_b^{jk}}{\partial t} + \frac{\partial Q_x^{jk}}{\partial x} + \frac{\partial Q_y^{jk}}{\partial y} - v_s^{jk} c_b^{jk} + q_r^{jk} = 0 \qquad (153)$$

where

$s_b^{jk}$ is the amount per unit area of bedload sediment with diameter $D_j$ and specific gravity $s_k$;

$Q_x^{jk}$ and $Q_y^{jk}$ are the rates of bedload transport per unit width in the $x$ and $y$ directions, respectively, of bedload sediment with diameter $D_j$ and specific gravity $s_k$;

$v_s^{jk}$ is terminal settling velocity of particle with diameter $D_j$ and specific gravity $s_k$;

$c_b^{jk}$ is concentration of suspended sediment with diameter $D_j$ and specific gravity $s_k$ just above the sea bed;

$q_r^{jk}$ is the resuspension rate of bedload sediment with diameter $D_j$ and specific gravity $s_k$.

The study domain of the BLT model is the bottom boundary of the SST model projected on the horizontal plain (Figure 10), since the value of variable $s_b^{jk}$ and parameters $Q_x^{jk}$ , $Q_y^{jk}$ and $q_r^{jk}$ are the values on the horizontal planes.

In the weighted residual method, the variable $s_b^{jk}$ is replaced by approximate function $\hat{s}_b^{jk}$ which is written in terms of its nodal values as follows:

$$\hat{s}_b^{jk} = \sum_{i=1}^{n_b} N_i S_{bi}^{jk} = \boldsymbol{N}^{\boldsymbol{T}} \boldsymbol{S}_b^{jk} \tag{154}$$

in which

$S_{bi}^{jk}$ is the amount per unit area at node *i* for of bedload sediment with diameter $D_j$ and specific gravity $s_k$;

$N_i$ is interpolation function;

$\boldsymbol{S}_b^{jk}$ is matrix of $S_{bi}^{jk}$;

$\boldsymbol{N}$ is matrix of $N_i$;

$n_b$ is total number of nodes in the study domain.

When $s_b^{jk}$ in Eq.(153) is replaced by $\hat{s}_b^{jk}$, an error or residual will occur. This residual is multiplied with a weighting function $w_s$ and the integral of their product over the whole study domain is set to zero. This results in the $D_j$ following weighted residual equation:

$$\iint_A w_s \left\{ \frac{\partial \hat{s}_b^{jk}}{\partial t} + \frac{\partial Q_x^{jk}}{\partial x} + \frac{\partial Q_y^{jk}}{\partial y} - v_s^{jk} c_b^{jk} + q_r^{jk} \right\} dA = 0 \tag{155}$$

In Galerkin's technique, the interpolation function $N_i$ ($i$ =1,2,..,$n_b$) are used as a weighting function. Therefore, the following set of weighted residual equations is obtained:

$$\iint_A N_i \left\{ \frac{\partial \hat{s}_b^{jk}}{\partial t} + \frac{\partial Q_x^{jk}}{\partial x} + \frac{\partial Q_y^{jk}}{\partial y} - v_s^{jk} c_b^{jk} + q_r^{jk} \right\} dA = 0 \quad (i = 1,2,..,n_b) \tag{156}$$

which can be written in the matrix form as:

$$\iint_A \boldsymbol{N}\left\{\frac{\partial \hat{s}_b^{jk}}{\partial t}+\frac{\partial Q_x^{jk}}{\partial x}+\frac{\partial Q_y^{jk}}{\partial y}-v_s^{jk}c_b^{jk}+q_r^{jk}\right\}dA=\mathbf{0} \tag{157}$$

Besides $\hat{s}_b^{jk}$, the parameters $Q_x^{jk}, Q_y^{jk}$ and $c_b^{jk}$ can be expresses in term of the nodal values as:

$$Q_x^{jk}=\sum_{i=1}^{n}N_i Q_{xi}^{jk}=\boldsymbol{N^T Q}_x^{jk} \tag{158}$$

$$Q_y^{jk}=\sum_{i=1}^{n}N_i Q_{yi}^{jk}=\boldsymbol{N^T Q}_y^{jk} \tag{159}$$

$$c_b^{jk}=\sum_{i=1}^{n}N_i C_{bi}^{jk}=\boldsymbol{N^T C}_b^{jk} \tag{160}$$

When substituting into Eq.(157) we obtain:

$$\iint_A \boldsymbol{N}\left\{\frac{\partial}{\partial t}\left(\boldsymbol{N^T S}_b^{jk}\right)+\frac{\partial\left(\boldsymbol{N^T Q_x^{jk}}\right)}{\partial x}+\frac{\partial\left(\boldsymbol{N^T Q_y^{jk}}\right)}{\partial y}-v_s^{jk}\boldsymbol{N^T C_b^{jk}}+q_r^{jk}\right\}dA=\mathbf{0} \tag{161}$$

Because matrix $\hat{s}_b^{jk}$, $Q_x^{jk}, Q_y^{jk}$ and $c_b^{jk}$ are matrixs of variable and parameter at nodal that is already assigned position. So it not be function of *x* and *y* and matrix ***N*** will not vary with time. Therefore Eq. (161) can be arranged as:

$$\iint_A \boldsymbol{NN^T}dA\frac{\partial \boldsymbol{S_b^{jk}}}{\partial t}+\iint_A \boldsymbol{N}\frac{\partial \boldsymbol{N^T}}{\partial x}dA\boldsymbol{Q_x^{jk}}+\iint_A \boldsymbol{N}\frac{\partial \boldsymbol{N^T}}{\partial y}dA\boldsymbol{Q_y^{jk}}-\iint_A v_s^{jk}\boldsymbol{NN^T}dA\boldsymbol{C_b^{jk}}+\iint_A q_r^{jk}\boldsymbol{N}dA=\mathbf{0} \tag{162}$$

or in a compact form as:

$$\boldsymbol{M}\frac{d\boldsymbol{S}_{\boldsymbol{b}}^{\boldsymbol{jk}}}{dt}+\boldsymbol{M}_{\boldsymbol{x}}\boldsymbol{Q}_{\boldsymbol{x}}^{\boldsymbol{jk}}+\boldsymbol{M}_{\boldsymbol{y}}\boldsymbol{Q}_{\boldsymbol{y}}^{\boldsymbol{jk}}-\boldsymbol{M}_{\boldsymbol{v}}^{\boldsymbol{jk}}\boldsymbol{C}_{\boldsymbol{b}}^{\boldsymbol{jk}}+\boldsymbol{M}_{\boldsymbol{b}}^{\boldsymbol{jk}} \tag{163}$$

where

$$\boldsymbol{M}=\iint_{A}\boldsymbol{N}\boldsymbol{N}^{\boldsymbol{T}}dA \tag{164}$$

$$\boldsymbol{M}_{\boldsymbol{x}}=\iint_{A}\boldsymbol{N}\frac{\partial\boldsymbol{N}^{\boldsymbol{T}}}{\partial x}dA \tag{165}$$

$$\boldsymbol{M}_{\boldsymbol{y}}=\iint_{A}\boldsymbol{N}\frac{\partial\boldsymbol{N}^{\boldsymbol{T}}}{\partial y}dA \tag{166}$$

$$\boldsymbol{M}_{\boldsymbol{v}}^{\boldsymbol{jk}}=\iint_{A}v_{s}^{jk}\boldsymbol{N}\boldsymbol{N}^{\boldsymbol{T}}dA \tag{167}$$

$$\boldsymbol{M}_{\boldsymbol{b}}^{\boldsymbol{jk}}=\iint_{A}q_{r}^{jk}\boldsymbol{N}dA \tag{168}$$

In finite element method, study area is divide into elements. Variable and parameter of each element are present to function of each node of element. When integral whole study area, it is equal summary of integral in each element. System matrix can be substituted with symbol in Eq. (164) to Eq. (168) as union of element matrix as follow:

$$\boldsymbol{M}=\bigcup_{e=1}^{m_b}\boldsymbol{M}^{\boldsymbol{e}}=\bigcup_{e=1}^{m_b}\left\{\iint_{A^e}\boldsymbol{N}^{\boldsymbol{e}}\boldsymbol{N}^{\boldsymbol{eT}}dA\right\} \tag{169}$$

$$\boldsymbol{M}_{\boldsymbol{x}}=\bigcup_{e=1}^{m_b}\boldsymbol{M}_{\boldsymbol{x}}^{\boldsymbol{e}}=\bigcup_{e=1}^{m_b}\left\{\iint_{A^e}\boldsymbol{N}^{\boldsymbol{e}}\frac{\partial\boldsymbol{N}^{\boldsymbol{eT}}}{\partial x}dA\right\} \tag{170}$$

$$\boldsymbol{M}_{\boldsymbol{y}}=\bigcup_{e=1}^{m_b}\boldsymbol{M}_{\boldsymbol{y}}^{\boldsymbol{e}}=\bigcup_{e=1}^{m_b}\left\{\iint_{A^e}\boldsymbol{N}^{\boldsymbol{e}}\frac{\partial\boldsymbol{N}^{\boldsymbol{eT}}}{\partial y}dA\right\} \tag{171}$$

$$\boldsymbol{M}_{\boldsymbol{v}}=\bigcup_{e=1}^{m_b}\boldsymbol{M}_{\boldsymbol{v}}^{\boldsymbol{e}}=\bigcup_{e=1}^{m_b}\left\{\iint_{A^e}v_{s}^{jk}\boldsymbol{N}^{\boldsymbol{e}}\boldsymbol{N}^{\boldsymbol{eT}}dA\right\} \tag{172}$$

$$\boldsymbol{M}_{\boldsymbol{b}}^{\boldsymbol{jk}}=\bigcup_{e=1}^{m_b}M_{b}^{jke}=\bigcup_{e=1}^{m_b}\left\{\iint_{A^e}q_{r}^{jke}\boldsymbol{N}^{\boldsymbol{e}}dA\right\} \tag{173}$$

Where superscript "*e*" above on matrix symbol is element matrix of each element. Total elements are equal $m_b$.

Eq. (163) is a set of first order differential equations. Initial condition is necessary for calculated $s^{jk}$ at various time. We set sediment concentration which size $D_j$ and specific gravity $s_k$ at each node at $t = t_0$ as following:

$$\boldsymbol{S}_{\boldsymbol{b}}^{\boldsymbol{jk}}(t_0) = \boldsymbol{S}_{\boldsymbol{b0}}^{\boldsymbol{jk}} \tag{174}$$

In this study, bedload sediment transport model, we use isoparametric element (Figure 10) in two-dimensional modeling. Quadrilateral elements are difficult to integral, so we transform *x*-*y* coordinate into natural coordinates for this geometry are call $\xi - \mu$ coordinate and call isoparametric coordinates which consists of 4 nodes as number 1, 2, 3 and 4. These coordinates are illustrated in Figure 10 which distances from $\xi$.and $\eta$ are -1 to 1

Isoparametric element is termed for an element type that the Cartesian coordinates can be written in terms of their values at nodes within the element in the same form of the approximate function. That is, for instance, *x*, *y* coordinates and variable $\bar{u}$ can be written as (Liengcharernsit, 2009)

$$x = \sum_{i=1}^{n^e} \mathbf{N}_i^e \mathbf{x}_i^e = \mathbf{N}^{e^{\mathrm{T}}} \mathbf{x}^{\mathbf{e}} \tag{175}$$

$$y = \sum_{i=1}^{n^e} \mathbf{N}_i^e \mathbf{y}_i^e = \mathbf{N}^{e^{\mathrm{T}}} \mathbf{y}^{\mathbf{e}} \tag{176}$$

$$\bar{u} = \sum_{i=1}^{n^e} \mathbf{N}_i^e \mathbf{u}_i^e = \mathbf{N}^{e^{\mathrm{T}}} \mathbf{u}^{\mathbf{e}} \tag{177}$$

where $\mathbf{x}_i^e$ and $\mathbf{y}_i^e$ are *x* and *y* coordinates at node *i*, respectively;

$\mathbf{u}_i^e$ is variable at node *i*;

$\mathbf{N}^{e^{\mathrm{T}}}$ is matrix of shape function;

$n$ is the number of nodes in each element..

In this study, we use isoparametric elements in the two-dimensional model. The natural coordinate system for the isoparametric element shown in Figure 12. The Cartesian coordinates ($x$,$y$) are written in the term of the natural coordinates ($\xi, \eta$) by

$$x = x(\xi,\eta) \;\; ; \;\; y = y(\xi,\eta) \tag{178}$$

That is, for every point given by its $\xi, \eta$-coordinates in the parent domain, there exists a corresponding point given by its $x$,$y$-coordinate in the global domain.

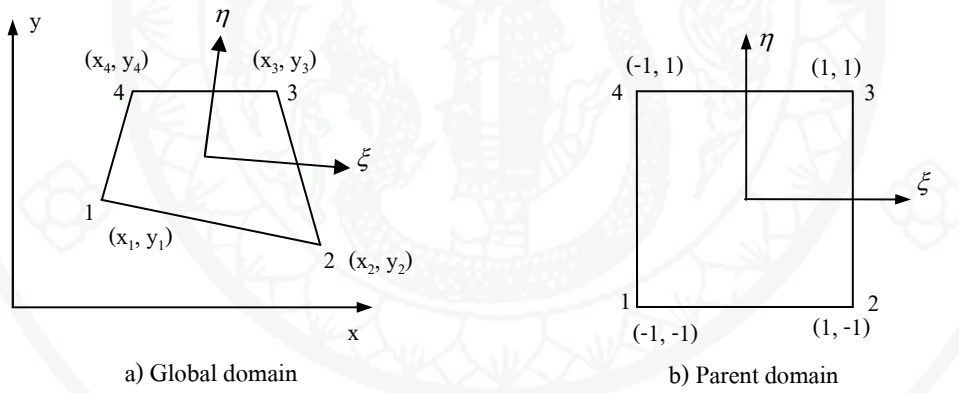


**Figure 12** Transformation from parent domain to global domain.

In the transformation between these two domains, it is required that one point in the parent domain should correspond to one point in the global domain and vice versa. To find this relationship, let $x$, $y$- coordinates are the function of parameter $a_i$ and $b_i$ as follows.

$$x = a_1 + a_2\xi + a_3\eta + a_4\xi\eta \tag{179}$$

$$y = b_1 + b_2\xi + b_3\eta + b_4\xi\eta \tag{180}$$

From Equation (179), substitution coordinate $x_i$ ($i$ = 1, 2, 3, 4) in $x$-$y$ coordinate system and coordinates $\xi_i$ and $\eta_i$ in natural coordinate system, and then solving for $a_1$, $a_2$, $a_3$ and $a_4$. The results are

$$a_1 = \frac{1}{4}\left(x_1 + x_2 + x_3 + x_4\right) \tag{181}$$

$$a_2 = \frac{1}{4}\left(-x_1 + x_2 + x_3 - x_4\right) \tag{182}$$

$$a_3 = \frac{1}{4}\left(-x_1 - x_2 + x_3 + x_4\right) \tag{183}$$

$$a_4 = \frac{1}{4}\left(x_1 - x_2 + x_3 - x_4\right) \tag{184}$$

Substitution of Equations (181) through (184) and rearrangement to yield

$$x = \frac{1}{4}(\xi-1)(\eta-1)x_1 - \frac{1}{4}(\xi+1)(\eta-1)x_2 + \frac{1}{4}(\xi+1)(\eta+1)x_3 - \frac{1}{4}(\xi-1)(\eta+1)x_4 \tag{185}$$

In a similar manner, the y coordinate can be written in terms of its nodal values as:

$$y = \frac{1}{4}(\xi-1)(\eta-1)y_1 - \frac{1}{4}(\xi+1)(\eta-1)y_2 + \frac{1}{4}(\xi+1)(\eta+1)y_3 - \frac{1}{4}(\xi-1)(\eta+1)y_4 \tag{186}$$

As a result, coordinate of $x$ and $y$ can be expressed in terms of their nodal values as:

$$x = \sum_{i=1}^{4} \mathbf{N}_i^e \mathbf{x}_i^e = \mathbf{N}^{e^{\mathbf{T}}} \mathbf{x}^{\mathbf{e}} \tag{187}$$

$$y = \sum_{i=1}^{4} \mathbf{N}_i^e \mathbf{y}_i^e = \mathbf{N}^{e^{\mathbf{T}}} \mathbf{y}^{\mathbf{e}} \tag{188}$$

where $\mathbf{x^e}$, $\mathbf{y^e}$ are matrices of $x_i$, $y_i$, respectively, and matrix of interpolation function $\mathbf{N}^e$ for the bilinear quadrilateral element in terms of natural coordinates involves:

$$N_1 = \frac{1}{4}(\xi-1)(\eta-1) \quad (189)$$

$$N_2 = -\frac{1}{4}(\xi+1)(\eta-1) \quad (190)$$

$$N_3 = \frac{1}{4}(\xi+1)(\eta+1) \quad (191)$$

$$N_4 = -\frac{1}{4}(\xi-1)(\eta+1) \quad (190)$$

As mentioned above, the isoparametric element, the approximate variable $\bar{u}$ can be written in terms of nodal values within the element and shape function in the same form as in *x*-*y* coordinate system. That is

$$\bar{u} = \sum_{i=1}^{4} \mathbf{N}_i^e \mathbf{u}_i^e = \mathbf{N}^{e^{\mathrm{T}}} \mathbf{u^e} \quad (193)$$

To determine the partial derivatives of $\bar{u}$, $\frac{\partial \bar{u}}{\partial x}$ and $\frac{\partial \bar{u}}{\partial y}$, the chain rule is applied to yield

$$\frac{\partial \bar{u}}{\partial x} = \frac{\partial \bar{u}}{\partial \xi}\frac{\partial \xi}{\partial x} + \frac{\partial \bar{u}}{\partial \eta}\frac{\partial \eta}{\partial x} \quad (194)$$

$$\frac{\partial \bar{u}}{\partial y} = \frac{\partial \bar{u}}{\partial \xi}\frac{\partial \xi}{\partial y} + \frac{\partial \bar{u}}{\partial \eta}\frac{\partial \eta}{\partial y} \quad (195)$$

However, the *x*,*y*-coordinates are written as a function of $\xi$ and $\eta$. It is convenient to find $\frac{\partial \bar{u}}{\partial \xi}$ and $\frac{\partial \bar{u}}{\partial \eta}$ by the chain rule as

$$\frac{\partial \bar{u}}{\partial \xi} = \frac{\partial \bar{u}}{\partial x}\frac{\partial x}{\partial \xi} + \frac{\partial \bar{u}}{\partial y}\frac{\partial y}{\partial \xi} \tag{196}$$

$$\frac{\partial \bar{u}}{\partial \eta} = \frac{\partial \bar{u}}{\partial x}\frac{\partial x}{\partial \eta} + \frac{\partial \bar{u}}{\partial y}\frac{\partial y}{\partial \eta} \tag{197}$$

which can be expressed in the form of matrix as follows;

$$\begin{bmatrix} \frac{\partial \bar{u}}{\partial \xi} \\ \frac{\partial \bar{u}}{\partial \eta} \end{bmatrix} = \begin{bmatrix} \frac{\partial x}{\partial \xi} & \frac{\partial y}{\partial \xi} \\ \frac{\partial x}{\partial \eta} & \frac{\partial y}{\partial \eta} \end{bmatrix} \begin{bmatrix} \frac{\partial \bar{u}}{\partial x} \\ \frac{\partial \bar{u}}{\partial y} \end{bmatrix} = \mathbf{J} \begin{bmatrix} \frac{\partial \bar{u}}{\partial x} \\ \frac{\partial \bar{u}}{\partial y} \end{bmatrix} \tag{198}$$

where

$$\mathbf{J} = \begin{bmatrix} \frac{\partial x}{\partial \xi} & \frac{\partial y}{\partial \xi} \\ \frac{\partial x}{\partial \eta} & \frac{\partial y}{\partial \eta} \end{bmatrix} \tag{199}$$

The matrix **J** is called the Jacobian matrix. The determinant of **J**, i.e., det **J**, is called the Jacobain.

$$\mathbf{J} = \begin{bmatrix} \frac{\partial x}{\partial \xi} & \frac{\partial y}{\partial \xi} \\ \frac{\partial x}{\partial \eta} & \frac{\partial y}{\partial \eta} \end{bmatrix} \tag{200}$$

From Equation (198), terms $\frac{\partial \bar{u}}{\partial x}$ and $\frac{\partial \bar{u}}{\partial y}$ can be determined by

$$\begin{bmatrix} \frac{\partial \bar{u}}{\partial x} \\ \frac{\partial \bar{u}}{\partial y} \end{bmatrix} = \mathbf{J}^{-1} \begin{bmatrix} \frac{\partial \bar{u}}{\partial \xi} \\ \frac{\partial \bar{u}}{\partial \eta} \end{bmatrix} \tag{201}$$

Terms $\frac{\partial \bar{u}}{\partial \xi}$ and $\frac{\partial \bar{u}}{\partial \eta}$ can be determined by;

$$\begin{bmatrix} \frac{\partial \bar{u}}{\partial \xi} \\ \frac{\partial \bar{u}}{\partial \eta} \end{bmatrix} = \begin{bmatrix} -\frac{1}{4}(1-\eta) & \frac{1}{4}(1-\eta) & \frac{1}{4}(1+\eta) & -\frac{1}{4}(1+\eta) \\ -\frac{1}{4}(1-\xi) & -\frac{1}{4}(1+\xi) & \frac{1}{4}(1+\xi) & \frac{1}{4}(1-\xi) \end{bmatrix} \begin{bmatrix} u_1 \\ u_2 \\ u_3 \\ u_4 \end{bmatrix} \tag{202}$$

The above equation is written in more compact form as

$$\begin{bmatrix} \frac{\partial \bar{u}}{\partial \xi} \\ \frac{\partial \bar{u}}{\partial \eta} \end{bmatrix} = \mathbf{D}_{\mathrm{N}} \begin{bmatrix} u_1 \\ u_2 \\ u_3 \\ u_4 \end{bmatrix} = \mathbf{D}_{\mathrm{N}} \mathbf{u}^{\mathrm{e}} \tag{203}$$

where

$$\mathbf{D}_{\mathrm{N}} = \begin{bmatrix} -\frac{1}{4}(1-\eta) & \frac{1}{4}(1-\eta) & \frac{1}{4}(1+\eta) & -\frac{1}{4}(1+\eta) \\ -\frac{1}{4}(1-\xi) & -\frac{1}{4}(1+\xi) & \frac{1}{4}(1+\xi) & \frac{1}{4}(1-\xi) \end{bmatrix} \tag{204}$$

In a similar manner, terms $\frac{\partial x}{\partial \xi}$, $\frac{\partial x}{\partial \eta}$, $\frac{\partial y}{\partial \xi}$, $\frac{\partial y}{\partial \eta}$ represented in terms of $x_i$ and $y_i$ can be written in the matrix form as follows;

$$\mathbf{J} = \begin{bmatrix} \frac{\partial x}{\partial \xi} & \frac{\partial y}{\partial \xi} \\ \frac{\partial x}{\partial \eta} & \frac{\partial y}{\partial \eta} \end{bmatrix} = \mathbf{D}_{\mathrm{N}} \begin{bmatrix} x_1 & y_1 \\ x_2 & y_2 \\ x_3 & y_3 \\ x_4 & y_4 \end{bmatrix} \tag{205}$$

Let

$$\mathbf{J} = \begin{bmatrix} \mathbf{J}_{11} & \mathbf{J}_{12} \\ \mathbf{J}_{21} & \mathbf{J}_{22} \end{bmatrix} \tag{206}$$

Inverse of $\mathbf{J}$ can be determined by

$$\mathbf{J}^{-1} = \frac{1}{|\mathbf{J}|}\begin{bmatrix} \mathbf{J}_{22} & -\mathbf{J}_{12} \\ -\mathbf{J}_{21} & \mathbf{J}_{11} \end{bmatrix} \quad (207)$$

where $|\mathbf{J}| = \mathbf{J}_{11}\mathbf{J}_{22} - \mathbf{J}_{12}\mathbf{J}_{21}$

The difference volume ($dA$) can be defind in term $d\xi$ and $d\eta$ as;

$$dA = |\mathbf{J}|\, d\xi\, d\eta \quad (208)$$

By transforming isoparametric element, element matrices can be calculated by using the numerical integration method according to the Guass integration scheme (sometimes termed Gauss-Legendre integration) as

$$\iint_{A^e} f(x,y)\,dxdy = \int_{-1}^{1}\int_{-1}^{1} f(\xi,\eta)|\mathbf{J}(\xi,\eta)|d\xi d\eta = \sum_{j=1}^{m}\sum_{i=1}^{n} W_i W_j f(\xi,\eta)|\mathbf{J}(\xi_i,\eta_j)| \quad (209)$$

where

| | |
|---|---|
| $m$ and $n$ | are the number of Gauss points; |
| $W_i$ and $W_j$ | are weights of Gauss points at $i$ = 1, 2, 3, 4 and $j$ = 1, 2, 3, 4, respectiverly; |
| $\xi_i$ , $\eta_j$ | are Gauss point locations; |
| $\|\mathbf{J}(\xi_i,\eta_j)\|$ | is the determinant of Jacobian matrix. |

In a case of rectangular element with $n = m = 2$, weights of Gauss points $W_i$ = 1 , $W_j$ = 1 and Gauss point locations are ;

$$\begin{bmatrix} \xi_1 & \eta_1 \\ \xi_2 & \eta_2 \\ \xi_3 & \eta_3 \\ \xi_4 & \eta_4 \end{bmatrix} = \begin{bmatrix} -1/\sqrt{3} & -1/\sqrt{3} \\ 1/\sqrt{3} & -1/\sqrt{3} \\ 1/\sqrt{3} & 1/\sqrt{3} \\ -1/\sqrt{3} & 1/\sqrt{3} \end{bmatrix}$$

In the finite element method, the study domain is divided into elements with nodal points. The variables and parameters at a point in each element are expressed in terms of the values at nodal points of that element. The matrices $\boldsymbol{M}$, $\boldsymbol{P}$ and $\boldsymbol{Q}$ in Eq.(111) and the matrices $\boldsymbol{M}$, $\boldsymbol{M}_x$, $\boldsymbol{M}_y$, $\boldsymbol{M}_v$ and $\boldsymbol{M}_b$ in Eq.(163) can be determined for each element which result in element matrices. These element matrices are then assembled to form system matrices.

**3. Computation Procedure**

Computation of suspended sediment transport and bedload transport will be made alternately using Eq.(111) and Eq.(163), respectively. The computation procedure and can be described as follows (Figure 13 to Figure 15):

1) From sediment sampling data, grain size of sediment particles and specific gravity are divided into groups. Let $D_j$ and $s_k$ be mean diameter and specific gravity of group *jk*. Total sediment load from watershed area is estimated. The load of each group is determined based on the grain size distribution data which are previously analyzed.

2) For each group of grain size and specific gravity, the terminal settling velocity is determined. Also, the sediment resuspension rate is estimated from some empirical formula. With these parameters together with flow velocity data, which are normally obtained from the hydrodynamic model, the matrices $\boldsymbol{M}$, $\boldsymbol{P}$ and $\boldsymbol{Q}$ in Eq.(111) can be computed.

3) Given initial values of suspended sediment concentrations at all nodal points in the study domain, the nodal concentrations at the next time step can be determined from Eq.(111).

4) From flow velocity data, water depth, wind and wave data at each nodal point, bed shear stress can be estimated. Then, Shields parameter $\theta_s$ is computed from Eq.(151). Also, the critical bed shear stress $\tau_{cr}$ and the critical Shields parameter $\theta_{cr}$ can be determined from Eq.(152). Then, the bedload transport rate factor $\Phi$ is computed from Eq.(150) and the rate of bedload transport rate per unit width $q_b^{jk}$ can be computed from Eq.(149).

5) At each nodal point, multiply $q_b^{jk}$ with bedload sediment bulk density and gravitational acceleration *g* to obtain the bedload transport rate $Q_n^{jk}$ in terms of weight per unit width per unit time.

6) Compute $Q_x^{jk}$ and $Q_y^{jk}$ from the following equations:

$$Q_x^{jk} = \frac{u}{|V|} Q_n^{jk} \tag{210}$$

and

$$Q_y^{jk} = \frac{v}{|V|} Q_n^{jk} \tag{211}$$

in which

*u* and *v* are current velocities in the *x* and *y* directions, respectively;

$|V| = \sqrt{u^2 + v^2}$ is overall current velocity.

8) Arrange the values of $Q_x^{jk}$ and $Q_y^{jk}$ at all nodal points on the bed to form matrices $\boldsymbol{Q_x^{jk}}$ and $\boldsymbol{Q_y^{jk}}$, respectively.

9) From the selected element configuration on the sea bed, determine element matrices and then assembled to the system matrices $\boldsymbol{M}$, $\boldsymbol{M_x}$, $\boldsymbol{M_y}$, $\boldsymbol{M_v}$ and $\boldsymbol{M_b}$ by using Eqs (164) – (168).

10) Given initial values of bedload sediment at all nodal points in the study domain, the nodal values at the next time step can be determined from Eq.(163).

11) Computation in the next time step is then repeated following the procedures from (2) to (9) described above.

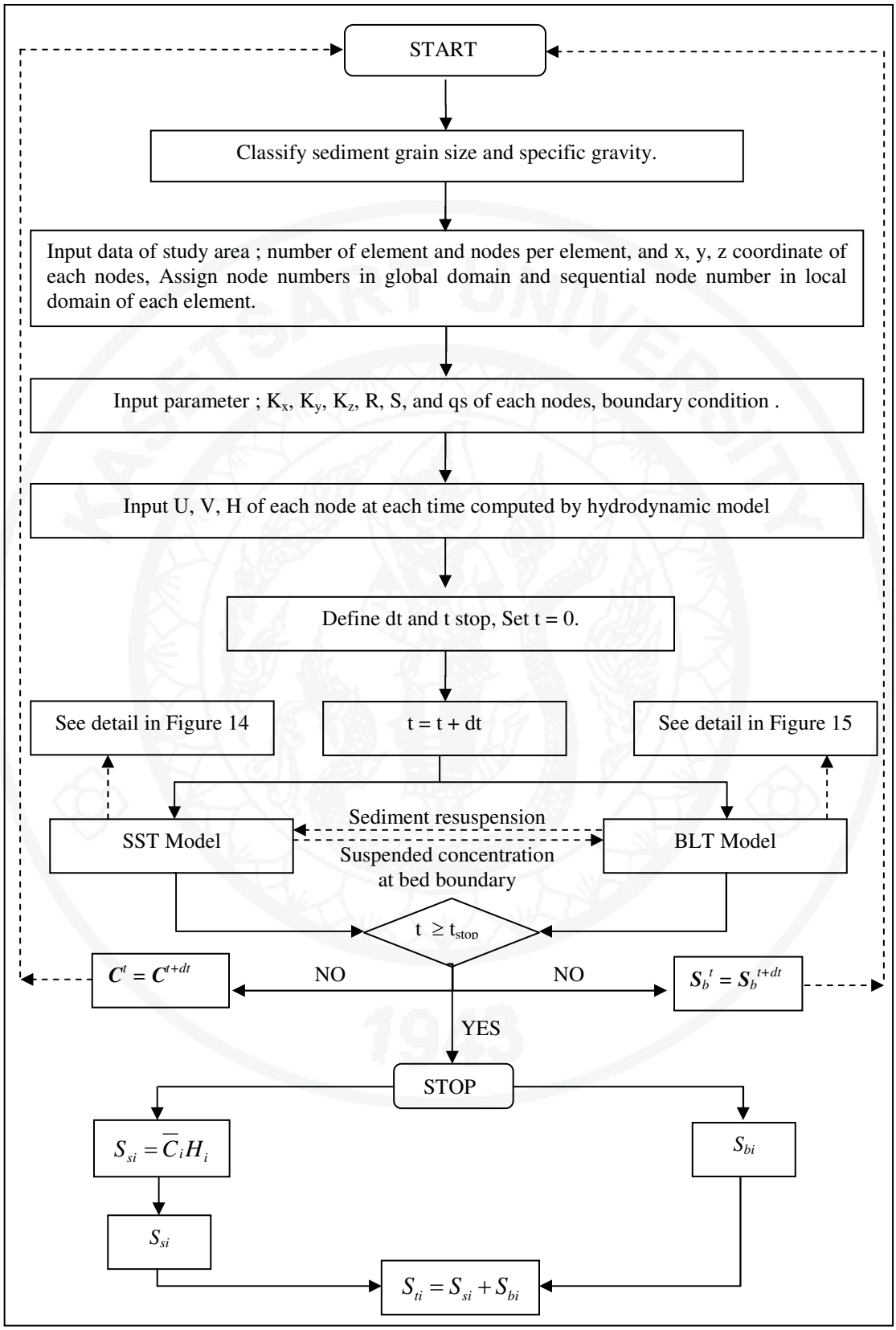


**Figure 13** computation procedure for sediment transport model.

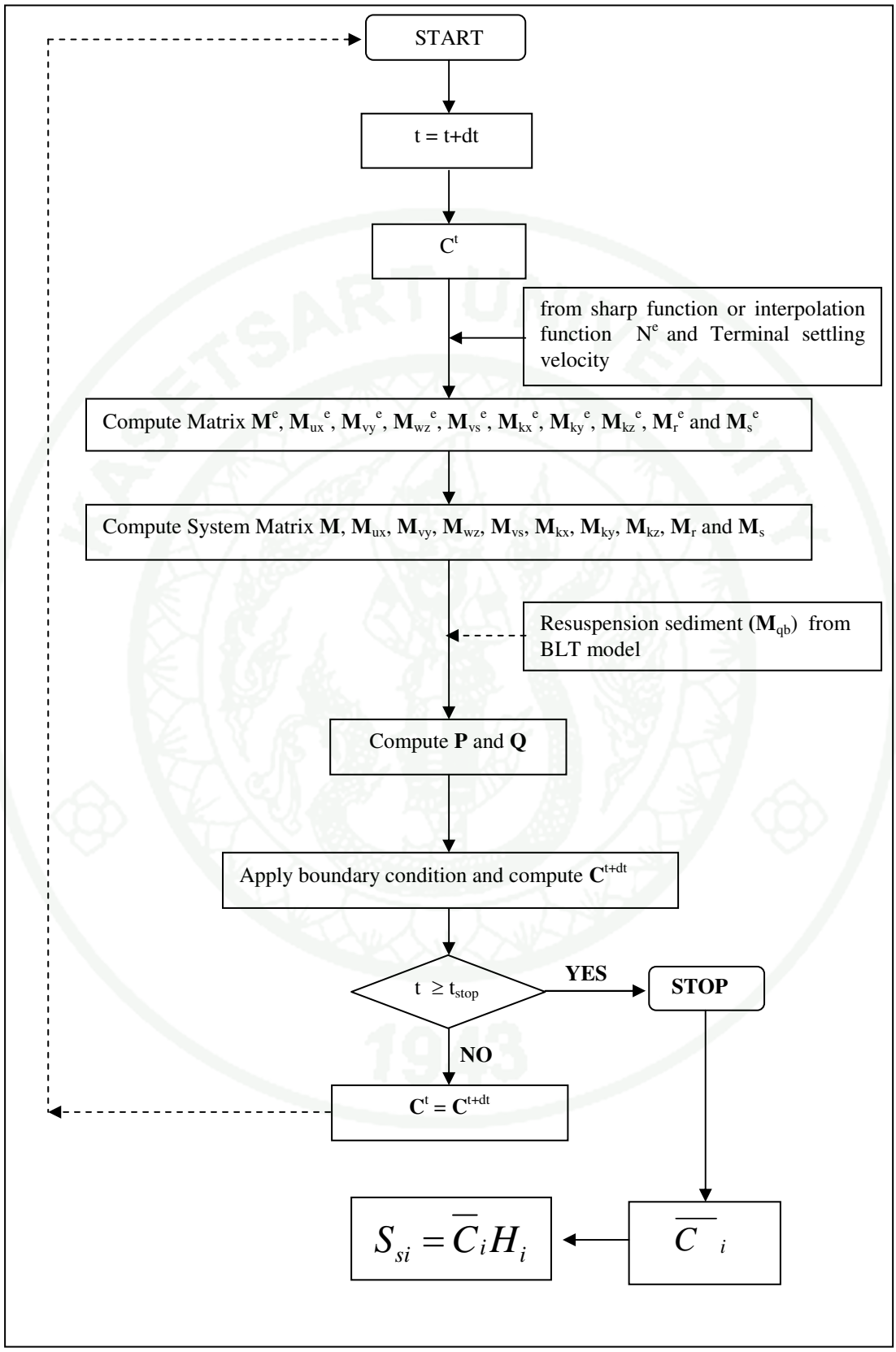


**Figure 14** computation procedure for suspended sediment transport (SST) model.

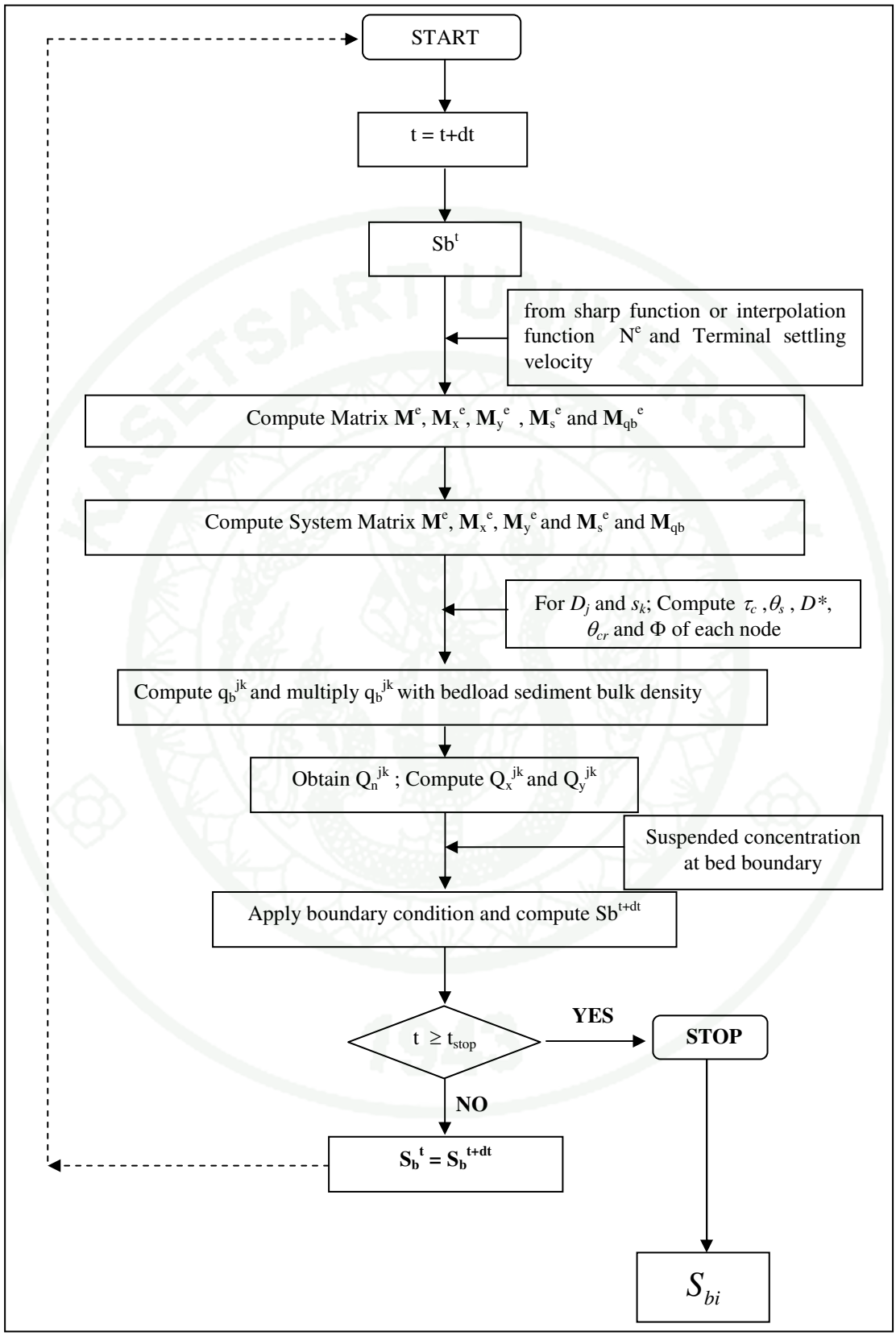


**Figure 15** computation procedure for bedload sediment transport (BLT) model.

## 4. Model Verification

For a uniform channel with constant flow velocity and assuming constant value of the dispersion coefficient, the substance balance equation can be written as

$$\frac{\partial c}{\partial t} + U\frac{\partial c}{\partial x} - K_x\frac{\partial^2 c}{\partial x^2} + Kc = 0 \qquad (212)$$

where $c$ is substance concentration;
$U$ is flow velocity in the $x$ axis;
$K_x$ is dispersion coefficient;
$K$ is the decaying rate of the substance;
$t$ is time.

Once, the initial and boundary conditions are specified, the solution of Eq.(212) can be obtained. The following cases are considered.

For a uniform channel with specified substance concentration at the upper end, Figure (16), the boundary and initial conditions are given by (Ogata and Banks, 1961)

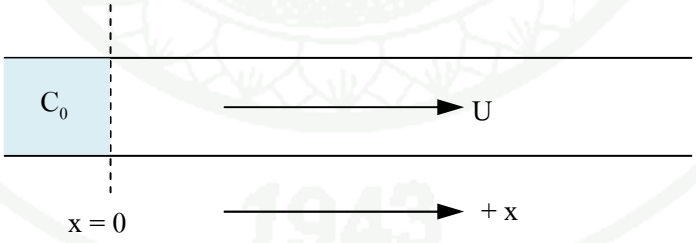


**Figure 16** Uniform channel with specified substance concentration at the upper end.

The boundary and initial conditions for uniform channel as shown in Figure 16 are given by :

$$c(0,t) = C_0 ; \qquad t \geq 0 \qquad (213)$$

$c(\infty,t) = 0 ; \qquad t \geq 0$ (214)

$c(x,t) = 0 ; \qquad x \geq 0$ (215)

For unsteady state can be determined substance concentration from Eq.(212) as: (Ogata and Banks, 1961)

$$\frac{c}{C_0} = \frac{1}{2}.e^{\frac{xU}{2K_x}}\left[\begin{array}{l}\exp\left(\frac{x}{2Kx}\sqrt{U^2+4K_xK}\right)erfc\left(\frac{x+\sqrt{U^2+4K_xK}.t}{\sqrt{4K_x.t}}\right)\\ +\exp\left(-\frac{x}{2K_x}\sqrt{U^2+4K_xK}\right)erfc\left(\frac{x-\sqrt{U^2+4K_xK}.t}{\sqrt{4K_x.t}}\right)\end{array}\right] \quad (216)$$

Verification for the developed sediment transport model is made by using a uniform cross-sectional channel with 20 km in length, 1 km in width, and 5 m in depth. The channel is divided into 20 rectangular elements with 42 nodal points. Each element has a length of 1 km and a width of 1 km as shown in Figure 17. The analytical results are also computed using Eq. (216) and Eq. (220) for the same case to test for validity of the developed model. The same values of flow velocity, dispersion coefficient and decaying rate are used in both model and analytical computation.

For model verification, the initial conditions are specified (Chao *et al*., 2008); the flow velocity in x direction is 0.03 m/s, dispersion coefficient in x direction are 30, 50 and 100 $m^2/s$, and decaying rate is 1.0 $day^{-1}$. The computation is started with substance concentration of 30 mg/L. In addition, flow velocity in the y direction is set to 0 m/s and the dispersion coefficient in the y direction is 0 $m^2/s$.

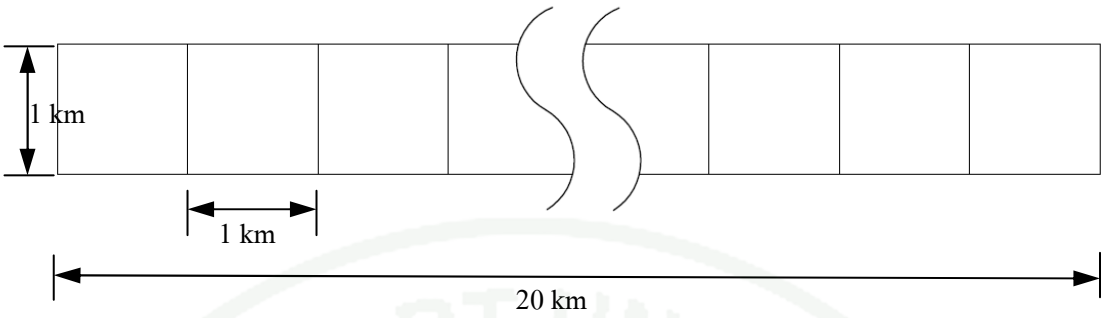


**Figure 17** Finite element grid of a uniform channel with specified concentration at one end.

In this verification, the time increments of 3,600 and 7,200 seconds respectively. The results of model verification depicted in Figures 18, 19 and 20. The substance concentration obtained from the developed model is quite close to the analytical solutions.

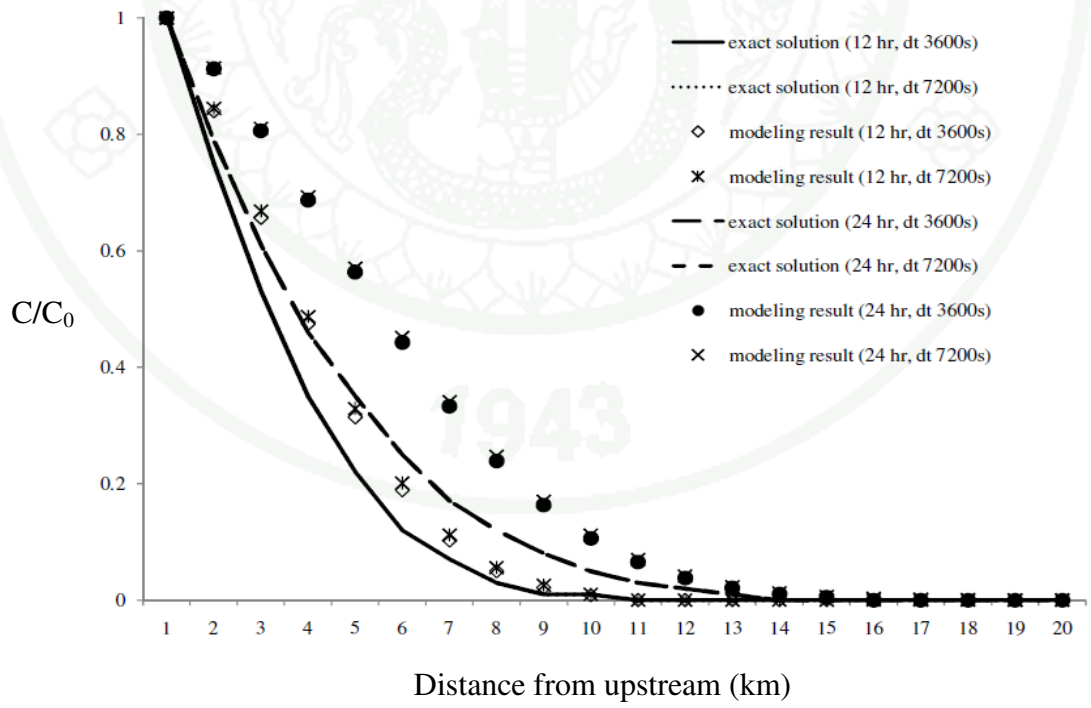


**Figure 18** Finite element grid for uniform channel with specified concentration at one end (Kx = 100 $m^2/s$).

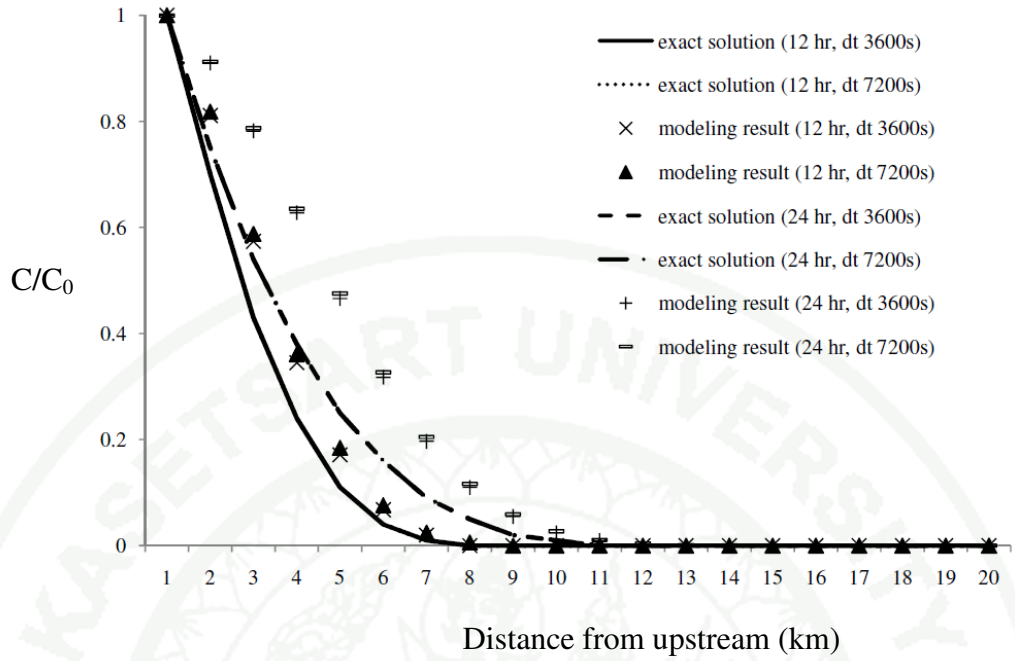


**Figure 19** Finite element grid for uniform channel with specified concentration at one end (Kx = 50 $m^2$/s).

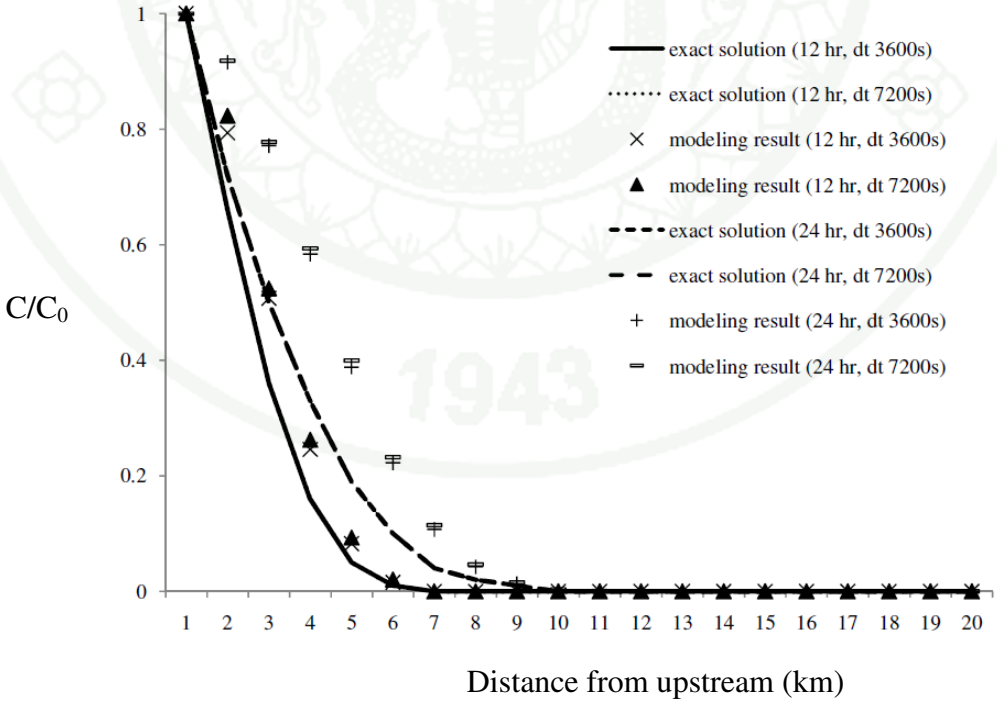


**Figure 20** Finite element grid for uniform channel with specified concentration at one end (Kx = 30 $m^2$/s).

## 5. Model Application

The developed model is applied to study sediment transport in the Songkhla Lake which is one of the most important water resources in the southern part of Thailand.

The Songkhla Lake is a natural lake (lagoon) located in the south of Thailand. It has very unique characteristics, with 3 water ecosystems, i.e. fresh water, brackish water and saline water. The lake covers about 1,042 $km^2$ whereas the catchment area covers about 8,754 $km^2$ consisting of 13 sub-basins. Water depth in the lake varies in the range of 1-4 m.

### 5.1 Suspended Sediment Sampling and Analyses

In this study, water samples are collected at 41 stations which include 16 stations in canals from the sub-basins and 25 stations inside the lake (Figure 21). The sediment is divided into 3 groups based on its grain size as shown in Table 3, since there is no significant difference in specific gravity of sediment from various sources. Total suspended solid concentrations obtained from field sampling are determined. The results are shown in Table 4, Table 5 and Figure 22.

**Table 3** Sediment grain size of water sampling.

| Sediment grain size (μm) | Typical (μm) | Percentage (%) |
|---|---|---|
| < 20 | 10 | 43.81 |
| 20-50 | 35 | 49.79 |
| 50-80 | 65 | 6.40 |

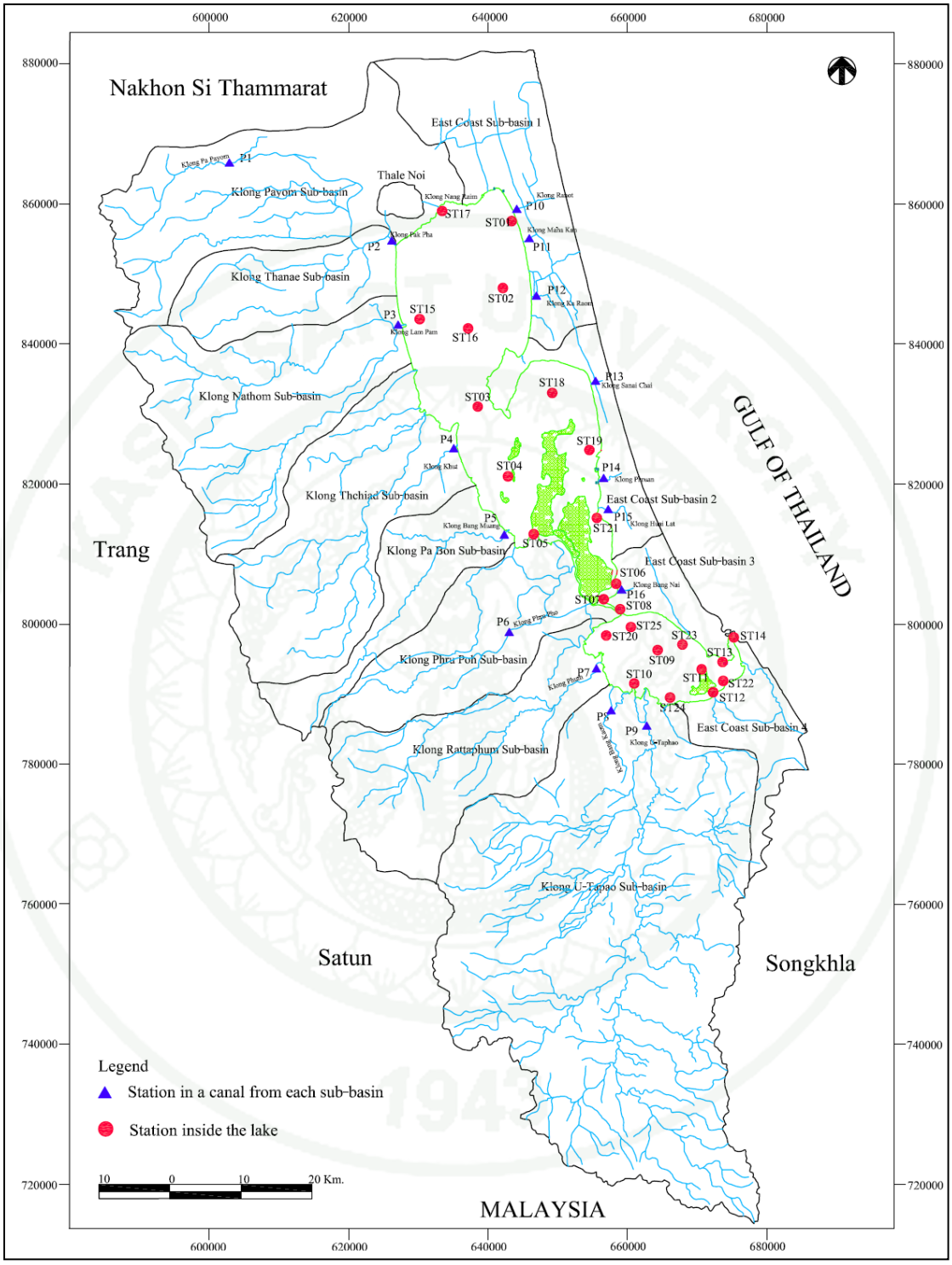


**Figure 21** Sampling stations in Songkhla Lake Basin.

**Table 4** Total suspended solids in Songkhla Lake Subbasin.

| Station | Subbasin | TSS (mg/L) | | | | |
|---|---|---|---|---|---|---|
| | | April 06 | June 06 | July 06 | Aug 06 | Sep 06 |
| P1 | Klong Pa Payom | 14.20 | 3.00 | 5.25 | 1.00 | 2.00 |
| P2 | Klong Thanae | 41.00 | 51.00 | 45.00 | 22.50 | 12.00 |
| P3 | Klong Nathom | 47.80 | 42.50 | 31.50 | 5.50 | 8.00 |
| P4 | Klong Tachiad | 28.20 | 17.50 | 11.75 | 12.50 | 6.00 |
| P5 | Klong Pa Bon | 26.40 | 13.00 | 24.00 | 2.50 | 4.00 |
| P6 | Klong Phru Poh | 16.20 | 18.00 | 9.75 | 2.50 | 3.75 |
| P7 | Klong Rattaphum | 89.00 | 42.50 | 32.50 | 7.50 | 8.75 |
| P8 | Klong Bang Klao (Bang Yee Tample) | 24.50 | 27.50 | 16.00 | 5.00 | 12.00 |
| P9 | Klong U-Tapao | 37.00 | 17.50 | 17.50 | 6.50 | 47.00 |
| P10 | Klong Ranot (East Coast 1) | | | | | 4.25 |
| P11 | Klong Maha Kan (East Coast 1) | | | | | 3.00 |
| P12 | Klong Ka Ram (East Coast 1) | | | | | 17.00 |
| P13 | Klong Sanam Chai (East Coast 2) | | | | | 8.25 |
| P14 | Klong Phruan (East Coast 2) | | | | | 20.00 |
| P15 | Klong Huai Lat (East Coast 2) | | | | | |
| P16 | ıg Nai (East Coast 3) | | | | | |

**Table 4** (Continued)

| Station | Subbasin | TSS (mg/L) | | | | | |
|---|---|---|---|---|---|---|---|
| | | Oct 06 | Nov 06 | Dec 06 | Jan 07 | Feb 07 | Mar 07 |
| P1 | Klong Pa Payom | 1.00 | 8.25 | 44.00 | 4.50 | 4.25 | 5.00 |
| P2 | Klong Thanae | 12.50 | 14.00 | 19.75 | 13.50 | 31.00 | 92.00 |
| P3 | Klong Nathom | 11.00 | 10.75 | 12.25 | 10.00 | 18.25 | 17.50 |
| P4 | Klong Tachiad | 12.50 | 8.50 | 8.25 | 4.75 | 31.00 | 24.00 |
| P5 | Klong Pa Bon | 8.50 | 13.50 | 10.75 | 6.00 | 23.25 | 4.25 |
| P6 | Klong Phru Poh | 13.50 | 6.25 | 27.00 | 5.25 | 6.50 | 20.50 |
| P7 | Klong Rattaphum | 15.00 | 25.00 | 58.50 | 33.25 | 20.00 | 7.83 |
| P8 | Klong Bang Klao (Bang Yee Tample) | 12.00 | 14.50 | 15.00 | 15.25 | 18.50 | 8.50 |
| P9 | Klong U-Tapao | 22.50 | 7.25 | 9.00 | 7.50 | 13.50 | 15.00 |
| P10 | Klong Ranot (East Coast 1) | 74.50 | 37.50 | 51.50 | 34.50 | 46.50 | 24.50 |
| P11 | Klong Maha Kan (East Coast 1) | 38.00 | 15.00 | 34.50 | 35.50 | 62.17 | 52.50 |
| P12 | Klong Ka Ram (East Coast 1) | 53.00 | 20.00 | 22.00 | 59.00 | 49.00 | 57.00 |
| P13 | Klong Sanam Chai (East Coast 2) | 24.75 | 34.00 | 26.50 | 13.75 | 30.00 | 27.00 |
| P14 | Klong Phruan (East Coast 2) | 42.00 | 16.50 | 20.00 | 21.00 | 12.75 | 4.17 |
| P15 | Klong Huai Lat (East Coast 2) | | | | | | 23.50 |
| P16 | Klong Bang Nai (East Coast 3) | | | | | | 16.25 |

**Table 5** Total suspended solids in Songkhla Lake.

| Station* | Area | TSS (mg/L) | | |
|---|---|---|---|---|
| | | Sep 06 | Dec 06 | Feb 07 |
| ST01 | Thale Luang | 6.25 | 29.50 | 41.50 |
| ST02 | Thale Luang | 29.00 | 19.00 | 25.00 |
| ST03 | Thale Luang | 101.50 | 26.50 | 108.00 |
| ST04 | Thale Sab | 1.00 | 61.00 | 87.00 |
| ST05 | Thale Sab | 12.50 | 17.00 | 41.00 |
| ST06 | Thale Sab | 114.50 | 14.00 | 31.67 |
| ST07 | Thale Sab | 20.25 | 15.00 | 51.00 |
| ST08 | Thale Sab | 13.25 | 13.25 | 92.00 |
| ST09 | Thale Sab Songkhla | 10.25 | 17.00 | 11.83 |
| ST10 | Thale Sab Songkhla | 25.50 | 12.50 | 66.50 |
| ST11 | Thale Sab Songkhla | 40.50 | 7.00 | 28.00 |
| ST12 | Thale Sab Songkhla | 7.50 | 14.00 | 13.00 |
| ST13 | Thale Sab Songkhla | 20.00 | 5.25 | 70.75 |
| ST14 | Thale Sab Songkhla | 19.75 | 21.50 | 11.25 |
| ST15 | Thale Luang | 26.50 | 16.50 | 46.50 |
| ST16 | Thale Luang | 47.00 | 29.00 | 31.00 |
| ST17 | Thale Luang | 17.75 | 8.00 | 61.00 |
| ST18 | Thale Sab | 150.50 | 11.00 | 153.00 |
| ST19 | Thale Sab | 65.50 | 23.00 | 174.50 |
| ST20 | Thale Sab Songkhla | 11.50 | 22.00 | 58.50 |
| ST21 | Thale Sab | 17.50 | 46.50 | 86.00 |
| ST22 | Thale Sab Songkhla | 9.00 | 16.75 | 16.75 |
| ST23 | Thale Sab Songkhla | 8.75 | 2.25 | 20.50 |
| ST24 | Thale Sab Songkhla | 14.00 | 14.00 | 5.25 |
| ST25 | Thale Sab Songkhla | 12.50 | 19.25 | 49.50 |

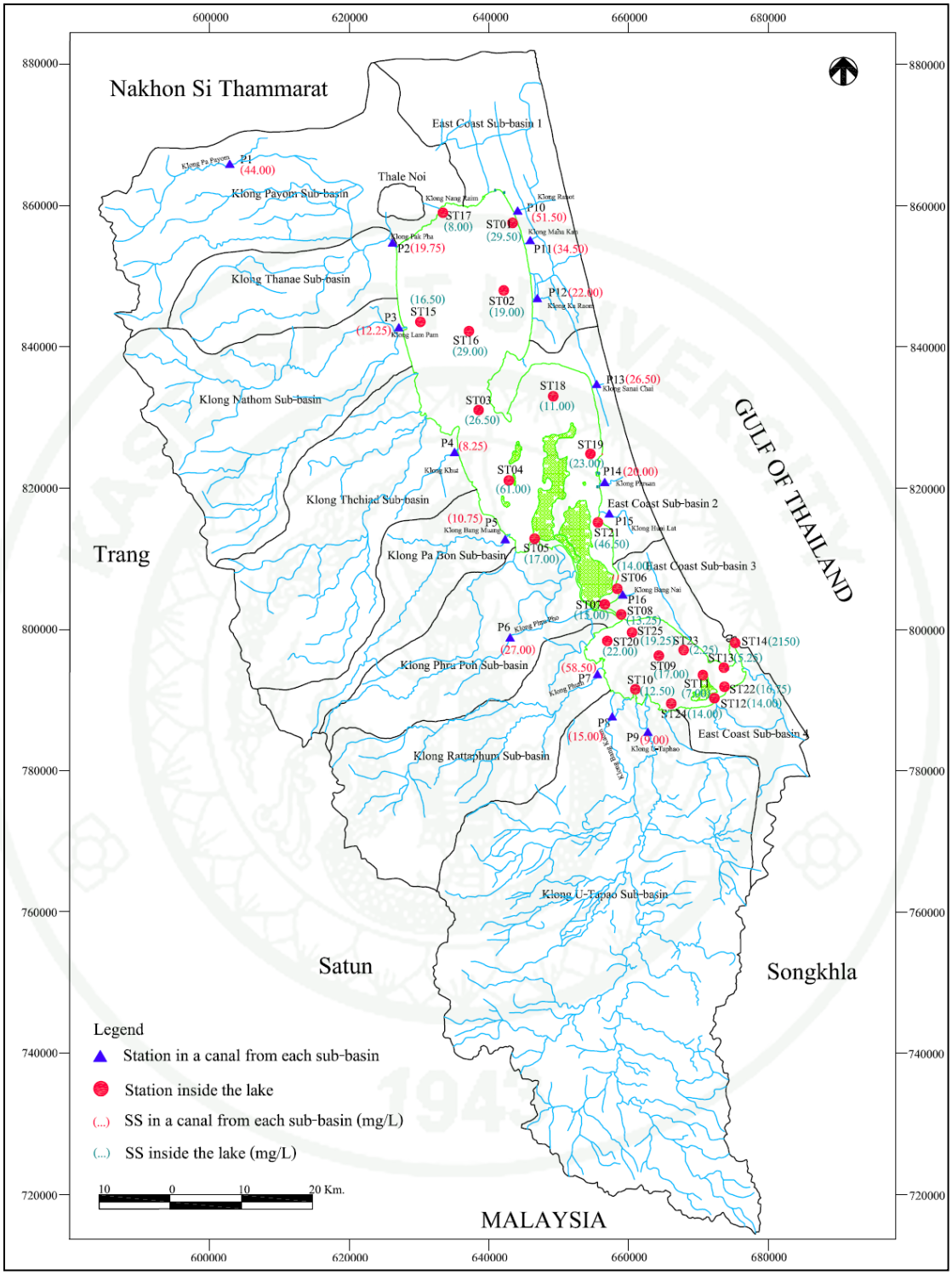


**Figure 22** Suspended Solids in Songkhla Lake Basin, December (2006).

## 5.2 Element Configuration

In this study, the hexahedral elements are used for the three-dimensional suspended sediment transport (SST) model and the bilinear quadrilateral elements are used for the two-dimensional bedload transport (BLT) model. The total area of 1,042 $km^2$ of Songkhla lake is divided into 414 hexahedral elements with 880 nodal points. The bottom boundary of the lake projected on a horizontal plane is divided into 138 bilinear quadrilateral elements with 220 nodal points as shown in Figure 23.

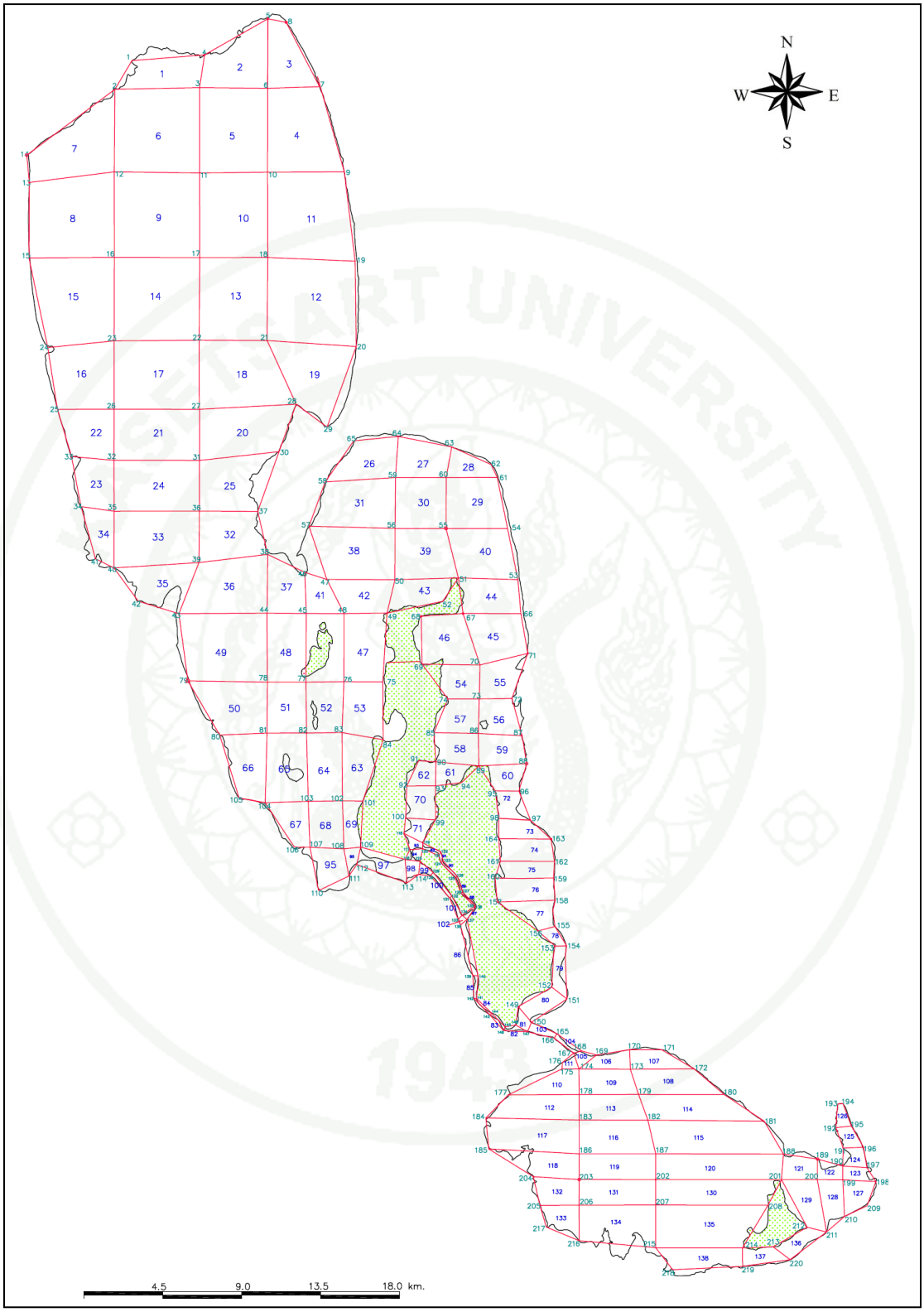


**Figure 23** Element configuration on Songkhla Lake.

## 5.3 Model Input Data

Besides coordinates of all nodal points in the study domain, the sediment transport model requires data on flow velocities at each nodal point, water depth, sediment load and sediment resuspension rate (for each group of grain size). Since the Songkhla Lake is a shallow lake, the vertically average hydrodynamic model is used to simulate flow velocities *u* and *v* and water depth *h* at nodal points of the isoparametric elements on the bottom plane while the vertical component of velocity *w* is neglected. Data on suspended sediment concentrations obtained from field sampling are used as initial values of the SST model. Initial values of bedload sediment are assumed for all groups of grain size equal zero. So, the results obtained from the BLT model will reveal whether there occurs accumulation or erosion of bedload sediment at the nodal point by comparing the computed bedload amount with the assumed initial values. In this study, the effect of wind driven wave is not considered due to the lack of reliable wind data.

The mean depth of the Songkhla Lake is rather low, so the average depth model is reasonably applied to the lake. The dispersion and advection values are equal for all direction i.e., Kx = Ky = Kz = 100 $m^2/s$. The equation to calculate the parameter which use in model application is shown in Table 6. The variable values associated with the model are listed in Table 7.

**Table 6** Equation for Parameter and variable in model application.

| Parameter/variable | Equation |
|---|---|
| Bed shear stress ( $\tau_b$ )[1] | $\tau_b = \rho C_D V_h^2$ |
| Shield parameter ( $\theta$ )[2] | $\theta = \frac{\tau_b}{(\rho_s - \rho)gD}$ |
| Critical Shield parameter ( $\theta_{cr}$ )[2] | $\theta_{cr} = \frac{0.3}{1+1.2D^*} + 0.055\left[1 - \exp\left(-0.02D^*\right)\right]$ |
| Critical shear stress ( $\tau_{cr}$ )[2] | $\theta_{cr} = \frac{\tau_{cr}}{(\rho_s - \rho)gD}$ |
| bedload transport rate factor ( $\Phi$ )[2] | $\Phi = \frac{q_b}{\left[g(s-1)D^3\right]^{\frac{1}{2}}}$ |
| [3] | $\Phi = 12\theta_s^{\frac{1}{2}}(\theta_s - \theta_{cr})$ |
| Terminal settling velocity ( $vs$ )[4] | $vs = \frac{(s-1)gD^2}{18\upsilon}$ for $1 < D \leq 100$ μm |
| Sediment resuspension rate[5] | $E_b = 0$ for $\tau_b < \tau_{cr}$ |
| | $E_b = M\left(\frac{\tau_b}{\tau_{ce}} - 1\right)$ for $\tau_b > \tau_{cr}$ |

**Sources :** [1] Reeve *et al*. (2004)

[2] Shields (1936)

[3] Nielsen (1992)

[4] Van Rijn (1993)

[5] Partheniades E (1965)

**Table 7** Variables values associated with the model.

| Variables | Values |
|---|---|
| Specific gravity (s) | 1.06 |
| Water density (ρ) | $1.026 \times 10^3$ g/m$^3$ |
| Particle density ($\rho_s$) | $2.65 \times 10^3$ g/m$^3$ |
| Acceleration due to gravity (g) | 9.81 m/s$^2$ |
| Kinematic viscosity (υ) | $1.19 \times 10^{-6}$ m$^2$/s |

From Table 6, Table 7 as well as values of *u* and *v* from a hydronamic model, we can calculate bed shear stress ($\tau_b$), Shields parameter ($\theta$), bedload transport rate factor ($\Phi$) and sediment resuspension rate at each nodal point at various time. For sediment grain size, we can calculate critical Shields parameter ($\theta_{cr}$), critical shear stress ($\tau_{cr}$) and terminal settling velocity (*vs*) as shown in Table 8.

**Table 8** Values of variables associated with sediment grain size.

| Variable | Values for each sediment grain size | | |
|---|---|---|---|
| | 10 μm | 35 μm | 65 μm |
| Critical Shields parameter ($\theta_{cr}$) | 0.2754 | 0.2287 | 0.1902 |
| Critical shear stress ($\tau_{cr}$): N/m$^2$ | 0.0446 | 0.1296 | 0.2001 |
| Terminal settling velocity (*vs*): m/s | $2.7479 \times 10^{-6}$ | $3.3662 \times 10^{-5}$ | $1.1610 \times 10^{-4}$ |

All parameters and variables as mentioned above are used for model application in the Songkhla Lake. In addition, sediment loading is drained to the lake at some elements as shown in Table 9.

**Table 9** Sediment loading in the Songkhla lake

| Subbasin | Element number of draining | Sediment loading (g/s) | | | | | | | | | | | |
|---|---|---|---|---|---|---|---|---|---|---|---|---|---|
| | | Jan | Feb | Mar | Apr | May | June | Jul | Aug | Sep | Oct | Nov | Dec |
| Pa Payom and Thanae | 7 | 0.012 | 0.011 | 0.013 | 0.037 | 0.008 | 0.008 | 0.014 | 0.003 | 0.005 | 0.003 | 0.021 | 0.115 |
| Nathom | 16 | 0.016 | 0.036 | 0.106 | 0.047 | 0.059 | 0.059 | 0.052 | 0.026 | 0.014 | 0.014 | 0.016 | 0.023 |
| Thachiad | 23 | 0.021 | 0.039 | 0.038 | 0.103 | 0.091 | 0.091 | 0.068 | 0.012 | 0.017 | 0.024 | 0.023 | 0.026 |
| Pa Bon | 67 | 0.008 | 0.049 | 0.038 | 0.045 | 0.028 | 0.028 | 0.019 | 0.020 | 0.010 | 0.020 | 0.014 | 0.013 |
| Phru Poh | 82 | 0.230 | 0.893 | 0.163 | 1.014 | 0.499 | 0.499 | 0.922 | 0.096 | 0.154 | 0.327 | 0.519 | 0.413 |
| Rattaphum | 132 | 0.030 | 0.037 | 0.118 | 0.093 | 0.104 | 0.104 | 0.056 | 0.014 | 0.022 | 0.078 | 0.036 | 0.156 |
| U-Tapao | 134 | 0.373 | 0.224 | 0.088 | 0.998 | 0.477 | 0.477 | 0.365 | 0.084 | 0.098 | 0.168 | 0.280 | 0.656 |
| U-Tapao | 134 | 0.255 | 0.359 | 0.264 | 0.690 | 0.505 | 0.505 | 0.376 | 0.129 | 0.662 | 0.387 | 0.244 | 0.269 |

The sediment transport in the Songkhla lake is simulated based on current flow data and sediment load data in November 2006 which is the rainy season in this region. The results obtained from the model show the total sediment transport in Figure 24, suspended sediment and bedload sediment transport in Figure 25 and Figure 26, respectively. The average sediment transport is equal to 537 $g/m^2$ and total sediment is equal to 559,121 tons. However, run off in 2006 which drained to the Songkhla Lake is equal to 4,896 million cubic meters or 155 cubic meters per second (Royal Irrigation Department, 2009). ONEP (2006) used empirical formulation to calculate the sediment inflow to the Songkhla Lake which is equal to 498,738 tons. Therefore the total sediment from model is more than the sediment inflow only 1.3 times.

Suspended sediment transport rate is approximately 488 $g/m^2$, it is different for various area. The suspended sediment transport is usually high around the drainage points and decreasing by distances. Sediment grain size effect on sediment transport due to there affect to terminal settling velocities and sediment resuspension from bottom. From these reason, the terminal settling velocities varies with sediment grain size. Resuspension sediment, the important factor affecting suspended sediment transport rate is increasing. Then, the area which has resuspended sediment occur, the suspended sediment transport rate is higher than other area such as the Middle Songkhla lake.

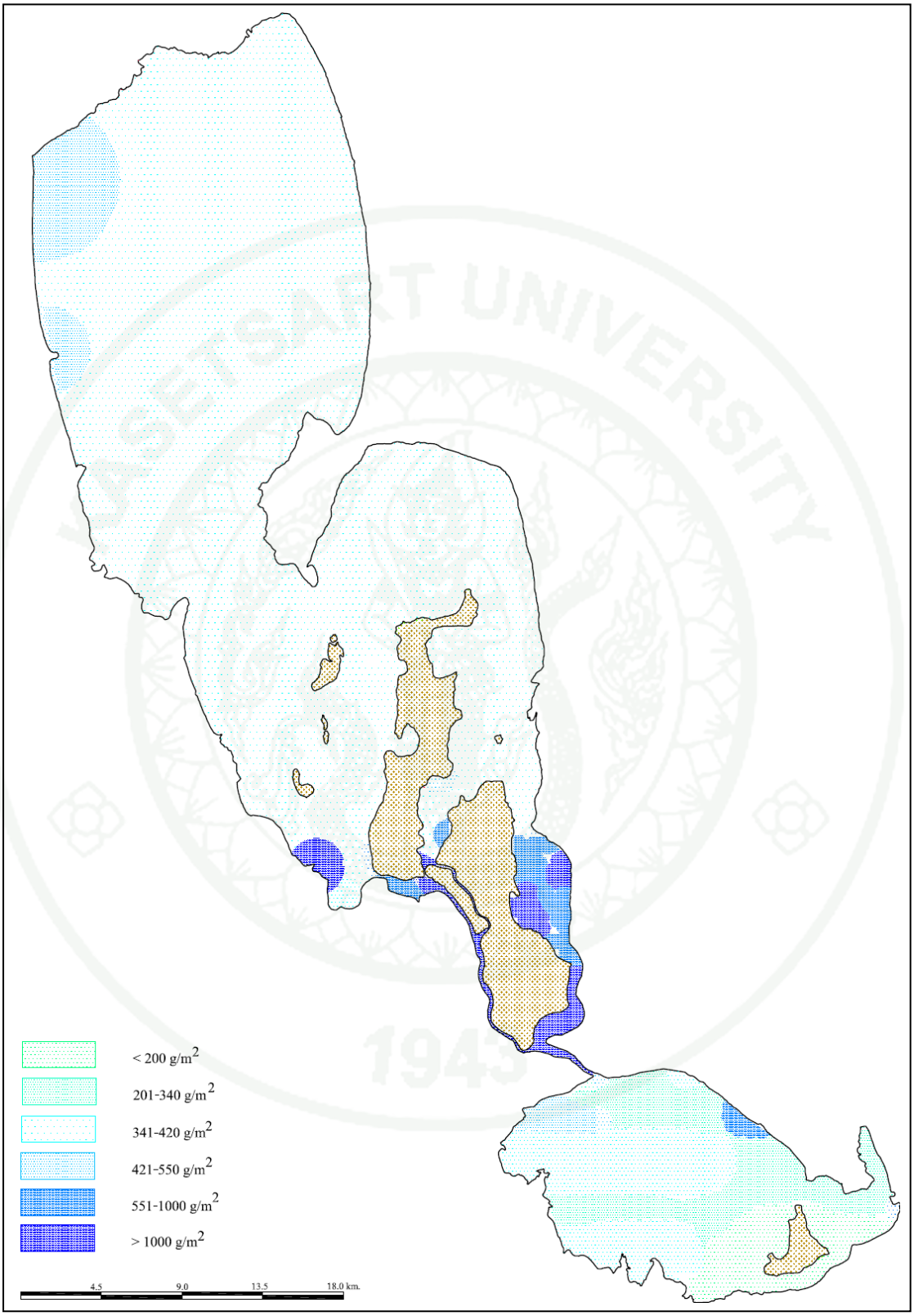


**Figure 24** Total sediment transport (g/m$^2$) in Songkhla lake.

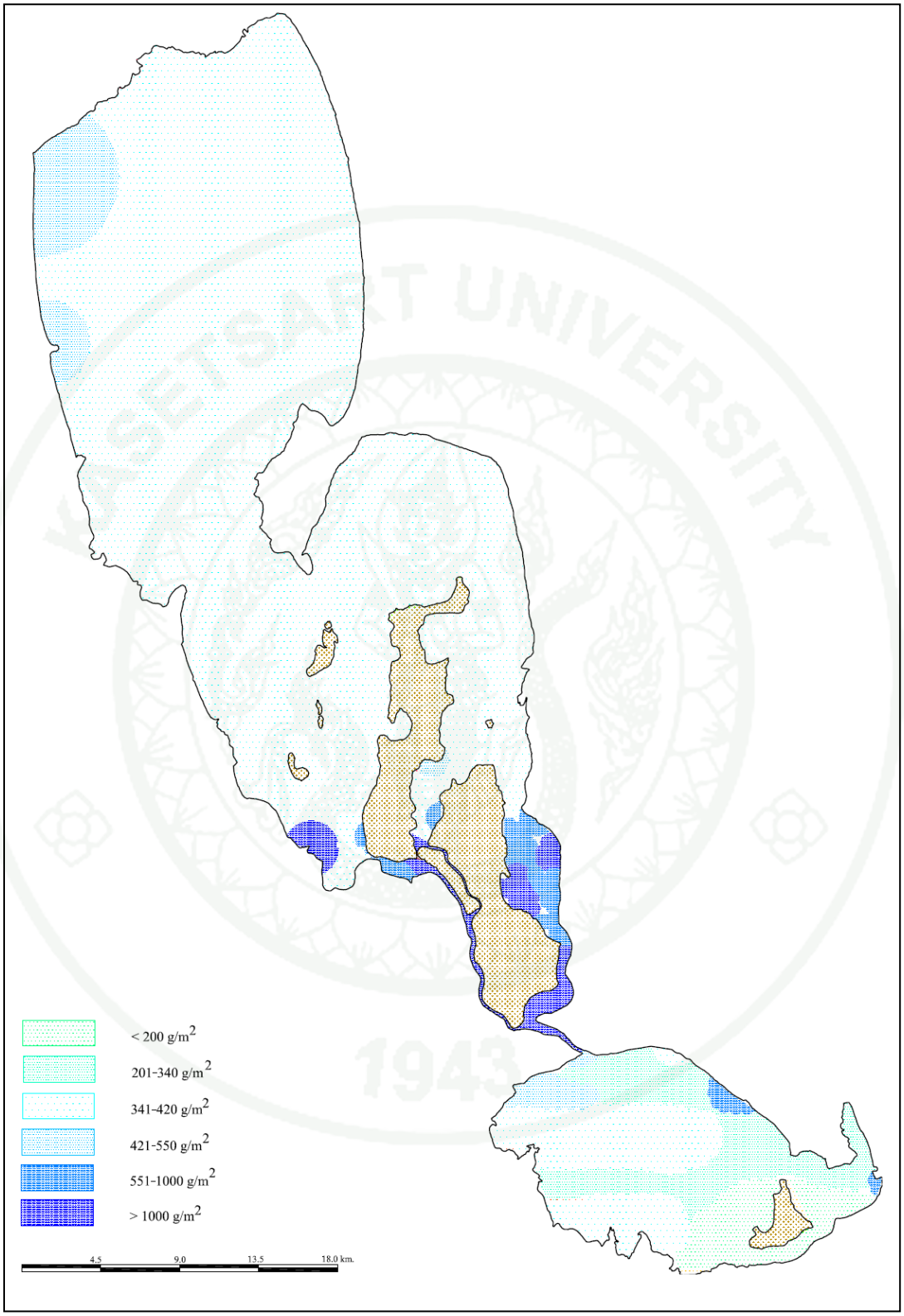


**Figure 25** Suspended sediment transport ($g/m^2$) in Songkhla lake.

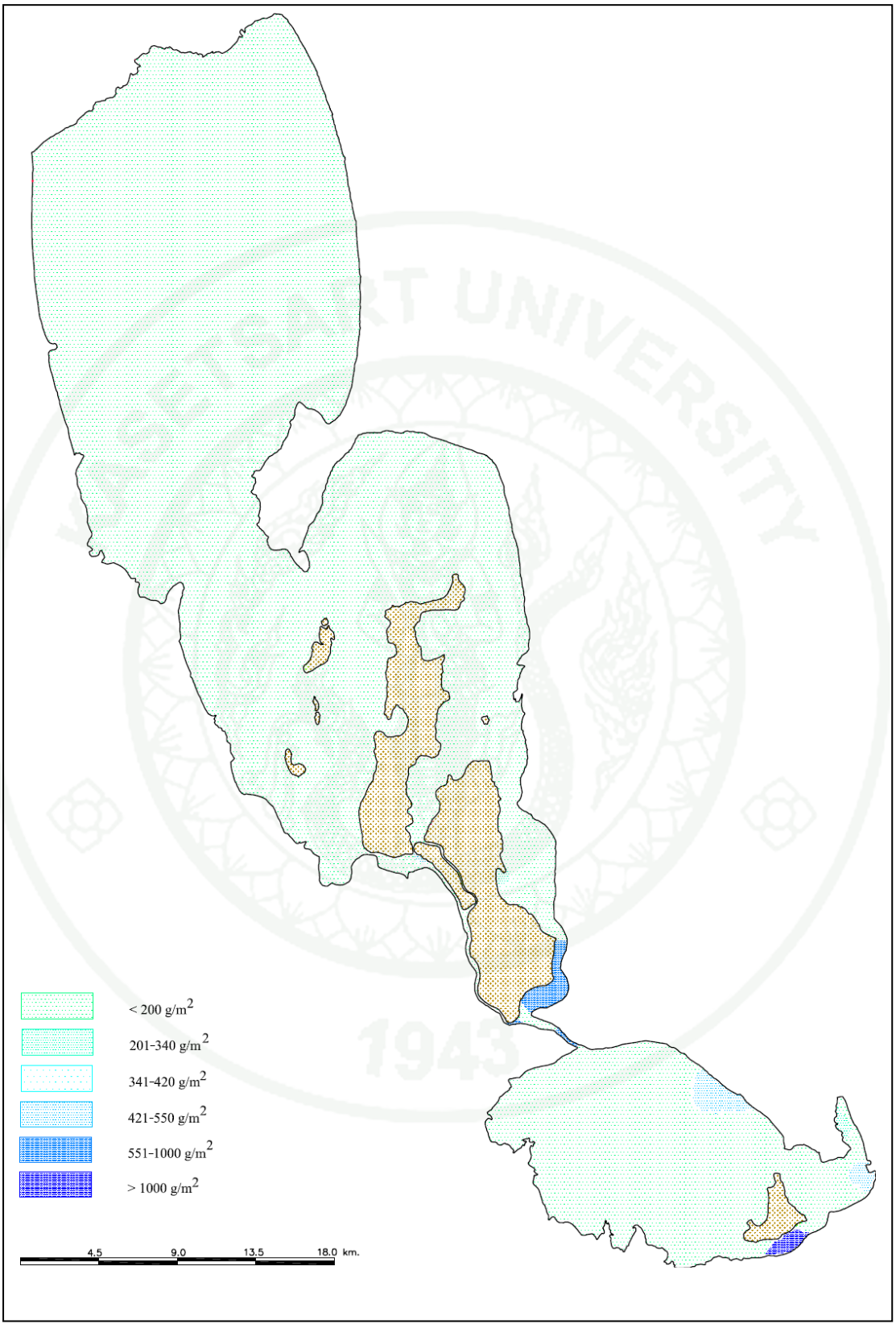


**Figure 26** Bedload sediment transport ($g/m^2$) in Songkhla lake.

Bedload sediment transport rate is approximately 48 g/m$^2$. Due to bedload sediment transport depend on bed shear stress ( $\tau_b$ ), Shields parameter ( $\theta$ ), critical Shields parameter ( $\theta_{cr}$ ), bedload transport rate factor ( $\Phi$ ), if Shields parameter ( $\theta$ ) of the sediment more than critical Shields parameter ( $\theta_{cr}$ ) then sediment transport will occur. Moreover, resuspension sediment can occur if the bed shear stress ( $\tau_b$ ) more than critical shear stress ( $\tau_{cr}$ ), then its is a sink of bedload sediment. However, both suspended sediment and bedload sediment transport are depended on sediment grain size ($D$) and specific gravity ($s$).

The sediment transport rate in the Songkhla Lake is high amount in the areas near the coastline of the lake. It is found that there is still some difference between the simulated results and the field sampling data. This might be caused by significant difference in the resuspension rate used in the model and the rate actually occurred in the lake. Wind wave might have significant effect on the resuspension rate because the lake is very shallow. So, reliable wind data should be used in the simulation.

# CONCLUSION AND RECOMMENDATION

1) In this study, a sediment transport model is developed in which suspended sediment and bedload sediment are interrelated to each other. The developed sediment transport model is a reliable, appropiate and effective tool for determine sediment transport in the Songkhla Lake with unsteady flow and multiple discharge points. Moreover, the developed model is an effective tool for predicting sediment transport pattern in the future.

2) Sediment grain size and specific gravity are important parameters affecting settling rate of suspended sediment and resuspension of bedload sediment which are significant source and sink terms of the sediment transport model. Therefore, in this study the sediment load from various sources are divided into groups based on its grain size and specific gravity. Then, transport pattern of each group is calculated and combined together to get the total amount of suspended sediment and bedload sediment at each location (nodal point) in the study domain. With this technique, the transport pattern simulated from the model is expected to be more realistic.

3) The finite element method is used in model development in this study. Three-dimensional model is developed for the suspended sediment transport model whereas two-dimensional model is developed for the bedload transport model. The bottom boundary of the suspended load transport study domain projected on the horizontal plane is used as the study domain of the bedload transport model.

4) The sediment transport process which has occurred in the past affects distribution patterns of both suspended sediment and bedload sediment at present. In order to simulate the sediment transport patterns in the future, it is necessary that reliable initial values which are suspended sediment and bedload sediment distributions at present or at the beginning of the simulation time (t = 0) are given. Field sampling and analyses are needed to collect these data.

5) For shallow water body like the Songkhla lake, wind driven wave plays an important role on sediment transport. Therefore, detailed study on wind data and wave generation by wind is necessary so as to obtain a reliable sediment transport model.

6) The developed model will be considered as a useful tool for predicting the sediment transport in the Songkhla lake basin, which is important component for water quality and ecology simulations.

# LITERATURE CITED

Aksoy, H. and Kavvas, M.L. 2005. A review of hillslope and watershed scale erosion and sediment transport models. **Catena**. 64: 247-271.

American Public Health Association, American Water Works Association, water Environment Federation. 1998. Standard Methods for the Examination of Water and Wastewater. 20th Ed. .

Brebbia, C.A. 1953. **The Boundary Element Method for Engineers**. Wiley, New York.

Brooks, K.N., Ffolliott, P.F., Gregersen, H.M. and Thames, J.L. 1991. **Hydrology and the management of watershed**. Iowa State University Press, USA.

Camenen, B., and Larson, M. 2005. A general formula for non-cohesive bed load sediment transport. **Estuarine, Coastal and Shelf Sciences**. 63: 249-260.

Chao, X., Jia, Y., Shields, D., Wang S.S.Y., and Cooper, C.M., 2008. Three-dimensional numerical modeling of cohesive sediment transport and wind wave impact in a shallow oxbow lake. **Advances in Water Resources**. 31: 1004-1014.

Chapra, S.C. 1997. **Surface Water-Quality Modeling**. The McGraw-Hill Companies, Inc., Singapore.

Chittrakarn, T., Bhongsuwan, T., Nunnin, P. and Thong-jerm, T. 1996. **The determination of sedimentation rate in Songkhla Lake using Isotopic Technique.** Physics Department, Faculty of Science, Prince of Songkhla University.

Conner, J.J. and C.A. Brebbia. 1976. **Finite Element Techniques for Fluid Flow**. Newnes Butterworths, London.

Danielsson, A. Jonsson, A. and Rahm, L. 2007. Resuspension patterns in the Baltic proper. **Journal of Sea Research**. 57: 257-269.

Don, N. Cao., Araki, H., Yamanishi, H., Ohgushi, K., Hang, N. T. Minh. and Tokunaga, T. 2007. Sediment Transport and Short-term Sedimentation Processes in the Tidal Flats of the Ariake Sea, West Coast of Kyushu, Japan. **Journal of Coastal Research**. SI 50: 837-841.

Folly, A., Quinton, J.N. and Smith, R.E. 1999. Evaluation of the EUROSEM model using data from the Catsop watershed, the Netherlands. **Catena**. 37: 507-519.

Hakanson, L., Gyllenhammar, A. and Brolin, A. 2004. A dynamic compartment model to predict sedimentation and suspended particulate matter in coastal areas. **Ecological Modelling.** 175: 353-384.

Heppner, C.S., Ran, Q., VanderKwaak, J.E. and Loague, K. 2006. Adding sediment transport to the integrated hydrology model (InHM) : Development and testing. **Advances in Water Resources**. 29: 930-943.

Hu, K., Ding, P., Wang, Z. and Yang, S. 2009. A 2D/3D hydrodynamic and sediment transport model for the Yangtze Estuary, China. **Journal of Marine Systems**. 77: 114-136.

Huebner, K.H, Thornton, E.A, Byrom, T.G. 1995. **Elements and interpolation functions**. In: The Finite Element Method for Engineers, 3rd edn. Wiley-Interscience Publication, New York.

Hutton, D.V. 2004. **Method of weighted residuals**. **In: Fundamentals of finite element analysis**, Int edn. McGraw-Hill, New York.

Ippen, A.T. 1966. **Estuary and Coastline Hydrodynamics**. McGraw-Hill book company, Inc. USA.

John Taylor and Sons. 1985. **Songkhla Lake Basin Plining Study: Final Report**. Submitted to National Economic and Social Development Boaed and National Environal Environment Board.

Lewis, P. E. and J. P. Ward. 1991. **The Finite Element Method, Principles and Applications**. Addison-Wesley Publishing Company, London.

Li, M., Pan, S. and O'Connor, B. A. 2008. A two-phase numerical model for sediment transport predictionunder oscillatory sheet flows. **Coastal Engineering**. 55: 1159-1173.

Liengcharernsit, W. 1979. **Mathematical Models for Hydrodynamic Circulation and Dispersion of Selected Water Quality Constituents with Application to The Upper Gulf of Thailand**. Ph.D. thesis, Asian Institute of Technology.

Liengcharernsit, W. 2009. **Environmental Modeling**. Department of Environmental Engineering, Faculty of Engineering, Kasetsart University, Bangkok.

Liu, X. and Huang, W. 2009. Modeling sediment resuspension and transport induced by storm wind in Apalachicola Bay, USA. **Environmental Modelling & Software**. 24:1302-1313.

Liu, W.C. 2005. Modeling the influence of settling velocity on cohesive sediment transport in Tanshui River estuary. Environmental Geology. 47: 535-546.

Meyer-Peter, E. and Muller, R. 1984. **Formula for bedload transport**. In: Report on the 2nd Meeting of the International Association of Hydraulic Structure Research. Stockholm, Sweden.

Moehansyah, H., Maheshwari, B.L. and Armstrong, J. 2004. Field Evaluation of Selected Soil Erosion Models for Catchment Management in Indonesia. **Biosystems Engineeting.** 88: 491-506.

Muttiah, R. S., Harmel, R. D. and Richardson, C. W. 2005. Discharge and sedimentation periodicities in small sized watersheds. **Catena**. 61: 241-255.

Neilsen, P. 1992. **Coastal Bottom Boundary Layers and Sediment Transport**. World Scientific Publishing, Singapore. Advanced Series on Ocean Engineering, Vol. 4.

Neilsen, P. and Callagham, D. P. 2003. Shear stress and sediment transport calculations for sheet flow under waves. **Coastal Engineering**. 47: 347-354.

Nguyen, K. D., Guillou, S., Chauchat, J. and Barbry, N. 2009. A two-phase numerical model for suspended-sediment transport in estuaries. **Advances in Water Resources**. 32: 1187-1196.

Office of Natural Resources and Environmental Policy and Planning. 2006. **Master Plan for Songkhla Lake Basin Development**. Neo Point Press, Hat Yai. Thailand.

Paphitis, D. and Collins, M.B. 2005. Sediment resuspension events within the (microtidal) coastal waters of Thermaikos Gulf, northern Greece. **Continental Shelf Research**. 25:2350-2365.

Partheniades E. 1965. **Erosion and deposition of cohesive soils**. J Hydraul Div, ASCE: 91(HY1):105-39.

Perianez, R. 2002. Modelling the suspended matter dynamics in a marine environment using a three dimensional σ coordinate model: application to the eastern Irish Sea. **Applied Mathematical Modelling**. 26: 583-601.

Pierre Y. J. 1998. **Erosion and Sedimentation.** 2 ed. Cambridge university Press, United States of America.

Polesky, S. P., Dechaumphai, P., Glass, C. E. and Pandey, A. K. 1992. Three-Dimensional Thermal-Structural Analysis of a Swept Cowl Leading Edge Subjected to Skewed Shock-Shock Interference Heating. **AIAA Journal of Thermophysics and Heat Transfer**. 6: 48-54.

Reeve, D., Chadwick, A. and Fleming, C. 2004. **Coastal Engineering Process, Theory and Design Practice.** Spon Press, London.

Ribbe, J. and Holloway, P. E. 2001. A model of suspended sediment transport by internal tides. **Continental Shelf Research**. 21: 395-422.

Ribberink, J. S. 1998. Bed-load transport for steady flows and unsteady oscillatory flows. **Coastal Engineering**. 34:59-82.

Rodriguez, H. N. and Metha, A.J. 2000. Longshore transport of fine-grained sediment. **Continental Shelf Research**. 20: 1419-1432.

Royal Irrigation Department. 2009. **Annual Report 2006**. Available Source: http://www.rid.go.th/2009/_data/docs/AnnualReportRID49.rar.

Songrukkiat, K., 2006. **Evaluation of Soil Erosion in Songkhla Lake Watershed by Mathematical Model**. M. Eng. Thesis, Kasetsart University.

Soulsby, R.L., 1997. **Dynamics of Marine Sands**. A Manual for Practical Applications. Thomas Telford, London, UK.

Soulsby, R.L., Clarke, S., 2004. **Bed Shear-Stresses Under Combined Waves and Currents on Smooth and Rough Beds**. Report TR 137. HR Wallingford Ltd., Wallingford, UK.

Soulsby, R.L., Damgaard, J.S., 2005. **Bedload Sediment Transport in Coastal Waters**. Report TR 152. HR Wallingford Ltd., Wallingford, UK.

Van Rijn LC. 1989. **Handbook sediment transport by currents and waves**. Report H461. Delft Hydraulics.

Velegrakis, A.F., Michel, D., Collins, M.B., Lafite, R., Oikonomou, E.K., Dupont, J.P., Huault, M.F., Lecouturier, M., Salomon, J.C. and Bishop, C. 1999. Sources, sinks and resuspension of suspended particle matter in the eastern English Channel. **Continental Shelf Research**. 19: 1933-1957.

VKI, DHI, PEMconsult A/S, COWI A/S, PSU and Seatec International Ltd. 1999. The EMSONG Project. **Environmental Management in the Songkhla Lake Basin**. DANCED and Ministry of Science, Technology and Environment, Thailand.

Wang, X.H., Pinardi, N. and Malacic, V. Sediment transport and resuspension due to combined motion of wave and current in the northern Adriatic Sea during a Bora event in January 2001: A numerical modeling study. **Continental Self Research**. 27: 613-633.

Warner, J. C., Sherwood, C. R., Signell, R. P., Harris, C. K. and Arango, H. G. 2008. Development of a three-dimensional, regional, coupled wave, current, and sediment-transport model. **Computer & Geosciences**. 34:1284-1306.

Wolanski, E., Huan, N. H., Dao, L. T., Nhan, N. H. and Thuy, N. N. 1996. **Estuarine, Coastal and Shelf Science**. 43: 565-582.

You, Z.J. 2005. Fine sediment resuspension dynamics in a large semi-enclosed bay. **Ocean Engineering**. 32:1982-1993.

Stronach, J.A., Webb, A.j., Murty, T.S. and Cretney. 1993. A Three-Dimensional Numerical Model of Suspended Sediment Transport in Howe Sound, British Columbia. Atmosphere-Ocean. 31: 73-79.

# APPENDICES

# Appendix A

Source Code of Computer Program for Sediment Transport Model

```
Sediment Transport Model=Suspened sediment model+Bedload sediment model
Suspended Sediment Model <UnSteady State>
-------------------------------------------------------------------------
Input element : node values
-------------------------------------------------------------------------
NodeE=xlsread('SLB_element','element');
Node=[NodeE(:,2) NodeE(:,3) NodeE(:,4) NodeE(:,5) NodeE(:,6) NodeE(:,7)
NodeE(:,8) NodeE(:,9)];   %node squence
[e,a]=size(Node);                % e = row number  a = column number
nel=e;                           %number of elements
clear NodeE
-------------------------------------------------------------------------
Input coordinate x y z
-------------------------------------------------------------------------
coordinate=xlsread('SLB_element','coordinate(4)');
coordinateN=[coordinate(:,2) coordinate(:,3) coordinate(:,4)]; %coordinate squence
[n,b]=size(coordinateN);
nnode=n;                         %total number of nodes in system
-------------------------------------------------------------------------
Define element coordinate
-------------------------------------------------------------------------
for i=1 : nel
   for j=1:8
      x(i,j)=coordinate(Node(i,j),2);       %%x coordinate
      y(i,j)=coordinate(Node(i,j),3);       %%y coordinate
      z(i,j)=coordinate(Node(i,j),4);       %%z coordinate
   end
end
-------------------------------------------------------------------------
Input node sequence for each element for Mqs
-------------------------------------------------------------------------
NodeS=xlsread('SLB_element','elementSS');
```

```
NodeSS=[NodeS(:,2) NodeS(:,3) NodeS(:,4) NodeS(:,5)];   %node sequence
[s,k]=size(NodeSS);                    %% s = row number  k = column number
snel=s;                                %% number of elements
clear NodeS
-------------------------------------------------------------------------
Input coordinate x y
-------------------------------------------------------------------------
coordinateSS=[coordinate(:,2) coordinate(:,3)]; %coordinate squence
[p,r]=size(coordinate);
snode=p;              %total number of nodes in system
-------------------------------------------------------------------------
Define element coordinate
-------------------------------------------------------------------------
for i=1:snel
   for j=1:4
      Xx(i,j)=coordinate(NodeSS(i,j),2);      %% x coordinate
      Yy(i,j)=coordinate(NodeSS(i,j),3);      %% y coordinate
   end
end


-------------------------------------------------------------------------
Input data for control parameters
-------------------------------------------------------------------------
Kx=100;                    %mixing coefficients in x direction**
Ky=100;                    %mixing coefficients in y direction**
Kz=100;                    %mixing coefficients in z direction**
R=xlsread('SLB_element','RS');
Qq=xlsread('SLB_element','Qq');
Vq=xlsread('SLB_element','R(2)');
S=xlsread('SLB_element','S');
Ww=xlsread('SLB_element','W');      %%velocity in z direction (m/s)
W=Ww(:,2);
```

```
Qs=xlsread('SLB_element','Qs');      %% SS concentration of each element
-------------------------------------------------------------------------
Input (XI, ETA, MU) and weight(w) for numerical intergration (3-D)
-------------------------------------------------------------------------
XI=[(-1/(sqrt(3))); (1/(sqrt(3))); (1/(sqrt(3))); (-1/(sqrt(3))); (-1/(sqrt(3))); (1/(sqrt(3)));
(1/(sqrt(3))); (-1/(sqrt(3)))]; %%integration point in xi-axis
ETA=[(-1/(sqrt(3))); (-1/(sqrt(3))); (1/(sqrt(3))); (1/(sqrt(3))); (-1/(sqrt(3))); (-
1/(sqrt(3))); (1/(sqrt(3))); (1/(sqrt(3)))];%%integration point in eta-axis
MU=[(-1/(sqrt(3))); (-1/(sqrt(3))); (-1/(sqrt(3))); (-1/(sqrt(3))); (1/(sqrt(3)));
(1/(sqrt(3))); (1/(sqrt(3))); (1/(sqrt(3)))]; %%integration point in mu-axis
w=1.0;                                  %%weighting coefficient
-------------------------------------------------------------------------
Input (XI, ETA) and weight(w) for numerical intergration(2-D)
-------------------------------------------------------------------------
XII=[(-1/(sqrt(3)));(1/(sqrt(3)));(1/(sqrt(3)));(-1/(sqrt(3)))];
ETAA=[(-1/(sqrt(3)));(-1/(sqrt(3)));(1/(sqrt(3)));(1/(sqrt(3)))];
w=1.0;
-------------------------------------------------------------------------
Input data for initial condition (SST model)
-------------------------------------------------------------------------
C_Ct0=zeros(nnode,1,3);
Mqr_t0=zeros(nnode,1,3);            %%Sediment resuspension from BST model
C0=xlsread('SLB_element','C0');      %% initial value of SS
Qbr=xlsread('SLB_element','Qbr');    %% initial value of Mqbr
for i=1:nnode
   for j=1:3
      C_Ct0(i,1,j)=C_Ct0(i,1,j)+C0(i,j);
      Mqr_t0(i,1,j)=Mqr_t0(i,1,j)+Qbr(i,j);
   end
end
clear C0
clear Qbr
```

```
-------------------------------------------------------------------
Input data for boundary conditions(Inlet SS)
-------------------------------------------------------------------
Bound=[193;194;413;414;633;634;853;854];        %% SST boundary
cBound=[0.0 0.0 0.0;0.0 0.0 0.0;0.0 0.0 0.0;0.0 0.0 0.0;
       0.0 0.0 0.0;0.0 0.0 0.0;0.0 0.0 0.0;0.0 0.0 0.0];
[cc,oo]=size(Bound);
bound=cc;

SBound=[193; 194];                          %% BST boundary
cSBound=[0.0 0.0 0.0;0.0 0.0 0.0];
[bb,oo]=size(SBound);
sbound=bb;

-------------------------------------------------------------------
Input element : node values (BST model)
-------------------------------------------------------------------
NodeB=xlsread('SLB_elementbed','elementbed');
NodeBB=[NodeB(:,2) NodeB(:,3) NodeB(:,4) NodeB(:,5)];   %node squence
[b,d]=size(NodeBB);             % b = row number  d = column number
bnel=b;                         %number of elements
clear NodeB
-------------------------------------------------------------------
Input coordinate x y
-------------------------------------------------------------------
coordinateB=xlsread('SLB_elementbed','coordinatee');
coordinateBB=[coordinateB(:,2) coordinateB(:,3)]; %coordinate squence
[m,o]=size(coordinateB);
bnode=m;                    %total number of nodes in system
```

```
-----------------------------------------------------------------------
Define element coordinate
-----------------------------------------------------------------------
for i=1 : bnel
   for j=1:4
      X(i,j)=coordinateBB(NodeBB(i,j),1);        %%x coordinate
      Y(i,j)=coordinateBB(NodeBB(i,j),2);        %%y coordinate
   end
end
-----------------------------------------------------------------------
Define Particle Diameter : 3 sizes
-----------------------------------------------------------------------
D=[0.00001; 0.000035; 0.000065];     %% sediment diameter (m)
Pd=[0.4381; 0.4979; 0.064];          %% % sediment for each size
[n,a]=size(d);

rs=zeros(nnode,1);
for i=1:nnode
   for j=1:12
      for k=1:3
      if Vq(i)==0
         rs(i,j)=0;
      else
         rs(i,j,k)=R(i,j)*Pd(k)*Qq(i)/Vq(i);
      end
      end
   end
end
-----------------------------------------------------------------------
Calculate Terminal settling velocity (vs),D*,
Critical Shield Parameter (CSP),Critical shear stress (Tcs)
-----------------------------------------------------------------------
```

```
s=1.06;
vis=1.19*10^(-6);
M=0.000025;                 %% erodibility coefficient (kg/m^2/s)
h=1.5;
den=1.0*10^(3);             %% water density (g/m3)
denS=2.65*10^(3);           %% sedimenr density (g/m3)
g=9.81;                     %% acceleration due gravity (m/s2)
vis=1.19*10^(-6);           %% kinematic viscosity (m2/s)
D50=23.29*10^(-6);          %% m
ks=2.5*D50;
Z0=ks/30;
CD=(0.4/(1+log(Z0/h)))^2;

vs=zeros(3,1);
Dstr=zeros(3,1);
CSP=zeros(3,1);
Tcs=zeros(3,1);
for id=1:3
   vs(id)=(g*(s-1)/(18*vis))*D(id)^(2);
   Dstr(id)=(g*(s-1)/(vis^2))^(1/3)*D(id);
   CSP(id)=(0.3/(1+1.2*Dstr(id)))+0.055*(1-exp(-0.02*Dstr(id)));
   Tcs(id)=CSP(id)*((denS-den)*g*D(id));
end

-------------------------------------------------------------------------
Input data for initial condition (BST model)
-------------------------------------------------------------------------
Sb_t0=zeros(bnode,1,3);
Sb0=xlsread('SLB_elementbed','Si');
for i=1:bnode
   for j=1:3
      Sb_t0(i,1,j)=Sb_t0(i,1,j)+Sb0(i,j);
```

```
   end
end
clear Sb0
-------------------------------------------------------------------------
Define U and V from Hydrodynamic model
-------------------------------------------------------------------------
uv=textread('SLB_hydro_edit1.txt');
uu=(uv(:,3)); vv=(uv(:,4)); hh=(uv(:,2));
clear uv;

UV=[hh uu vv; hh uu vv; hh uu vv; hh uu vv; hh uu vv; hh uu vv; hh uu vv;
   hh uu vv; hh uu vv; hh uu vv; hh uu vv; hh uu vv; hh uu vv];
Uu=UV(:,2); Vv=UV(:,3); Hh=UV(:,1);
clear hh uu vv
-------------------------------------------------------------------------
t=1;                          %% Set t start
count1=1;
tt=24*3600;                   %% Set t stop (month*day*hour*sec)
dt=30*30;                     %% delta t (sec*min)
nt=tt/dt;

CAns=zeros(nnode,1,3) ;       %% Sediment Answer at t=0
Sbiii=zeros(bnode,1,3);
r = 221;
for st=1:nt                   %% Set t stop=6 hour (t<21601 sec)
   U = [Uu(r:1:r+219); Uu(r:1:r+219); Uu(r:1:r+219); Uu(r:1:r+219)];
   V = [Vv(r:1:r+219); Vv(r:1:r+219); Vv(r:1:r+219); Vv(r:1:r+219)];
   u = Uu(r:1:r+219);
   v = Vv(r:1:r+219);
   H = Hh(r:1:r+219);
```

```
for nt=1:2880
    RR=rs(:,1,:);
  end

  for nt=2881:5760
    RR=rs(:,2,:);
  end

  for nt=5761:8640
    RR=rs(:,3,:);
  end

  for nt=8641:11520
    RR=rs(:,4,:);
  end

  for nt=11521:14400
    RR=rs(:,5,:);
  end

  for nt=14401:17280
    RR=rs(:,6,:);
  end

  for nt=17281:20160
    RR=rs(:,7,:);
  end

  for nt=20161:23040
    RR=rs(:,8,:);
  end
```

```
   for nt=23041:25920
      RR=rs(:,9,:);
   end

   for nt=25921:28800
      RR=rs(:,10,:);
   end

   for nt=28800:31680
      RR=rs(:,11,:);
   end

   for nt=31680:34560
      RR=rs(:,12,:);
   end

r = r+220;

-------------------------------------------------------------------
Calculate element+system matrix M,Mux,Mvy,Mwz,Mkx,Mky,Mkz,Mvs
-------------------------------------------------------------------
Msys=zeros(nnode);
MuxSys=zeros(nnode);
MvySys=zeros(nnode);
MwzSys=zeros(nnode);
MkxSys=zeros(nnode);
MkySys=zeros(nnode);
MkzSys=zeros(nnode);
MvsSys=zeros(nnode);
for i=1:nel
   Mele=zeros(8);
   MUele=zeros(8);
```

```
MVele=zeros(8);
MWele=zeros(8);
MKxele=zeros(8);
MKyele=zeros(8);
MKzele=zeros(8);
MVsele=zeros(8);
nd=Node(i,:);
XYZ=[x(i,1) y(i,1) z(i,1);
   x(i,2) y(i,2) z(i,2);
   x(i,3) y(i,3) z(i,3);
   x(i,4) y(i,4) z(i,4);
   x(i,5) y(i,5) z(i,5);
   x(i,6) y(i,6) z(i,6);
   x(i,7) y(i,7) z(i,7);
   x(i,8) y(i,8) z(i,8)];
Ux=[U(Node(i,1));
   U(Node(i,2));
   U(Node(i,3));
   U(Node(i,4));
   U(Node(i,5));
   U(Node(i,6));
   U(Node(i,7));
   U(Node(i,8))];
Vy=[V(Node(i,1));
   V(Node(i,2));
   V(Node(i,3));
   V(Node(i,4));
   V(Node(i,5));
   V(Node(i,6));
   V(Node(i,7));
   V(Node(i,8))];
Wz=[W(Node(i,1));
```

```
    W(Node(i,2));
    W(Node(i,3));
    W(Node(i,4));
    W(Node(i,5));
    W(Node(i,6));
    W(Node(i,7));
    W(Node(i,8))];
  for j=1:8;
  xi=XI(j); eta=ETA(j); mu=MU(j);
  phi=[(1/8)*(1-xi)*(1-eta)*(1-mu);
    (1/8)*(1+xi)*(1-eta)*(1-mu);
    (1/8)*(1+xi)*(1+eta)*(1-mu);
    (1/8)*(1-xi)*(1+eta)*(1-mu);
    (1/8)*(1-xi)*(1-eta)*(1+mu);
    (1/8)*(1+xi)*(1-eta)*(1+mu);
    (1/8)*(1+xi)*(1+eta)*(1+mu);
    (1/8)*(1-xi)*(1+eta)*(1+mu)];
  B=[(-1/8)*(1-eta)*(1-mu) (1/8)*(1-eta)*(1-mu) (1/8)*(1+eta)*(1-mu) (-
1/8)*(1+eta)*(1-mu) (-1/8)*(1-eta)*(1+mu) (1/8)*(1-eta)*(1+mu)
(1/8)*(1+eta)*(1+mu) (-1/8)*(1+eta)*(1+mu);
    (-1/8)*(1-xi)*(1-mu) (-1/8)*(1+xi)*(1-mu) (1/8)*(1+xi)*(1-mu) (1/8)*(1-xi)*(1-
mu) (-1/8)*(1-xi)*(1+mu) (-1/8)*(1+xi)*(1+mu) (1/8)*(1+xi)*(1+mu) (1/8)*(1-
xi)*(1+mu);
    (-1/8)*(1-xi)*(1-eta) (-1/8)*(1+xi)*(1-eta) (-1/8)*(1+xi)*(1+eta) (-1/8)*(1-
xi)*(1+eta) (1/8)*(1-xi)*(1-eta) (1/8)*(1+xi)*(1-eta) (1/8)*(1+xi)*(1+eta) (1/8)*(1-
xi)*(1+eta)];
  J=B*XYZ;
  J_inv=inv(J);
  d_phiT=J_inv*B;
  d_phiTx=d_phiT(1,:);          %% d_phiTx=d_phiT/dx
  d_phiTy=d_phiT(2,:);          %%d_phiTx=d_phiT/dy
  d_phiTz=d_phiT(3,:);          %%d_phiTx=d_phiT/dz
```

```
   Mele=Mele+w*phi*phi'*abs(det(J));
   MUele=MUele+w*phi*phi'*Ux*d_phiTx*abs(det(J));
   MVele=MVele+w*phi*phi'*Vy*d_phiTy*abs(det(J));
   MWele=MWele+w*phi*phi'*Wz*d_phiTz*abs(det(J));
   MKxele=MKxele+Kx*w*d_phiTx'*d_phiTx*abs(det(J));
   MKyele=MKyele+Ky*w*d_phiTy'*d_phiTy*abs(det(J));
   MKzele=MKzele+Kz*w*d_phiTz'*d_phiTz*abs(det(J));
   MVsele=MVsele+w*phi*d_phiTz*abs(det(J));
   end

%% System
   for ni=1:8;
      ii=nd(ni);
      for nj=1:8;
         jj=nd(nj);
         Msys(ii,jj)=Msys(ii,jj)+Mele(ni,nj);
         MuxSys(ii,jj)=MuxSys(ii,jj)+MUele(ni,nj);
         MvySys(ii,jj)=MvySys(ii,jj)+MVele(ni,nj);
         MwzSys(ii,jj)=MwzSys(ii,jj)+MWele(ni,nj);
         MkxSys(ii,jj)=MkxSys(ii,jj)+MKxele(ni,nj);
         MkySys(ii,jj)=MkySys(ii,jj)+MKyele(ni,nj);
         MkzSys(ii,jj)=MkzSys(ii,jj)+MKzele(ni,nj);
         MvsSys(ii,jj)=MvsSys(ii,jj)+MVsele(ni,nj);
      end
   end
end

MVSys=zeros(nnode,nnode,3);
for k=1:3
   MVSys(:,:,k)=vs(k,1)*MvsSys;
end
```

```
------------------------------------------------------------------------
Calculate element+system matrix of Mr, Md
------------------------------------------------------------------------
MrSys=zeros(nnode,1);
MdSys=zeros(nnode,1);
for i=1:nel
   MRele=zeros(8,1);
   MDele=zeros(8,1);
   nd=Node(i,:);
   XYZ=[x(i,1) y(i,1) z(i,1);
     x(i,2) y(i,2) z(i,2);
     x(i,3) y(i,3) z(i,3);
     x(i,4) y(i,4) z(i,4);
     x(i,5) y(i,5) z(i,5);
     x(i,6) y(i,6) z(i,6);
     x(i,7) y(i,7) z(i,7);
     x(i,8) y(i,8) z(i,8)];
   for j=1:8                    %%loop for computation of element matrices
   xi=XI(j); eta=ETA(j); mu=MU(j);
   phi=[(1/8)*(1-xi)*(1-eta)*(1-mu);
      (1/8)*(1+xi)*(1-eta)*(1-mu);
      (1/8)*(1+xi)*(1+eta)*(1-mu);
      (1/8)*(1-xi)*(1+eta)*(1-mu);
      (1/8)*(1-xi)*(1-eta)*(1+mu);
      (1/8)*(1+xi)*(1-eta)*(1+mu);
      (1/8)*(1+xi)*(1+eta)*(1+mu);
      (1/8)*(1-xi)*(1+eta)*(1+mu)];
   B=[(-1/8)*(1-eta)*(1-mu) (1/8)*(1-eta)*(1-mu) (1/8)*(1+eta)*(1-mu) (-
1/8)*(1+eta)*(1-mu) (-1/8)*(1-eta)*(1+mu) (1/8)*(1-eta)*(1+mu)
(1/8)*(1+eta)*(1+mu) (-1/8)*(1+eta)*(1+mu);
```

```
    (-1/8)*(1-xi)*(1-mu) (-1/8)*(1+xi)*(1-mu) (1/8)*(1+xi)*(1-mu) (1/8)*(1-xi)*(1-
mu) (-1/8)*(1-xi)*(1+mu) (-1/8)*(1+xi)*(1+mu) (1/8)*(1+xi)*(1+mu) (1/8)*(1-
xi)*(1+mu);
    (-1/8)*(1-xi)*(1-eta) (-1/8)*(1+xi)*(1-eta) (-1/8)*(1+xi)*(1+eta) (-1/8)*(1-
xi)*(1+eta) (1/8)*(1-xi)*(1-eta) (1/8)*(1+xi)*(1-eta) (1/8)*(1+xi)*(1+eta) (1/8)*(1-
xi)*(1+eta)];
  J=B*XYZ;
  MRele=MRele+w*phi*abs(det(J));
  MDele=MDele+w*phi*abs(det(J));
  end
  for ni=1:8
    MrSys(Node(i,ni),1)=MrSys(Node(i,ni),1)+MRele(ni,1);
    MdSys(Node(i,ni),1)=MdSys(Node(i,ni),1)+MDele(ni,1);
  end
end

MRSys=zeros(nnode,1,3);
MDSys=zeros(nnode,1,3);
for i=1:nnode
 for j=1:3
    MRSys(i,1,j)=RR(i,1,j)*MrSys(i,1);
    MDSys(i,1,j)=S(i,j)*MdSys(i,1);
 end
end

-------------------------------------------------------------------------
Calculate element+system matrix of Mqs
-------------------------------------------------------------------------
MqsSys=zeros(snode,1);
for i=1:snel
  MQsele=zeros(4,1);
  for j=1:4                %%loop for computation of element matrices
```

```
   xxi=XII(j,1); eeta=ETAA(j,1);
   phe=[(1/4)*(1-xxi)*(1-eeta); (1/4)*(1+xxi)*(1-eeta); (1/4)*(1+xxi)*(1+eeta);
(1/4)*(1-xxi)*(1+eeta)];
   B1=[(-1/4)*(1-eeta) (1/4)*(1-eeta) (1/4)*(1+eeta) (-1/4)*(1+eeta); (-1/4)*(1-xxi) (-
1/4)*(1+xxi) (1/4)*(1+xxi) (1/4)*(1-xxi)];
   XYB=[Xx(i,1) Yy(i,1);
     Xx(i,2) Yy(i,2);
     Xx(i,3) Yy(i,3);
     Xx(i,4) Yy(i,4)];
   J1=B1*XYB;

   MQsele=MQsele+w*phe*abs(det(J1));
   end
   %%
   for ni=1:4
      MqsSys(NodeSS(i,ni),1)=MqsSys(NodeSS(i,ni),1)+MQsele(ni,1);
   end
end

MQSSys=zeros(snode,1,3);
for i=1:snode
  for j=1:3
     MQSSys(i,1,j)=Qs(i,j)*MqsSys(i,1);
  end
end

-------------------------------------------------------------------
Element matrix in compacted form
-------------------------------------------------------------------
P=zeros(nnode,nnode,3);
Q=zeros(nnode,1,3);
for k=1:3
```

```
        P(:,:,k)=MuxSys+MvySys+MwzSys-
MVSys(:,:,k)+MkxSys+MkySys+MkzSys;
        Q(:,1,k)=MRSys(:,1,k)-MDSys(:,1,k)+Mqr_t0(:,1,k)+MQSSys(:,1,k);
        MT=(Msys/dt)+(P(:,:,k)/2);
        MF=(Msys/dt)-(P(:,:,k)/2);
        MFF=(MF*C_Ct0(:,1,k))+Q(:,1,k);
-------------------------------------------------------------------------
Apply boudary condition value
-------------------------------------------------------------------------
for ib=1:bound
   MT(Bound(ib),:)=0;
   MT(Bound(ib),Bound(ib))=1;
   MFF(Bound(ib,1))=cBound(ib);
end
-------------------------------------------------------------------------
Solve the matrix equation
-------------------------------------------------------------------------
CAns(:,1,k)=inv(MT)*MFF;
C_Ct0(:,1,k)=CAns(:,1,k);
end


-------------------------------------------------------------------------
Bedload Sediment Transport Model (UnSteady State)
-------------------------------------------------------------------------


Vh=zeros(bnode,1);
BedShear=zeros(bnode,1);
for i=1:bnode
   Vh(i)=sqrt(u(i)^2+v(i)^2);
   BedShear(i)=den*CD*Vh(i)^2;
End
```

```
---------------------------------------------------------------------
Calculate Shields Parameter (Shield)
---------------------------------------------------------------------
Shield=zeros(bnode,1,3);
for i=1:bnode
for j=1:3
   Shield(i,1,j)=BedShear(i)/(g*(denS-den)*D(j));
end
end

---------------------------------------------------------------------
Calculate Bedload Transport Rate Factor (BTR)
---------------------------------------------------------------------
BTR=zeros(bnode,1,3);
for i=1:bnode
   for j=1:3
      if Shield(i,1,j)<CSP(j);
         BTR(i,1,j)=0;
      else
      BTR(i,1,j)=12*((sqrt(Shield(i,1,j)))*(Shield(i,1,j)-CSP(j)));
      end
   end
end
---------------------------------------------------------------------
Calculate Bedload (qb),Qx and Qy
qb*Bulk density (Bu=1.0-1.6 g/cm3, =1.0-1.6 *10^3 g/m3)
qb (g/m/s)
---------------------------------------------------------------------
Vf=zeros(bnode,1);
for i=1:bnode
   Vf(i)=Vh(i,1);
end
```

```
 qb=zeros(bnode,1,3);
Qx=zeros(bnode,1,3);
Qy=zeros(bnode,1,3);

for i=1:bnode
   for j=1:3
     qb(i,1,j)=0.055*10^(6)*BTR(i,1,j)*(g*(s-1)*D(j)^3)^(0.5);
   if Vf(i)==0;
     Qx(i,1,j)=0;
     Qy(i,1,j)=0;
   else
     Qx(i,1,j)=((u(i))/Vf(i))*qb(i,1,j);
     Qy(i,1,j)=((v(i))/Vf(i))*qb(i,1,j);
   end
   end
end

-------------------------------------------------------------------------
  Matrix M
-------------------------------------------------------------------------
MSys=zeros(bnode);
MxSys=zeros(bnode);
MySys=zeros(bnode);
for i=1:bnel
   Mele=zeros(4);
   Mxele=zeros(4);
   Myele=zeros(4);
   nd=NodeBB(i,:);
   XYB=[X(i,1) Y(i,1);
     X(i,2) Y(i,2);
     X(i,3) Y(i,3);
     X(i,4) Y(i,4)];
```

```
   for j=1:4
   xxi=XI(j); eeta=ETA(j);
   phe=[(1/4)*(1-xxi)*(1-eeta); (1/4)*(1+xxi)*(1-eeta); (1/4)*(1+xxi)*(1+eeta);
(1/4)*(1-xxi)*(1+eeta)];
   B1=[(-1/4)*(1-eeta) (1/4)*(1-eeta) (1/4)*(1+eeta) (-1/4)*(1+eeta); (-1/4)*(1-xxi) (-
1/4)*(1+xxi) (1/4)*(1+xxi) (1/4)*(1-xxi)];
   J1=B1*XYB;
   J1_inv=inv(J1);
   d_phi=J1_inv*B1;
   d_phix=d_phi(1,:);
   d_phiy=d_phi(2,:);
   Mele=Mele+w*phe*phe'*(det(J1));
   Mxele=Mxele+w*phe*d_phix*(det(J1));
   Myele=Myele+w*phe*d_phiy*(det(J1));
   end

   for ni=1:4;
      ii=nd(ni);
      for nj=1:4;
         jj=nd(nj);
         MSys(ii,jj)=MSys(ii,jj)+Mele(ni,nj);
         MxSys(ii,jj)=MxSys(ii,jj)+Mxele(ni,nj);
         MySys(ii,jj)=MySys(ii,jj)+Myele(ni,nj);
      end
   end
end

---------------------------------------------------------------------
Calculate element+system matrix of Mv
---------------------------------------------------------------------
MvSys=zeros(bnode,bnode,3);
for i=bnode
```

```
   for j=1:bnode
   for k=1:3
    MvSys(i,j,k)=vs(k)*MSys(i,j);
   end
   end
end

---------------------------------------------------------------------
Calculate element+system matrix of Mqbr
---------------------------------------------------------------------
Qn=zeros(bnode,1,3);
for i=1:bnode
   for j=1:3
   if BedShear(i)<Tcs(j);
      Qn(i,1,j)=0;
   else
      Qn(i,1,j)=(M*((BedShear(i)/Tcs(j))-1))/h;
   end
   end
end

MqbrSys=zeros(bnode,1);
for i=1:bnel
   MQbrele=zeros(4,1);
   nd=NodeBB(i,:);
   XYB=[X(i,1) Y(i,1);
      X(i,2) Y(i,2);
      X(i,3) Y(i,3);
      X(i,4) Y(i,4)];
   for j=1:4                %%loop for computation of element matrices
   xxi=XI(j); eeta=ETA(j);
```

```
   phe=[(1/4)*(1-xxi)*(1-eeta); (1/4)*(1+xxi)*(1-eeta); (1/4)*(1+xxi)*(1+eeta);
(1/4)*(1-xxi)*(1+eeta)];
   B1=[(-1/4)*(1-eeta) (1/4)*(1-eeta) (1/4)*(1+eeta) (-1/4)*(1+eeta); (-1/4)*(1-xxi) (-
1/4)*(1+xxi) (1/4)*(1+xxi) (1/4)*(1-xxi)];
   J1=B1*XYB;
   MQbrele=MQbrele+w*phe*(det(J1));
   end

   for ni=1:4
      MqbrSys(NodeBB(i,ni),1)=MqbrSys(NodeBB(i,ni),1)+MQbrele(ni,1);
   end
end

Mqr=zeros(bnode,1,3);
for i=1:bnode
  for j=1:3
   Mqr(i,1,j)=Qn(i,j)*MqbrSys(i,1);
  end
end
 ---------------------------------------------------------------------
Define Mqr for Suspended sediment transport model
---------------------------------------------------------------------
Qr=zeros(660,1,3);
MQ=[Mqr;Qr];
Mqr_t0=MQ;
clear Qr
---------------------------------------------------------------------
Element matrix in compacted form
---------------------------------------------------------------------
G=zeros(bnode,1,3);
Sbi=zeros(bnode,1,3);
Sbii=zeros(bnode,1,3);
```

```
for j=1:3
      mt=MSys/dt;
      G(:,1,j)=-MxSys*Qx(:,1,j)-MySys*Qy(:,1,j)+MvSys(:,:,j)*CAns((1:220),1,j)-
Mqr(:,1,j);
      Sbi(:,1,j)=(mt*Sb_t0(:,1,j))+G(:,1,j);
------------------------------------------------------------------------
Apply boudary condition
------------------------------------------------------------------------
   for ib=1:sbound
      mt(SBound(ib))=zeros;
      mt(SBound(ib),SBound(ib))=1;
      Sbi(SBound(ib,1))=cSBound(ib);
   end
Sbii(:,1,j)=inv(mt)*Sbi(:,1,j);
end

Sbiii=zeros(bnode,1,3);
for i=1:bnode;
   for j=1:3;
   if Sbii(i,1,j)<0;
      Sbiii(i,1,j)=0;
   else
      Sbiii(i,1,j)=Sbii(i,1,j);
   end
   end
end
Sb_t0(:,1,j)=Sbiii(:,1,j);

csi=zeros(nnode,1);
for i=1:nnode
  csi(i)=(CAns(i,1,1))+(CAns(i,1,2))+(CAns(i,1,3));
end
```

```
 Ssi=zeros(bnode,1);
SSi=zeros(bnode,1,3);
for i=1:bnode;
   for j=1:3
   Ssi(i)=((csi(i)+csi(i+220)+csi(i+440)+csi(i+660))/4)*H(i);

SSi(i,1,j)=((CAns(i,1,j)+CAns((i+220),1,j)+CAns((i+440),1,j)+CAns((i+660),1,j))/4)
*H(i);
   end
end



if t==15552000
   data_CAns_6=CAns;
   data_Sbiii_6=Sbiii;
end

count1=count1+1;
disp(count1)

end
------------------------------------------------------------------------
Calculate Total Suspended sediment (Ssi)
------------------------------------------------------------------------
SBi=zeros(bnode,1);
for i=1:bnode
   SBi(i)=Sbiii(i,1,1)+Sbiii(i,1,2)+Sbiii(i,1,3);
end
```

```
------------------------------------------------------------------------
Calculate Total sediment (Tsi)
------------------------------------------------------------------------
Sti=zeros(bnode,1,3);
STi=zeros(bnode,1);
for i=1:bnode
   for j=1:3
   Sti(i,1,j)=SSi(i,1,j)+Sbiii(i,1,j);
   STi(i)=Sti(i,1,1)+Sti(i,1,2)+Sti(i,1,3);
   end
end

disp('finish');
```

# Appendix B

Elevation of water level at Songkhla station

**Appendix Table B1** Elevation of water level at Songkhla in November, 2009, predicted in meters above the lowest low water

| Date | Hours | | | | | | | | | | | |
|---|---|---|---|---|---|---|---|---|---|---|---|---|
| | 0 | 1 | 2 | 3 | 4 | 5 | 6 | 7 | 8 | 9 | 10 | 11 |
| 1 | 1.0 | 1.0 | 0.9 | 0.9 | 0.9 | 1.0 | 1.1 | 1.1 | 1.2 | 1.2 | 1.1 | 1.0 |
| 2 | 1.0 | 1.0 | 0.9 | 0.9 | 0.9 | 1.0 | 1.1 | 1.1 | 1.2 | 1.2 | 1.2 | 1.1 |
| 3 | 1.1 | 1.0 | 0.9 | 0.8 | 0.8 | 0.9 | 1.0 | 1.1 | 1.2 | 1.2 | 1.2 | 1.2 |
| 4 | 1.1 | 1.0 | 0.9 | 0.9 | 0.8 | 0.8 | 0.9 | 1.0 | 1.2 | 1.2 | 1.3 | 1.2 |
| 5 | 1.2 | 1.1 | 1.0 | 0.9 | 0.8 | 0.8 | 0.9 | 1.0 | 1.1 | 1.2 | 1.2 | 1.3 |
| 6 | 1.2 | 1.2 | 1.1 | 0.9 | 0.8 | 0.8 | 0.8 | 0.9 | 1.0 | 1.1 | 1.2 | 1.2 |
| 7 | 1.2 | 1.2 | 1.1 | 1.0 | 0.9 | 0.8 | 0.8 | 0.8 | 0.9 | 1.0 | 1.1 | 1.2 |
| 8 | 1.2 | 1.2 | 1.2 | 1.1 | 1.0 | 0.9 | 0.8 | 0.8 | 0.9 | 0.9 | 1.0 | 1.1 |
| 9 | 1.2 | 1.2 | 1.2 | 1.2 | 1.1 | 1.0 | 0.9 | 0.9 | 0.8 | 0.9 | 0.9 | 1.0 |
| 10 | 1.2 | 1.2 | 1.2 | 1.2 | 1.2 | 1.1 | 1.0 | 0.9 | 0.9 | 0.9 | 0.9 | 1.0 |
| 11 | 1.1 | 1.2 | 1.2 | 1.2 | 1.2 | 1.2 | 1.1 | 1.0 | 0.9 | 0.9 | 0.9 | 1.0 |
| 12 | 1.1 | 1.1 | 1.1 | 1.2 | 1.2 | 1.2 | 1.2 | 1.1 | 1.1 | 1.0 | 1.0 | 1.0 |
| 13 | 1.1 | 1.1 | 1.1 | 1.1 | 1.2 | 1.2 | 1.2 | 1.2 | 1.2 | 1.1 | 1.1 | 1.0 |
| 14 | 1.1 | 1.0 | 1.0 | 1.1 | 1.1 | 1.2 | 1.2 | 1.3 | 1.3 | 1.2 | 1.2 | 1.1 |
| 15 | 1.1 | 1.1 | 1.0 | 1.0 | 1.1 | 1.1 | 1.2 | 1.3 | 1.3 | 1.3 | 1.3 | 1.2 |
| 16 | 1.2 | 1.1 | 1.0 | 1.0 | 1.0 | 1.1 | 1.2 | 1.3 | 1.3 | 1.3 | 1.3 | 1.3 |
| 17 | 1.2 | 1.1 | 1.0 | 1.0 | 1.0 | 1.0 | 1.1 | 1.2 | 1.3 | 1.3 | 1.4 | 1.3 |
| 18 | 1.3 | 1.2 | 1.1 | 1.0 | 0.9 | 1.0 | 1.0 | 1.1 | 1.3 | 1.3 | 1.4 | 1.3 |
| 19 | 1.3 | 1.2 | 1.1 | 1.0 | 1.0 | 1.1 | 1.2 | 1.3 | 1.3 | 1.3 | 1.3 | 1.3 |
| 20 | 1.3 | 1.3 | 1.2 | 1.1 | 1.0 | 0.9 | 0.9 | 1.0 | 1.1 | 1.2 | 1.3 | 1.3 |
| 21 | 1.3 | 1.3 | 1.2 | 1.1 | 1.0 | 1.0 | 0.9 | 1.0 | 1.0 | 1.1 | 1.2 | 1.3 |
| 22 | 1.3 | 1.3 | 1.3 | 1.2 | 1.1 | 1.0 | 1.0 | 1.0 | 1.0 | 1.1 | 1.2 | 1.2 |
| 23 | 1.3 | 1.3 | 1.3 | 1.2 | 1.1 | 1.0 | 1.0 | 1.0 | 1.0 | 1.0 | 1.1 | 1.2 |
| 24 | 1.2 | 1.3 | 1.3 | 1.2 | 1.2 | 1.1 | 1.0 | 1.0 | 1.0 | 1.0 | 1.0 | 1.1 |
| 25 | 1.2 | 1.2 | 1.2 | 1.2 | 1.2 | 1.1 | 1.1 | 1.0 | 1.0 | 1.0 | 1.0 | 1.1 |
| 26 | 1.2 | 1.2 | 1.2 | 1.2 | 1.2 | 1.2 | 1.1 | 1.1 | 1.0 | 1.0 | 1.0 | 1.0 |
| 27 | 1.1 | 1.1 | 1.2 | 1.2 | 1.2 | 1.2 | 1.2 | 1.2 | 1.1 | 1.1 | 1.1 | 1.1 |
| 28 | 1.1 | 1.1 | 1.1 | 1.1 | 1.2 | 1.2 | 1.2 | 1.2 | 1.2 | 1.2 | 1.1 | 1.1 |
| 29 | 1.1 | 1.1 | 1.1 | 1.1 | 1.2 | 1.2 | 1.2 | 1.3 | 1.3 | 1.2 | 1.2 | 1.1 |
| 30 | 1.1 | 1.1 | 1.0 | 1.0 | 1.1 | 1.2 | 1.2 | 1.3 | 1.3 | 1.3 | 1.3 | 1.2 |

**Appendix Table B1** (Continued)

| Date | Hours | | | | | | | | | | | |
|---|---|---|---|---|---|---|---|---|---|---|---|---|
| | 12 | 13 | 14 | 15 | 16 | 17 | 18 | 19 | 20 | 21 | 22 | 23 |
| 1 | 1.0 | 0.9 | 0.9 | 0.9 | 1.0 | 1.1 | 1.1 | 1.2 | 1.2 | 1.2 | 1.2 | 1.1 |
| 2 | 1.0 | 1.0 | 0.9 | 0.9 | 1.0 | 1.0 | 1.1 | 1.2 | 1.2 | 1.3 | 1.2 | 1.2 |
| 3 | 1.1 | 1.0 | 1.0 | 1.0 | 1.0 | 1.0 | 1.1 | 1.1 | 1.2 | 1.2 | 1.3 | 1.2 |
| 4 | 1.2 | 1.1 | 1.0 | 1.0 | 1.0 | 1.0 | 1.0 | 1.1 | 1.1 | 1.2 | 1.2 | 1.3 |
| 5 | 1.2 | 1.1 | 1.1 | 1.0 | 1.0 | 1.0 | 1.0 | 1.1 | 1.1 | 1.2 | 1.2 | 1.2 |
| 6 | 1.2 | 1.2 | 1.1 | 1.1 | 1.1 | 1.0 | 1.0 | 1.1 | 1.1 | 1.1 | 1.2 | 1.2 |
| 7 | 1.2 | 1.2 | 1.2 | 1.1 | 1.1 | 1.1 | 1.0 | 1.1 | 1.1 | 1.1 | 1.1 | 1.2 |
| 8 | 1.2 | 1.2 | 1.2 | 1.2 | 1.1 | 1.1 | 1.1 | 1.1 | 1.1 | 1.1 | 1.1 | 1.2 |
| 9 | 1.1 | 1.1 | 1.2 | 1.2 | 1.2 | 1.2 | 1.1 | 1.1 | 1.1 | 1.1 | 1.1 | 1.1 |
| 10 | 1.0 | 1.1 | 1.1 | 1.2 | 1.2 | 1.2 | 1.2 | 1.2 | 1.1 | 1.1 | 1.1 | 1.1 |
| 11 | 1.0 | 1.1 | 1.1 | 1.2 | 1.2 | 1.2 | 1.2 | 1.2 | 1.2 | 1.2 | 1.1 | 1.1 |
| 12 | 1.0 | 1.0 | 1.1 | 1.1 | 1.2 | 1.2 | 1.3 | 1.3 | 1.3 | 1.2 | 1.2 | 1.1 |
| 13 | 1.0 | 1.0 | 1.0 | 1.1 | 1.2 | 1.2 | 1.3 | 1.3 | 1.3 | 1.3 | 1.2 | 1.2 |
| 14 | 1.1 | 1.0 | 1.0 | 1.1 | 1.1 | 1.2 | 1.3 | 1.3 | 1.3 | 1.3 | 1.3 | 1.2 |
| 15 | 1.2 | 1.1 | 1.1 | 1.1 | 1.1 | 1.2 | 1.2 | 1.3 | 1.3 | 1.4 | 1.3 | 1.3 |
| 16 | 1.2 | 1.2 | 1.2 | 1.1 | 1.1 | 1.2 | 1.2 | 1.3 | 1.3 | 1.4 | 1.4 | 1.3 |
| 17 | 1.3 | 1.2 | 1.2 | 1.2 | 1.2 | 1.2 | 1.2 | 1.2 | 1.3 | 1.3 | 1.4 | 1.4 |
| 18 | 1.3 | 1.3 | 1.2 | 1.2 | 1.2 | 1.2 | 1.2 | 1.2 | 1.2 | 1.3 | 1.3 | 1.4 |
| 19 | 1.3 | 1.2 | 1.2 | 1.2 | 1.2 | 1.2 | 1.2 | 1.2 | 1.2 | 1.3 | 1.3 | 1.3 |
| 20 | 1.3 | 1.3 | 1.3 | 1.2 | 1.2 | 1.2 | 1.2 | 1.2 | 1.2 | 1.2 | 1.3 | 1.3 |
| 21 | 1.3 | 1.3 | 1.3 | 1.2 | 1.2 | 1.2 | 1.2 | 1.2 | 1.2 | 1.2 | 1.2 | 1.3 |
| 22 | 1.3 | 1.3 | 1.2 | 1.2 | 1.2 | 1.2 | 1.2 | 1.2 | 1.2 | 1.2 | 1.2 | 1.2 |
| 23 | 1.2 | 1.3 | 1.2 | 1.2 | 1.2 | 1.2 | 1.2 | 1.2 | 1.2 | 1.2 | 1.2 | 1.2 |
| 24 | 1.2 | 1.2 | 1.2 | 1.2 | 1.2 | 1.2 | 1.2 | 1.2 | 1.2 | 1.2 | 1.2 | 1.2 |
| 25 | 1.1 | 1.2 | 1.2 | 1.2 | 1.2 | 1.2 | 1.2 | 1.2 | 1.2 | 1.2 | 1.2 | 1.2 |
| 26 | 1.1 | 1.1 | 1.2 | 1.2 | 1.3 | 1.3 | 1.3 | 1.3 | 1.2 | 1.2 | 1.2 | 1.2 |
| 27 | 1.1 | 1.1 | 1.2 | 1.2 | 1.3 | 1.3 | 1.3 | 1.3 | 1.3 | 1.2 | 1.2 | 1.2 |
| 28 | 1.1 | 1.1 | 1.2 | 1.2 | 1.3 | 1.3 | 1.3 | 1.3 | 1.3 | 1.3 | 1.2 | 1.2 |
| 29 | 1.1 | 1.1 | 1.1 | 1.2 | 1.2 | 1.3 | 1.3 | 1.3 | 1.3 | 1.3 | 1.3 | 1.2 |
| 30 | 1.1 | 1.1 | 1.1 | 1.2 | 1.2 | 1.3 | 1.3 | 1.3 | 1.3 | 1.3 | 1.3 | 1.2 |

**Source :** Hydrographic Department (2009)

# Appendix C

Climatological Data for Period 1980 – 2009

Songkhla Station

**Appendix Table C1** Climatological data for period 1980-2009 (Songkhla Station)

| Elements | | N-Years | JAN | FEB | MAR | APR | MAY | JUN | JUL | AUG | SEP | OCT | NOV | DEC | Annual |
|---|---|---|---|---|---|---|---|---|---|---|---|---|---|---|---|
| Pressure(hPa) | Mean | 30 | 1011.7 | 1011.9 | 1010.4 | 1009.8 | 1009.2 | 1009.7 | 1009.9 | 1010.2 | 1011.1 | 1011.0 | 1010.4 | 1012.3 | 1010.6 |
| | Mean Daily Range | 30 | -2.0 | -0.8 | -1.7 | -0.5 | -0.7 | 0.3 | 0.2 | 0.4 | 1.9 | 0.9 | -1.8 | 0.3 | -0.3 |
| | Ext.Max. | 29 | 1017.8 | 1017.7 | 1018.7 | 1015.3 | 1013.3 | 1014.5 | 1013.9 | 1015.0 | 1016.2 | 1016.1 | 1016.7 | 1017.1 | 1018.7 |
| | Ext.Min. | 29 | 1010.0 | 1010.0 | 1010.0 | 1010.0 | 1010.0 | 1010.0 | 1010.0 | 1010.0 | 1010.0 | 1010.0 | 1010.0 | 1010.0 | 1010.0 |
| Temperature | Mean Max. | 30 | 29.6 | 30.3 | 31.4 | 32.4 | 33.0 | 33.1 | 32.9 | 32.9 | 32.3 | 31.3 | 29.7 | 29.2 | 31.5 |
| (Celcius) | Ext.Max. | 30 | 32.8 | 34.3 | 35.3 | 36.8 | 36.8 | 37.1 | 36.6 | 37.3 | 35.8 | 38.5 | 34.0 | 32.3 | 38.5 |
| | Mean Min. | 30 | 24.6 | 24.7 | 25.0 | 25.3 | 25.3 | 25.1 | 24.7 | 24.7 | 24.5 | 24.3 | 24.3 | 24.4 | 24.7 |
| | Ext.Min. | 30 | 24.0 | 24.0 | 24.1 | 24.5 | 25.3 | 24.4 | 24.5 | 24.1 | 24.1 | 23.6 | 23.7 | 24.0 | 23.6 |
| | Mean | 30 | 27.1 | 27.5 | 28.1 | 28.9 | 28.8 | 28.6 | 28.4 | 28.2 | 27.9 | 27.3 | 26.9 | 26.8 | 27.9 |
| Dew Point Temp.(Celcius) | Mean | 30 | 22.6 | 22.8 | 23.6 | 24.3 | 24.3 | 23.8 | 23.4 | 23.2 | 23.4 | 23.7 | 23.9 | 23.2 | 23.5 |
| Relative Humidity(%) | Mean | 30 | 77 | 77 | 78 | 77 | 78 | 77 | 77 | 76 | 78 | 82 | 84 | 81 | 79 |
| | Mean Max. | 30 | 87 | 87 | 89 | 90 | 90 | 90 | 90 | 90 | 91 | 93 | 93 | 90 | 90 |
| | Mean Min. | 30 | 69 | 67 | 67 | 65 | 63 | 61 | 60 | 59 | 62 | 68 | 74 | 73 | 66 |
| | Ext.Min. | 30 | 64 | 64 | 66 | 60 | 55 | 56 | 55 | 51 | 58 | 62 | 67 | 72 | 51.0 |
| Visibility(Km.) | 07.00LST | 30 | 8 | 8 | 8 | 9 | 10 | 9 | 9 | 9 | 9 | 9 | 8 | 8 | 9 |
| Cloud Amount (1-10) | Mean | 30 | 6 | 5 | 5 | 6 | 7 | 7 | 7 | 7 | 7 | 8 | 8 | 7 | 7 |

**Appendix Table C1** (Continued)

| Elements | | N-Years | JAN | FEB | MAR | APR | MAY | JUN | JUL | AUG | SEP | OCT | NOV | DEC | Annual |
|---|---|---|---|---|---|---|---|---|---|---|---|---|---|---|---|
| Wind (Knots) | Prev.Wind | 30 | | | | | | N,NE | | N,NE | | | | | |
| | Mean | 30 | 5.2 | 4.9 | 3.9 | 2.9 | 2.4 | 2.4 | 2.7 | 3.0 | 2.8 | 2.4 | 3.2 | 4.7 | 3.4 |
| | Max. | 30 | 28.0 | 26.0 | 34.0 | 33.0 | 40.0 | 35.0 | 38.0 | 42.0 | 37.0 | 34.0 | 37.0 | 33.0 | 42.0 |
| Pan Evaporation(mm.) | Mean | 30 | 149 | 158 | 180 | 172 | 155 | 142 | 145 | 150 | 138 | 126 | 104 | 117 | 145 |
| Rainfall(mm) | Mean | 30 | 72.6 | 48.6 | 59.0 | 76.5 | 123.8 | 99.1 | 92.7 | 110.7 | 130.3 | 250.0 | 533.2 | 431.2 | 169.0 |
| | Mean Rainy Day | 30 | 9 | 5 | 6 | 8 | 13 | 12 | 12 | 13 | 15 | 20 | 22 | 20 | 13 |
| | Daily Max. | 30 | 182.0 | 353.6 | 148.2 | 67.4 | 193.2 | 86.0 | 99.5 | 91.0 | 110.2 | 150.8 | 521.8 | 286.0 | 521.8 |
| Phenomena(Days) | Fog | 30 | 0 | 0 | 0 | 0 | 0 | 0 | 0 | 0 | 0 | 0 | 0 | 0 | 0 |
| | Haze | 30 | 2 | 2 | 2 | 3 | 2 | 3 | 5 | 3 | 1 | 1 | 1 | 2 | 2 |
| | Hail | 30 | 0 | 0 | 0 | 0 | 0 | 0 | 0 | 0 | 0 | 0 | 0 | 0 | 0 |
| | ThunderStorm | 30 | 0 | 0 | 3 | 6 | 13 | 10 | 9 | 8 | 10 | 12 | 8 | 4 | 7 |
| | Squall | 30 | 0 | 0 | 0 | 0 | 0 | 0 | 0 | 0 | 0 | 0 | 0 | 0 | 0 |

# Appendix D

Example for Hydrodynamic Data
in Songkhla lake

**Appendix Table D1** Example for Hydrodynamic data of each node in Songkhla lake

| Node | H (m) | U (m/s) | V (m/s) | Node | H (m) | U (m/s) | V (m/s) |
|---|---|---|---|---|---|---|---|
| 1 | 1.500 | 0.000 | 0.000 | 32 | 1.500 | 0.000 | 0.000 |
| 2 | 1.500 | -0.001 | -0.001 | 33 | 1.500 | 0.000 | 0.000 |
| 3 | 1.500 | 0.000 | 0.000 | 34 | 1.500 | 0.000 | 0.000 |
| 4 | 1.500 | 0.000 | 0.000 | 35 | 1.500 | 0.000 | 0.000 |
| 5 | 1.500 | 0.000 | 0.000 | 36 | 1.500 | 0.000 | 0.000 |
| 6 | 1.500 | 0.000 | 0.000 | 37 | 1.500 | 0.000 | 0.000 |
| 7 | 1.500 | 0.000 | 0.000 | 38 | 1.500 | 0.000 | 0.000 |
| 8 | 1.500 | 0.001 | -0.001 | 39 | 1.500 | 0.000 | 0.000 |
| 9 | 1.500 | 0.000 | 0.000 | 40 | 1.500 | -0.001 | 0.001 |
| 10 | 1.500 | 0.000 | 0.000 | 41 | 1.500 | 0.000 | -0.001 |
| 11 | 1.500 | 0.000 | 0.000 | 42 | 1.500 | 0.000 | 0.000 |
| 12 | 1.500 | 0.000 | 0.000 | 43 | 1.500 | 0.000 | 0.000 |
| 13 | 1.500 | 0.000 | 0.000 | 44 | 1.500 | 0.000 | 0.000 |
| 14 | 1.500 | 0.002 | 0.002 | 45 | 1.501 | 0.000 | 0.001 |
| 15 | 1.500 | 0.000 | 0.000 | 46 | 1.500 | 0.000 | 0.000 |
| 16 | 1.500 | 0.000 | 0.000 | 47 | 1.500 | 0.000 | 0.000 |
| 17 | 1.500 | 0.000 | 0.000 | 48 | 1.500 | 0.000 | 0.000 |
| 18 | 1.500 | 0.000 | 0.000 | 49 | 1.500 | 0.000 | 0.000 |
| 19 | 1.500 | 0.000 | 0.000 | 50 | 1.500 | 0.000 | 0.000 |
| 20 | 1.500 | 0.000 | 0.000 | 51 | 1.500 | 0.000 | 0.000 |
| 21 | 1.500 | 0.000 | 0.000 | 52 | 1.500 | 0.001 | 0.000 |
| 22 | 1.500 | 0.000 | 0.000 | 53 | 1.500 | 0.000 | 0.000 |
| 23 | 1.500 | 0.000 | 0.000 | 54 | 1.500 | 0.000 | 0.000 |
| 24 | 1.500 | 0.000 | 0.000 | 55 | 1.500 | 0.000 | 0.000 |
| 25 | 1.500 | 0.000 | 0.000 | 56 | 1.500 | 0.000 | 0.000 |
| 26 | 1.500 | 0.000 | 0.000 | 57 | 1.500 | 0.000 | 0.000 |
| 27 | 1.500 | 0.000 | 0.000 | 58 | 1.500 | 0.000 | 0.000 |
| 28 | 1.500 | 0.000 | 0.000 | 59 | 1.500 | 0.000 | 0.000 |
| 29 | 1.500 | -0.001 | -0.001 | 60 | 1.500 | 0.000 | 0.000 |
| 30 | 1.500 | 0.000 | 0.000 | 61 | 1.500 | 0.000 | 0.000 |
| 31 | 1.500 | 0.000 | 0.000 | 62 | 1.500 | 0.000 | 0.000 |

**Appendix Table D1** (Continued)

| Node | H (m) | U (m/s) | V (m/s) | Node | H (m) | U (m/s) | V (m/s) |
|---|---|---|---|---|---|---|---|
| 63 | 1.500 | 0.000 | 0.000 | 94 | 1.497 | 0.006 | 0.003 |
| 64 | 1.500 | 0.000 | 0.000 | 95 | 1.500 | 0.000 | -0.001 |
| 65 | 1.500 | 0.000 | 0.000 | 96 | 1.500 | 0.000 | 0.000 |
| 66 | 1.500 | 0.000 | -0.001 | 97 | 1.500 | 0.001 | -0.001 |
| 67 | 1.500 | 0.001 | 0.001 | 98 | 1.500 | 0.000 | 0.000 |
| 68 | 1.500 | 0.000 | 0.000 | 99 | 1.476 | 0.008 | 0.036 |
| 69 | 1.500 | 0.000 | 0.000 | 100 | 1.512 | -0.029 | 0.023 |
| 70 | 1.500 | 0.000 | -0.001 | 101 | 1.500 | 0.000 | -0.001 |
| 71 | 1.500 | 0.000 | 0.000 | 102 | 1.499 | 0.000 | 0.001 |
| 72 | 1.500 | 0.000 | 0.000 | 103 | 1.500 | 0.000 | 0.000 |
| 73 | 1.500 | 0.000 | 0.000 | 104 | 1.500 | -0.001 | 0.001 |
| 74 | 1.500 | 0.000 | 0.000 | 105 | 1.500 | 0.000 | 0.000 |
| 75 | 1.500 | 0.000 | 0.000 | 106 | 1.499 | 0.001 | -0.002 |
| 76 | 1.500 | 0.000 | 0.000 | 107 | 5.000 | 0.000 | 0.000 |
| 77 | 1.500 | 0.000 | -0.001 | 108 | 1.500 | 0.000 | -0.002 |
| 78 | 1.500 | 0.000 | 0.000 | 109 | 3.000 | -0.003 | 0.005 |
| 79 | 1.499 | 0.000 | 0.000 | 110 | 1.499 | -0.005 | 0.002 |
| 80 | 1.500 | 0.000 | 0.001 | 111 | 1.499 | 0.006 | 0.004 |
| 81 | 1.500 | 0.001 | 0.000 | 112 | 3.000 | 0.000 | 0.000 |
| 82 | 1.500 | 0.000 | 0.000 | 113 | 3.000 | 0.009 | -0.001 |
| 83 | 1.500 | 0.000 | 0.000 | 114 | 5.011 | -0.022 | -0.007 |
| 84 | 1.500 | 0.000 | 0.000 | 115 | 4.991 | 0.018 | -0.041 |
| 85 | 1.500 | 0.000 | -0.001 | 116 | 2.999 | -0.015 | 0.001 |
| 86 | 1.500 | 0.000 | 0.000 | 117 | 2.931 | 0.002 | -0.053 |
| 87 | 1.500 | 0.000 | 0.000 | 118 | 4.942 | -0.016 | 0.116 |
| 88 | 1.500 | 0.000 | 0.000 | 119 | 5.105 | 0.046 | -0.265 |
| 89 | 1.500 | -0.001 | 0.000 | 120 | 5.079 | 0.312 | 0.095 |
| 90 | 1.498 | 0.003 | 0.006 | 121 | 4.559 | -0.565 | 0.424 |
| 91 | 1.500 | -0.007 | -0.006 | 122 | 5.130 | -2.229 | 1.978 |
| 92 | 1.498 | -0.001 | -0.004 | 123 | 4.609 | 0.219 | -0.327 |
| 93 | 1.506 | -0.016 | -0.023 | 124 | 5.263 | -0.084 | 0.115 |

**Appendix Table D1** (Continued)

| Node | H (m) | U (m/s) | V (m/s) | Node | H (m) | U (m/s) | V (m/s) |
|---|---|---|---|---|---|---|---|
| 125 | 5.145 | -0.577 | 0.867 | 156 | 3.500 | -0.001 | 0.001 |
| 126 | 5.114 | -0.526 | 0.829 | 157 | 3.500 | 0.000 | 0.000 |
| 127 | 1.349 | 0.107 | -0.173 | 158 | 3.500 | 0.000 | 0.000 |
| 128 | 4.847 | 0.313 | -0.277 | 159 | 3.500 | 0.000 | 0.000 |
| 129 | 5.001 | -0.041 | 0.045 | 160 | 3.500 | 0.000 | 0.000 |
| 130 | 4.996 | 0.026 | -0.020 | 161 | 3.500 | 0.000 | 0.000 |
| 131 | 5.001 | 0.001 | -0.002 | 162 | 3.500 | 0.000 | 0.000 |
| 132 | 5.000 | 0.006 | -0.010 | 163 | 3.500 | 0.000 | 0.000 |
| 133 | 5.004 | -0.005 | 0.012 | 164 | 3.500 | 0.000 | 0.000 |
| 134 | 4.993 | -0.001 | 0.000 | 165 | 4.999 | 0.006 | -0.003 |
| 135 | 5.083 | -0.003 | 0.062 | 166 | 5.001 | 0.003 | -0.001 |
| 136 | 5.033 | -0.009 | 0.058 | 167 | 5.000 | 0.000 | -0.001 |
| 137 | 4.988 | 0.000 | -0.015 | 168 | 5.002 | -0.003 | 0.002 |
| 138 | 5.007 | -0.003 | 0.012 | 169 | 3.500 | 0.001 | 0.000 |
| 139 | 4.996 | 0.001 | -0.006 | 170 | 3.500 | -0.001 | 0.000 |
| 140 | 5.005 | -0.001 | 0.008 | 171 | 3.501 | 0.002 | -0.001 |
| 141 | 5.000 | 0.005 | -0.013 | 172 | 3.499 | -0.004 | 0.003 |
| 142 | 5.002 | -0.001 | 0.002 | 173 | 3.500 | 0.001 | -0.001 |
| 143 | 4.999 | 0.019 | -0.021 | 174 | 3.500 | 0.000 | 0.000 |
| 144 | 5.000 | -0.047 | 0.047 | 175 | 3.500 | -0.001 | -0.001 |
| 145 | 4.995 | 0.014 | -0.007 | 176 | 3.500 | 0.000 | 0.000 |
| 146 | 5.002 | 0.008 | -0.003 | 177 | 3.501 | 0.001 | 0.001 |
| 147 | 5.002 | -0.004 | 0.001 | 178 | 5.000 | 0.000 | 0.000 |
| 148 | 4.997 | 0.002 | 0.004 | 179 | 5.000 | -0.003 | 0.002 |
| 149 | 5.000 | 0.012 | 0.013 | 180 | 3.502 | 0.009 | -0.006 |
| 150 | 4.999 | -0.001 | -0.004 | 181 | 3.493 | -0.046 | 0.046 |
| 151 | 3.500 | 0.000 | 0.001 | 182 | 5.002 | 0.015 | -0.015 |
| 152 | 3.501 | -0.001 | -0.001 | 183 | 5.000 | -0.003 | 0.004 |
| 153 | 3.499 | 0.002 | -0.001 | 184 | 3.500 | -0.001 | -0.003 |
| 154 | 3.500 | 0.000 | 0.001 | 185 | 3.500 | -0.001 | 0.001 |
| 155 | 3.500 | 0.000 | -0.001 | 186 | 5.002 | 0.004 | -0.003 |

**Appendix Table D1** (Continued)

| Node | H (m) | U (m/s) | V (m/s) | Node | H (m) | U (m/s) | V (m/s) |
|---|---|---|---|---|---|---|---|
| 187 | 4.993 | -0.013 | 0.008 | 216 | 3.502 | -0.002 | 0.000 |
| 188 | 5.020 | 0.035 | -0.025 | 217 | 3.502 | 0.036 | -0.033 |
| 189 | 4.956 | -0.078 | 0.016 | 218 | 3.496 | -0.009 | 0.002 |
| 190 | 7.090 | 0.231 | 0.098 | 219 | 4.999 | 0.015 | 0.001 |
| 191 | 6.827 | 0.034 | -0.188 | 220 | 4.949 | -0.025 | -0.010 |
| 192 | 7.138 | -0.028 | 0.161 | | | | |
| 193 | 5.993 | -0.112 | 0.638 | | | | |
| 194 | 5.993 | -0.151 | 0.415 | | | | |
| 195 | 6.682 | -0.250 | 0.687 | | | | |
| 196 | 7.252 | 0.213 | -0.568 | | | | |
| 197 | 6.628 | -0.237 | 0.657 | | | | |
| 198 | 5.450 | 0.004 | -0.912 | | | | |
| 199 | 6.988 | -0.300 | -0.082 | | | | |
| 200 | 7.042 | 0.120 | -0.034 | | | | |
| 201 | 4.983 | -0.155 | 0.144 | | | | |
| 202 | 5.010 | 0.051 | -0.046 | | | | |
| 203 | 4.994 | -0.011 | 0.009 | | | | |
| 204 | 3.506 | -0.022 | 0.024 | | | | |
| 205 | 3.497 | -0.001 | 0.004 | | | | |
| 206 | 4.998 | -0.006 | -0.007 | | | | |
| 207 | 5.005 | 0.016 | 0.022 | | | | |
| 208 | 4.988 | -0.045 | -0.078 | | | | |
| 209 | 5.399 | 2.203 | 2.450 | | | | |
| 210 | 4.422 | -0.153 | -0.099 | | | | |
| 211 | 5.177 | 0.080 | 0.064 | | | | |
| 212 | 4.865 | -0.006 | -0.049 | | | | |
| 213 | 5.035 | -0.006 | -0.002 | | | | |
| 214 | 5.011 | -0.003 | 0.023 | | | | |
| 215 | 3.496 | -0.002 | 0.001 | | | | |

**Sources :** Liengcharernsit, W. (2009).

# CURRICULUM VITAE

**NAME** : Ms. Sucheewan Yoyrurob

**BIRTH DATE** : May 17, 1973

**BIRTH PLACE** : Suphanburi, Thailand

**EDUCATION** :

| **YEAR** | **INSTITUTE** | **DEGREE/DIPLOMA** |
|---|---|---|
| 1992 | Thammasat Univ. | B.Sc.(Environmental) |
| 2000 | King Mongkut's Univ. of Technology Thonburi | M.Sc.( Environmental) |

**WORK PLACE** : Faculty of Science and Technology, Songkhla Rajabhat University

**SCHOLARSHIP/AWARDS** : University Development Commission (UDC) sponsored by Office of the Higher Education Commission.